Sandra Schein BSc

Investigation of phenotypical effects due to overexpression of Suppressor of Fused, a key component of the Hedgehog Signaling Pathway, in cisplatin-resistant NSCLC cells

MASTER'S THESIS

to achieve the university degree of

Master of Science

Master's degree programme:

Biochemistry and Molecular Biomedicine

submitted to

Graz University of Technology

Supervisor

Assoz. Prof. Priv.-Doz. Dr.rer.nat. Andelko Hrzenjak

Department of Internal Medicine, Division of Pulmonology

Medical University of Graz

Graz, March 2021

AFFIDAVIT

I declare that I have authored this thesis independently, that I have not used other than the declared sources/resources, and that I have explicitly indicated all material which has been quoted either literally or by content from the sources used. The text document uploaded to TUGRAZonline is identical to the present master's thesis.

Date, Signature

Danksagung

An dieser Stelle möchte ich mich bei jeder einzelnen Person bedanken die mit mir diesen Weg bestritten und auch geprägt hat.

Allen voran danke ich meiner gesamten Familie, wobei das größte Dank meinen Eltern und meiner Schwester gebührt. Ihr habt mit mir gelacht, gefeiert, geweint, getrauert, mich in jeder nur erdenklichen Situation unterstützt, seid hinter meinen Entscheidungen gestanden, habt meine Launen ertragen und habt mir immer Mut zugesprochen. Ohne EUCH wäre ich nicht an dieser Stelle angelangt und ohne EUCH hätte ich gewisse Situationen nicht bewältigen können. Für eure Unterstützung werde ich ein Leben lang dankbar sein.

Ein weiteres besonderes Dankeschön richtet sich an meinen Betreuer Assoz. Prof. Priv.-Doz. Dr.rer.nat. Andelko Hrzenjak mit samt seinem Team. Es war mir eine Ehre von euch lernen und mit euch arbeiten zu dürfen. Durch euch konnte ich meine Fähigkeiten vertiefen, enorm ausbauen und viel Neues erlernen. Nach ausgewogenen Besprechungen und Diskussionen konnte man selbstständig experimentelle Planungen durchführen und somit einen wesentlichen Einblick in die wissenschaftliche Forschung werfen. Bei Fragen konnte jederzeit um Rat und Tat gebeten werden und so fühlte man sich durchgehend hervorragend betreut. Ich kann mich nicht genug bedanken, ich kann nur sagen das ihr meinen weiteren beruflichen Verlauf geprägt habt und mich in meiner Entscheidung mich den Biowissenschaften zuzuwenden noch einmal untermauert habt. Die Zeit in diesem Team wird immer einen besonderen Stellenwert in meinem Leben haben.

Kurzfassung

Krebserkrankungen nehmen in der heutigen Gesellschaft den traurigen Stellenwert der zweit häufigsten Todesursache weltweit ein. Auf Lungenkrebs entfallen die meisten krebsassoziierten Todesopfer. Ein wesentliches Problem ist zum einen die rechtzeitige Früherkennung, zum anderen jedoch die Entwicklung einer Chemotherapieresistenz. Cisplatin ist ein Chemotherapeutikum der ersten Wahl bei der Behandlung von Lungenkrebs. Verschiedenste molekulare Resistenzmechanismen sind bereits beschrieben, durch Forschung will man diesen entgegenwirken, beziehungsweise diese wieder aufheben. Es gibt verschiedenste Signalwege die häufiger mit solchen Resistenzentwicklungen von Krebs in Verbindung gebracht werden. Ein sehr prominenter Vertreter ist der Hedgehog Signalweg. Dieser ist in der Embryonalentwicklung aktiv und ist im Adulten größtenteils inaktiv. Es ist jedoch beschrieben, dass er bei der Gewebsregeneration sehr wohl reaktiviert werden kann, so beispielsweise in der Regeneration von Lungengewebe. Kommt es hierbei zu Deregulierung des Signalwegs, kann dies zu Krebsentstehung führen. In dieser Arbeit wurde der Hedgehog Signalweg in Cisplatinresistenten nichtkleinzelligen Lungenkarzinom (NSCLC) Zellen untersucht und es wurde festgestellt, dass er in diesen aktiv ist. Durch eine Überexpression des negativen Regulators (Suppressor of Fused; SUFU) des Signalweges wollten wir den gesamten Signalweg inhibieren und somit eine Re-sensibilisierung gegenüber Cisplatin schaffen. SUFU ist in der Lage Gli Transkriptionsfaktoren im Cytoplasma zurückzuhalten und sie so in ihrer Funktion einzuschränken. Eine hohe Gli2 Aktivität wurde bereits mit Cisplatinresistenz in Verbindung gebracht. Einschränkungen in der Proliferation und Vitalität konnten nachgewiesen werden, jedoch konnte keine konkrete Aussage über eine verbesserte Sensitivität gegenüber Cisplatin getroffen werden. Auch lässt eine co-Transfektion mit miR-182-5p, welche die Gli2 Expression direkt reguliert, auch keine konkrete Aussage über eine verbesserte Cisplatin Wirkung zu.

Zur Überprüfung dieser Hypothese sollten weitere Untersuchungen am Hedgehog Signalweg, dem negativ Regulator SUFU, den Gli Transkriptionsfaktoren, sowie an anderen Signalwegen, die den Hedgehog Signalweg beeinflussen könnten, durchgeführt werden.

Abstract

In modern society, cancer is sadly the second leading cause of death worldwide. Lung cancer accounts for most of cancer associated deaths. Early detection is a major problem on the one hand, and the development of chemotherapy resistance in cancer cells on the other. Cisplatin is a chemotherapy drug of choice for lung cancer treatment. A wide variety of molecular resistance mechanisms have already been described. Intensive research tries to counteract these or to reverse them. There are various signaling pathways that are more often associated with such resistance developments. A very prominent one is the Hedgehog signaling pathway. The pathway is active in embryonic development and mostly inactive in adults. However, it is known that it can be reactivated in tissue regeneration, e.g. regeneration of lung tissue. If the Hedgehog pathway is deregulated, this can lead to cancer development. In this work the Hedgehog signaling pathway was investigated in cisplatin resistant NSCLC cells and it was found to be active in these. By overexpressing the negative regulator (suppressor of fused; SUFU) of the pathway, our aim was to inhibit the entire signaling pathway and, thus, regain a sensitivity to cisplatin. SUFU is able to retain the Gli transcription factors in the cytoplasm and thus restrict their function. A high Gli2 activity has already been linked to cisplatin resistance. Reduction of cell proliferation and viability could be demonstrated, but no concrete statement could be made about improved sensitivity to cisplatin. A co-transfection with miR-182-5p, which directly regulates Gli2 expression, also did not allow any specific statements about an improved cisplatin effect.

To test this hypothesis, further research has to be done on the Hedgehog signaling pathway, on the negative regulator SUFU, on the Gli transcription factors, as well as on other signaling pathways that could influence the Hedgehog signaling pathway.

Table of content

1. Introduction 1

1.1 Structure, function and histology of the respiratory organ 1

1.2 Lung cancer classification and development 2

1.3 Cisplatin- the lung cancer treatment of choice 3

1.4 Micro RNAs 6

1.4.1 General information, biogenesis and mode of action 6

1.4.2 miRNAs in cancer 9

1.4.3 miR-182-5p 9

1.5 Hedgehog signaling pathway 10

1.5.1 SHH signal transduction 10

1.5.2 SHH in cancer 12

1.5.3 GLI proteins 14

1.5.4 SUFU 15

2. Aims 17

3. Materials and Methods 18

3.1 General solutions 18

3.2 Buffer and Solutions 20

3.3 Primer and gBLOCKs 21

3.4 Cell culture 24

3.4.1 Cell cultivation 25

3.4.2 Starvation and non-starvation conditions 26

3.4.3 Cell counting and plate out 26

3.4.4 Transfection methods and protocols 27

3.5 RNA analysis 29

3.5.1 RNA harvesting 29

3.5.1.1 mRNA and miRNA isolation and measurement 29

3.5.2 cDNA Synthesis 30

3.5.2.1 mRNA 30

3.5.2.2 miRNA-based cDNA synthesis 30

3.5.3 RT-qPCR 31

3.5.3.1 RT-qPCR for mRNA expression level 31

3.5.3.2 RT-qPCR for miRNA expression level 32

3.5.3.3 Analysis of the RT-qPCR data 33

3.6 DNA analysis 34

3.6.1 Cloning 34

3.6.1.1 *In silico* cloning, restriction cloning and ligation for preparing the SUFU plasmid 34

3.6.1.2 *In silico* cloning and Gibson assembly – Preparation of the Gli2 plasmids 36

3.6.2 DNA isolation methods and sequencing 37

3.7 Protein analysis 38

3.7.1 Protein harvesting and isolation 38

3.7.2 BCA 39

3.7.3 SDS Page 39

3.7.4 Western Blot 41

3.7.5 Immunofluorescence 43

3.8 Phenotypical assays 44

3.8.1 Colony Forming Assay 44

3.8.2 AlamarBlue Assay 44

3.8.3 Scratch Assay 45

3.9 Interaction assays 45

3.9.1 Luciferase assay 45

3.10 Statistical analysis 46

4. Results 47

4.1 H460-CisR was chosen as working cell line 47

4.2 SUFU gene amplification and restriction cloning into transfection vector 49

4.3 Testing SUFU plasmid overexpression with different DNA amounts at certain time 51

4.4 SUFU plasmid overexpression in H460-CisR influences expression of Gli transcription factors 53

4.5 SUFU overexpression influences the localisation of Gli proteins 55

4.6 SUFU overexpression influences the colony forming ability upon cisplatin treatment 61

4.7 SUFU overexpression has an effect at the cell viability of cisplatin resistant H460 cells 62

4.8 Proliferation and migration of H460-CisR cells are not influenced by SUFU overexpression..... 64

4.9 Co-transfection experiments of H460-CisR cells with SUFU and miR-182-5p plasmid..... 65

4.9.1 Gli2-mut2 plasmid preparation by using Gibson Assembly..... 65

4.9.2 Gli2 3´UTR is a direct target of miR-182-5p..... 66

4.9.3 Co-transfection showed mild effects on SUFU and Gli2 protein level.... 67

4.9.4 Cell viability of H460-CisR is only negligibly affected after co-transfection and cisplatin treatment..... 68

4.9.5 Co-transfection and cisplatin treatment has less effects on colony forming ability as SUFU overexpression alone 70

5. Discussion..... 72

6. References..... 79

7. Supplemental information 86

1. Introduction

1.1 Structure, function and histology of the respiratory organ

The lung is essential for gas exchange between blood and inhaled air. Blood absorbs O_2 from the air and releases CO_2 in the alveoli, this exchange is being done by diffusion. The bigger the surface area, which reaches up to 140 m^2, the more effective is this passive exchange (1).

For reaching the alveoli, the air has to pass the airways. They can be split into extrapulmonal airways, which include the nasal cavity, pharynx, larynx, trachea and the main bronchi, and the intrapulmonal airways, containing the bronchial tree including bronchial tubes, bronchiole and alveoli. From the trachea to the alveoli there are about 23 branches (1,2). The airways are coated with a characteristic mucous membrane (*Tunica mucosa*), which consists of the *lamina epithelialis* and the *lamina propria*. The *lamina propria* has a high content of elastic fibers and seromucous glands. The *lamina epithelialis*, in this content also called respiratory epithelium, consists of multi-row, high prismatic ciliated epithelium with goblet cells, which produce mucines, as can be seen in Figure 1 A. This special structure is capable of moistening, heating and cleaning the air (1,2).

The branching begins with the *bronchi*. The first stage of branching is the *lobar bronchi*, followed by the *segment bronchi*. In the course of division, the multi- row epithelium is converted into a single- row epithelium. *Bronchioli terminalis* and *bronchioli respiratory* are the next branches, they no longer contain glands. The terminal branches, where the *alveoli* are found, consist of the *ductus alveolaris* and the *sacculi alveolaris* (Figure 1 B) (1).

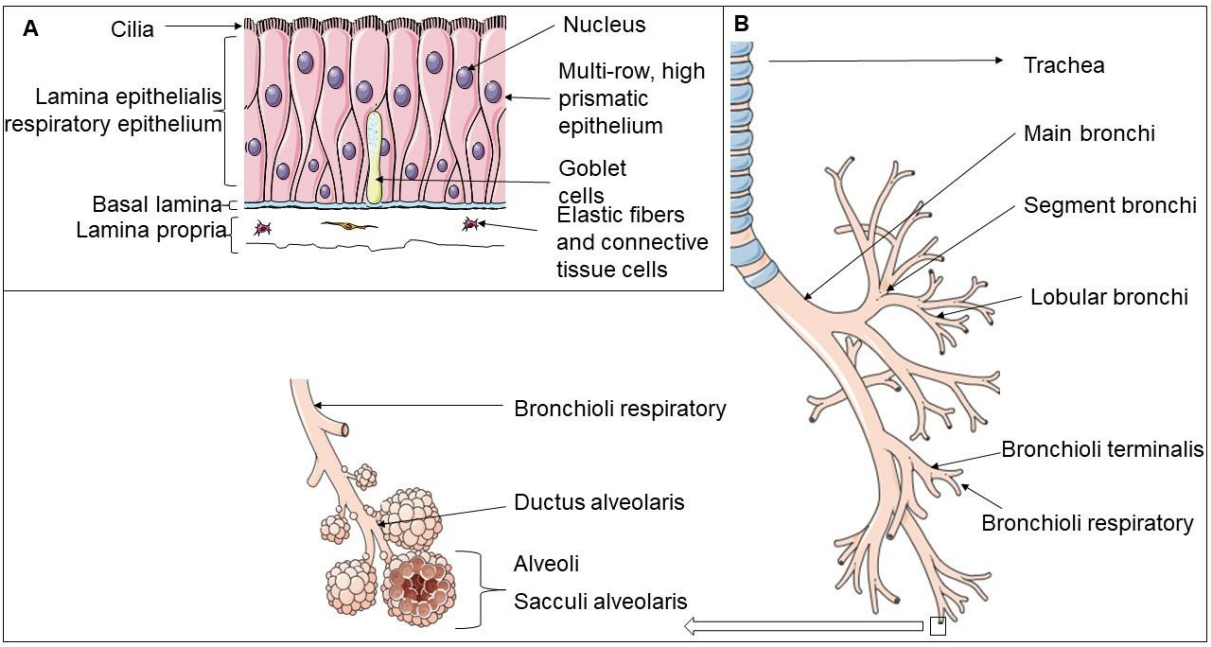

***Figure 1. Respiratory epithelium and intrapulmonal airways**. A: Histological structure and components of the respiratory epithelium. B: Intrapulmonal airways and overview of the debranching from trachea until sacculi alveolaris. B: Histological structure of the lung epithelium. (Figure was designed by using parts from Servier Medical ART: SMART (3))*

1.2 Lung cancer classification and development

Most of all human tumors have their origin in epithelial tissue and are called carcinomas. The epithelial tissue has the function of lining body cavities or vessels and covering the skin. Carcinomas are responsible for almost 80% of cancer deaths in the west world (4).

Lung carcinomas can be divided in two major classes, the squamous cell carcinomas (SCC) and adenocarcinomas (AC). SCC arises from the layer that has lining and protective function. AC arises from the layer in which specialized cells, e.g. glands with secretory function, are embedded. Lung cancer can be divided into 2 main classes. Non-small cell lung carcinomas (NSCLC), which make up to 85% of lung cancer and can be classified into SCC (up to 35%) and AC (more than 40%). Large cell carcinomas (LCC) cover the remaining part. Small cell lung carcinomas (SCLC) are the second main class of lung cancers and are considered more aggressive. It is assumed that these arise from neuroendocrine cells. They are distributed in the respiratory

epithelium and are hormone forming and storing cells. The classification of lung cancer is further enhanced by the high number of histological subgroups in each class. The development of lung cancer is not fully understood because of the great variety in influencing factors, however, smokers have a higher risk to develop cancer caused by carcinogens that are inhaled (1,4–10). In this work, the focus is set on NSCLC.

Cancer development is not a single step event, various factors are involved in the cancer formation. Divers sources, like mutations or gene deregulation, are found in the different cancer types. Lung cancer is a prominent example for high mutation rates. This high degree of genetic instability is achieved by inhaling a wide variety of carcinogens. The use of tobacco increases this risk for lung cancer. Consequences can occur on pathways of the DNA repair systems, either on DNA levels directly or at epigenetic level via hypermethylation. Through methylations tumor suppressor genes can be inactivated. For this reason, these reactions are very early events in cancer development. However, not only the indicated events lead to the cancer progression, also mutations or the incorrect regulation of certain signaling pathways plays a major role (1,4–12). Some signaling pathway deregulations, like the Hedgehog or the Wnt pathway, are also highly associated with cancer stem cells (CSC), which play a key role in tumor development and maintenance (4,7,8,11,12) which will be discussed in detail in chapter 1.5.2.

1.3 Cisplatin- the lung cancer treatment of choice

Cisplatin is used as a platinum-based chemotherapeutic for a variety of human cancer, e.g. lung cancer, ovarian cancer, breast cancer or brain cancer (13). In SCLC platinum-based drugs even represents the first- line method of treatment (9,13). In early – phase NSCLC the treatment consists of surgical removal followed by administration of cisplatin (9,10,13).

The molecular structure of cisplatin contains a double charged platinum ion with 4 bound ligands, as shown in Figure 2 A. The amine ligands ensure a better binding of the platinum ion and the two chloride ligands are responsible for the crosslink to the DNA, especially to purine bases. Cisplatin is given by intravenous injection and becomes active only in the cytoplasm. In the cytoplasm the chloride concentration is

lower than in the extracellular space and this leads to an exchange of Cl^- for H_2O (Figure 2 B). Because of this reaction, cisplatin becomes a strong electrophile and is in an active mode. It preferably reacts with the N7 residue of purine bases resulting in DNA damage. The most prominent DNA damage induced by cisplatin is the binding of two adjacent guanines (13–16).

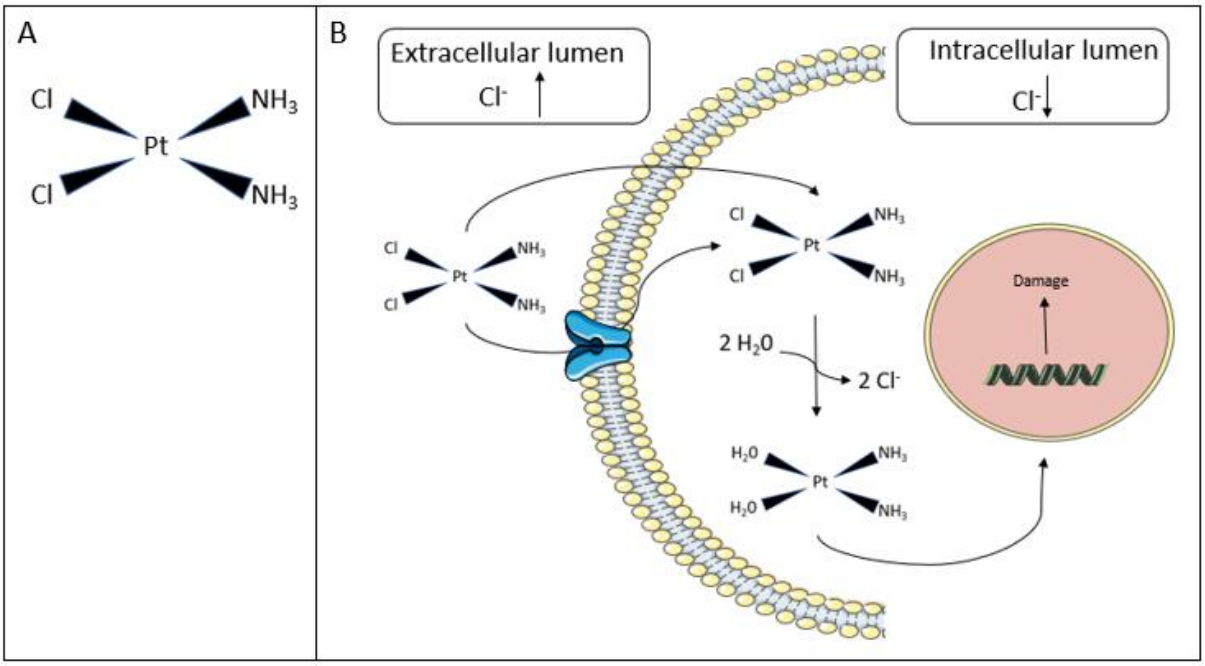

Figure 2. Cisplatin- Structure and mode of action. *A: Molecular structure of cisplatin. B: Uptake of cisplatin and intracellular activation mechanism as well as function of cisplatin. (Figure was designed by using parts from Servier Medical ART: SMART (3)).*

Beside the direct interaction with DNA, cisplatin also leads to increased oxidative stress and to an increased level of reactive oxygen species (ROS). As long as a certain point of DNA damage has not been exceeded, the cell cycle will be paused and the mistakes can be eliminated by the nucleotide excision repair system (NER). If the threshold is exceeded, apoptosis occurs. As mentioned above, oxidative stress is an important mechanism of the toxicity of cisplatin. The level of ROS is determined by the concentration and duration of the treatment by cisplatin. There are certain systems in the human body that can keep the level of ROS constantly low, but if the level is exceeded this will also lead to apoptosis (13,16).

The detailed uptake mechanism of cisplatin is not yet fully investigated. However, it is suggested that the cooper transporter 1 (Ctr1) is involved in the uptake, but cisplatin itself leads to an increase degradation of the transporter which in turn has a diminished uptake rate. Another assumption indicates a simple passive transport of cisplatin in term of the concentration gradient. That would suggest that the resistance occurs as an effect of increased efflux (13–15).

Cisplatin has a number of negative side effects. The most prominent are renal and neurotoxic effects. Especially due to kidney damage, there is a limitation of dose and duration of treatment and that is the main reason of emergence of resistance (13,14,16).

There are many different resistance mechanisms known, e.g. reduced intracellular accumulation, sequestration, NER and mismatch repair (MMR) system. The reduced accumulation and sequestration are so called “pre-target effects”. As already mentioned above, cisplatin downregulates the expression of the Ctr1, which leads to a decreased cell uptake. An increased efflux of cisplatin is also responsible for the reduced intracellular concentration. The multidrug resistance protein MRP2, which is a ABC ATPase, as well as the ATPases ATP7A and ATP7B are upregulated in cisplatin resistant cells (14,16).

Another “pre-target effect” is the sequestration through glutathione (GSH). Glutathione is present in every cell and is synthesized by γ-glutamylcysteine synthetase (γ-GCS). Glutathione is a tripeptide consisting of cysteine, glycine and glutamic acid. Apart from the DNA, activated cisplatin in the cytoplasm also binds to other nucleophiles, such as GSH. The binding to GSH is initiated by the glutathione-S-transferase (GST). This complex is exported through MRP2 (14,16–18).

So called “on target resistance” mechanism include the NER and the MMR systems. To a certain extent the injuries of cisplatin are repaired by NER. The mode of action is that damaged nucleotides are recognized, cut and removed from the DNA strand by special endonucleases and in the last step DNA synthesis and ligation is done to fill the gap. In this process, many proteins are involved, for example excision repair cross-complementing rodent repair deficiency, complementation group 1 (ERCC1). A high expression level of ERCC1 negatively correlates with the efficiency of cisplatin (16,19).

The MMR system is able to detect cisplatin lesions but not to repair them directly. This system usually affects the DNA replication. Important MMR-related proteins are mutS homolog 2 (MSH2) (20) and mutL homolog 1 (MLH1) (21). In the case of resistance development these two proteins are often mutated or downregulated. Acquired cisplatin resistance and downregulation of MSH2 is commonly observed (16).

1.4 Micro RNAs

1.4.1 General information, biogenesis and mode of action

There are different classes of RNA, with different function for this generic term. In general, RNAs are divided into coding and non-coding RNAs. The most widely known is mRNA, which is classified as coding RNA that encodes for proteins. The non-coding RNAs are involved in regulatory pathways. This group includes e.g. miRNAs (microRNAs), small interfering RNAs (siRNAs), long non coding RNAs (lncRNAs), or PIWI- interacting RNAs (piRNAs) (22). Since miRNAs are a major point in this work, only these will be discussed further.

miRNAs are relatively small single strand constructs of about 22 nucleotides (nt). They have crucial role in the regulation of gene expression. miRNAs are essential factors for e.g. cell proliferation, differentiation, cell death or the response to environmental factors. They are not only tissue-specific, but can be secreted into the extracellular lumen and act as chemical messenger. Their function as biomarker gets more and more popular, because aberrant expression could be an indication for a particular disease. The original discovery of them was more coincidental than planned. In 1993 two scientific groups were examining the *lin-4* gene in *Caenorhabditis elegans (C. elegans)*. It has been found that this gene is involved in the larval development, but encoded protein has never been found. After further investigations it was discovered that the short *lin-4* gene product is remarkable similar to the 3´UTR of *lin-14* gene, which is also involved in the development of *C. elegans*, and the level of *lin-4* regulates the expression of *lin-14* (23–27).

In order to obtain mature miRNA, a multi-step process is required. miRNAs are mainly processed from introns, very rarely from exons. There are 2 different pathways for the formation of the mature miRNA, the canonical pathway and the non- canonical pathway. The predominant pathway is the canonical one, which will be explained in detail (Figure 3). RNA polymerase II synthesizes a longer product, the so-called primary miRNA (pri-miRNA). A complex, consisting of the RNA binding protein DiGeorge Syndrome Critical Region 8 (DGCR8), which recognizes specific motifs, and Drosha, a ribonuclease III enzyme that cuts the specific hairpin, and the shorter precursor-miRNA (pre-miRNA) is produced. The typical 3´overhang of the pre-miRNA is also produced during this first step (26–28). The next step is the translocation from the nucleus to the cytoplasm. For this transport, exportin-5 (XPO5) is necessary. XPO5 binds the pre-miRNA by recognizing the 3`overhang, but only if it is associated with RanGTP. This complex passes the nuclear pore complex. In the cytoplasm, RanGTP is hydrolysed by RanGAP to RanGDP. The Exportin-RanGDP complex binds the pre-miRNA very weak and releases it to the cytoplasm. Exportin-RanGDP returns into the nucleus, RanGDP is exchanged to RanGTP, and the complex can bind a new pre-miRNA (26–33). In the cytoplasm the pre-miRNA is cut further by the DICER, a RNAse III endonuclease, and the mature miRNA is generated. Still double-stranded, it is loaded into the Argonaute protein AGO2. Then the passenger strand is degraded and the guide strand stays in complex with AGO2. Whether it is a 3p or a 5p miRNA depends on which strand is degraded. That in turn depends on many factors such as cell type or cell environment (26,27).

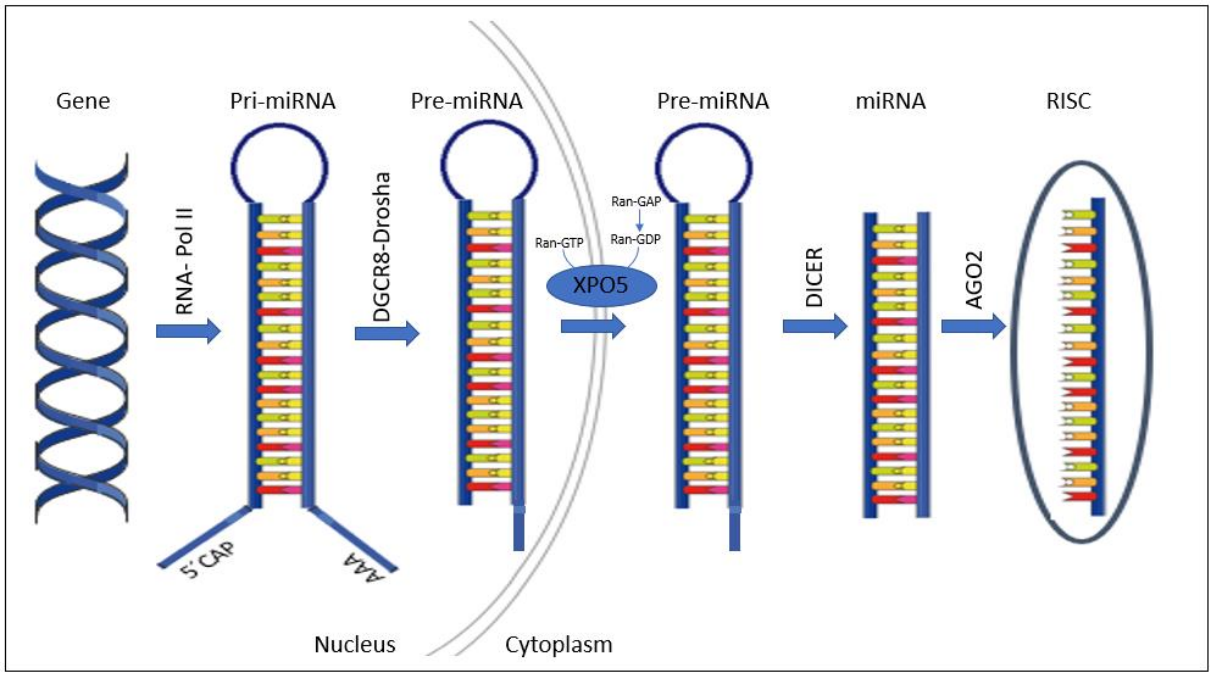

***Figure 3. miRNA maturation**. Transcription by RNA-Pol II leads to pri-miRNA, which is further processed by DGCR8-Drossha to pre-miRNA. pre-miRNA leaves the nucleus via XPO5 and is processed into mature miRNA by DICER. Figure was designed by using parts from Servier Medical ART: SMART (3)).*

The mature miRNA is able to bind specifically to the target mRNA, mostly in the 3´UTR (untranslated region), which leads to repression of translation or to degradation of the mRNA. miRNA binding at the 5´UTR or at the coding region is mostly associated with silencing effects but binding at the promoter could also lead to a stronger transcription (26). The binding takes place at so-called miRNA response elements (MRE) of the targeted mRNA, however, the motif is not completely complementary. The binding creates the miRNA induced silencing complex (RISC). This complex includes many factors. The AGO2 is in contact with the glycine- tryptophan repeat- containing protein (GW182) family, which are necessary for downstream effects. The GW 182 protein recruits then the CCR4-NOT and the PAN2/3 complex, as well as the poly A binding protein C (PABP). These components perform deadenylation of the mRNA. Decapping enzymes can then fulfil their function and the mRNA is further degraded by exoribonucleases (26,27,34).

1.4.2 miRNAs in cancer

miRNAs are becoming increasingly important in the detection, diagnosis, as well as in the therapy of various types of cancer. An abnormal regulation can have tremendous consequences (35,36). miRNAs can affect the tumor development in various ways because of their general regulatory functions. miRNAs could regulate oncogenes as well as tumor suppressor genes. The dysregulation of miRNAs can also have consequences for entire signaling pathways. These, in turn, play a major role in the development of cancer (37,38). Lung cancer is often diagnosed in an advanced stage of disease, for this reason there is an increased hope that miRNA profiling will counteract this diagnostic challenge. In the best case, miRNAs could act as biomarker for early lung cancer detection and prediction, as well as stage and subtype classification. By analysing different miRNAs, the course of diseases could be more easily monitored and also the effectiveness of treatment, especially chemotherapy, could be improved and adapted in the best possible way (39). These desired ideas are supported by the fact that there are differences in the expression levels of miRNAs between tumor tissue and non-malignant tissue. However, the enormous genetic diversity of tumors and cell lines makes investigation of “onco-miRNAs” very challenging (36,38).

1.4.3 miR-182-5p

The miR-182-5p is a regulatory miRNA that influences an entire signaling pathway. It is downregulated in cisplatin resistant lung adenocarcinomas as opposed to sensitive ones. It has been shown by our research group that this miRNA directly targets GLI2 and that the regulation of miR-182-5p consequently alters cisplatin sensitivity (40). GLI2 is a transcription factor in the Hedgehog (HH) signaling pathway. The HH signaling pathway is moving more and more in the focus of cancer research because this pathway is reactivated in cancer cells. By investigating deregulated miRNAs, with particular attention to miR-182-5p, a connection to the HH signaling pathway was established (40).

1.5 Hedgehog signaling pathway

The Hedgehog (HH) signaling pathway is a very important and therefore, highly conserved. It was first discovered in the model organism *Drosophila melanogaster* and years later in mammals. HH signaling pathway plays an enormously important role in embryonic development, since it controls cell proliferation, differentiation into tissues at given time, is responsible for tissue polarity and is also essential in brain development (41–45). Due to its crucial functions in embryonic development, it is not surprising that deregulation of HH signaling pathway has tremendous effects. Initial research at HH signaling pathway was limited to developmental defects, like general birth defects or neural defects (41–43). Lately it was found that the HH signaling pathway not only occurs in embryonic development but also plays a fundamental role in adults. In adults it is not permanently active, it is often silenced (41). However, if HH signaling pathway is active, it is capable of tissue homoeostasis like preservation, regeneration, renewal and repair. Therefore, it is active in the required stem cells and is responsible for their maintenance (41,43,45,46). The HH signaling pathway can be divided into 3 subclasses, depending on the involved ligand. The different proteins distinguish Sonic Hedgehog (SHH), Indian Hedgehog (IHH) and Desert Hedgehog (DHH) signaling pathway. IHH and DHH signaling pathways show their greatest effects on developing tissues and SHH signaling pathway occurs in developing, as well as in adult tissue and is, therefore, the most studied one (41–44). Central nervous tissue, lung tissue or teeth are examples where SHH signaling pathway is more common. Noteworthy, this pathway plays a crucial role in the regeneration of pulmonary epithelium (45).

1.5.1 SHH signal transduction

The SHH signaling pathway consists of a number of proteins that activate and regulate each other. There is also a canonical and a non-canonical pathway. The non-canonical pathway acts without a ligand (41,42,45). In this work only the canonical pathway and the most important proteins are discussed in detail.

In the first step, the mature ligand is secreted under the control of the dispatched (DPTCH) protein and binds to the patched receptor (PTCH1). PTCH1 is a 12-pass

trans membrane receptor. The binding activates the receptor and this means that the repression of the smoothened receptor (SMO) is inhibited. With its 7- transmembrane domain, SMO is reminiscent of a G-protein coupled receptor. How this receptor interaction takes place has not been clarified yet. It is only known that the inhibition of SMO repression is crucial for downstream signaling (41–45). Further, signal transduction takes place at primary cilia (PC), in close proximity to the above-mentioned receptors. The kinesin protein KIF7 is located at the top of PC and coordinates the signal transmission (42–44). The suppressor of fused (SUFU) and the GLI proteins form a complex. This complex dissociates through signal transmission and GLI can enter the nucleus. Since GLI proteins are transcription factors, they can regulate the HH signaling pathway target genes. There are several GLI proteins. Gli1 acts as activator and Gli2/Gli3 act as activator or repressor. Target genes are transcribed by the activators, including the *ptch* or *gli* genes, and create a positive feedback loop that maintains the pathway. Other target genes regulate the cell cycle, as well as growth, differentiation or repair (Figure 4) (41,43–45). If no ligand binds, there is no activation and signal transmission. In this scenario, KIF7 is located basal at PC and not at the top, and the SUFU-GLI complex is unable to dissociate. If this complex persists, it is not possible for the GLI proteins to translocate into the nucleus (43,45). It is known that a loss of SUFU leads to permanent pathway activation (42). It was also described that SUFU is involved in the maturation of Gli3, which acts as repressor (41). This findings suggests that SUFU is a strong negative regulator of the HH signaling pathway (43,45). SUFU is not the only negative regulator. The HH interacting protein1 (HHIP) and the growth-arrest specific protein1 (GAS1), which are secreted proteins, as well as the membrane proteins cysteine dioxygenase (CDO) and the brother of CDO (BOC), are able to interact with the HH ligands. This disrupts the actual interaction with the PTCH receptor (41).

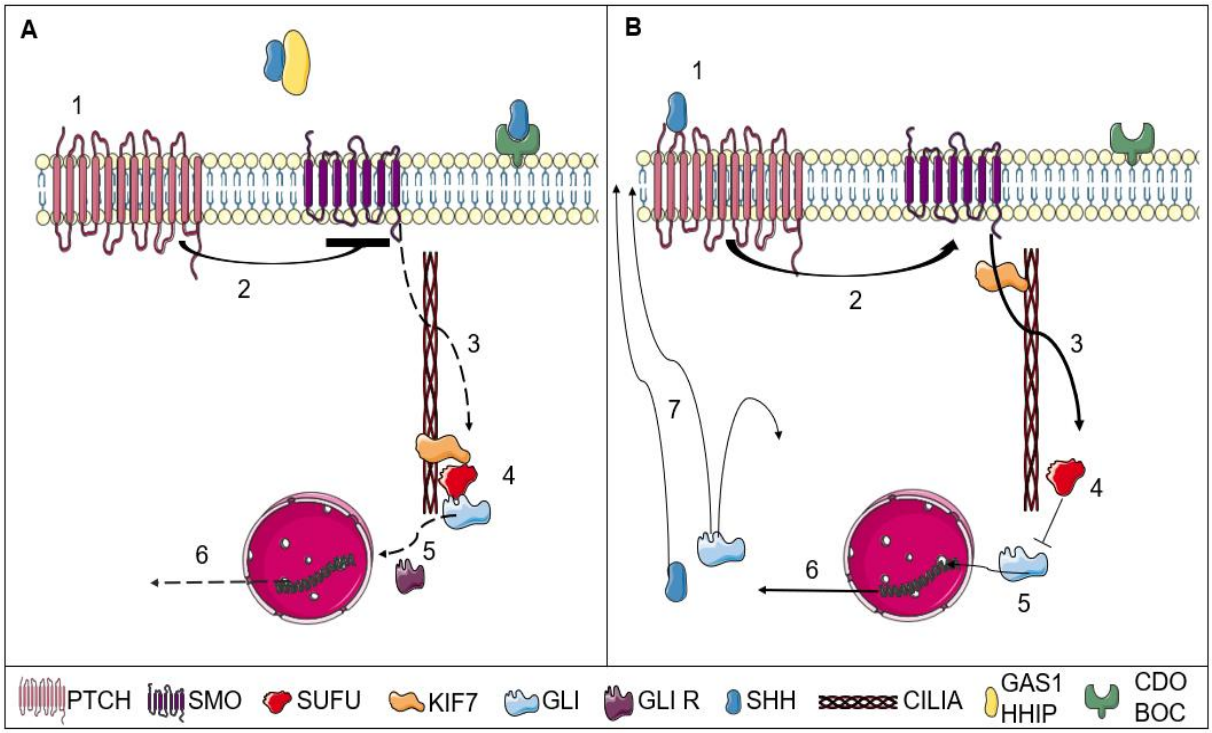

***Figure 4. Hedgehog Signaling Pathway**. A: Inactive HH signaling pathway. 1 = No ligand binding. 2 = No Signal transduction to smo receptor. 3 = No downstream signaling. 4 = No dissociation of SUFU-GLI complex. 5 = Gli Repressor form is generated. 6 = No transcription of target genes. B: Active HH signaling pathway. 1 = Ligand binding to patched receptor. 2 = Signal transduction to smo receptor. 3 = downstream signaling. 4 = SUFU Gli complex dissociates, no gli repressor form is generated. 5 = active Gli translocates in nucleus. 6 = Transcription of target genes. 7 = Secretion of target genes. Figure was designed by using components from Servier Medical ART: SMART (3)).*

1.5.2 SHH in cancer

Due to the sensitive functions of HH signaling pathway already mentioned in chapter 1.5, a connection between abnormal regulation and tumorigenesis was assumed (41–45). The HH signaling pathway is not only involved in the initial tumor development, but also in the maintenance, the further growth as well as invasion. There are various ways in which HH signaling pathway acts or influences cancer. For this, 4 basic model types for a better overview are described. The first type is the ligand independent activation. Loss of function as well as gain of function mutations in core components of the pathway make it constitutively active. The second type is the so-called ligand depended and autocrine activation with observed ligand overexpression. Through a positive feedback loop, the pathway activates itself and causes overexpression of cancer-related molecules, e.g. proliferation factors. Type III is ligand dependent and paracrine activation. In this case, the cell, which overexpresses the ligand, isn´t

regulating itself, ligands act on neighbouring cells. The last type, type IV, deals with the aberrant activation of HH signaling pathway in cancer stem cells (41–46). Although cells with stem cell properties have been discovered in some types of tumors, the term cancer stem cell (CSC) should be used with caution because their origin is puzzling and not yet exactly identified (45–47). They are said to have unlimited self-renewable potential, can differentiate into other cell types and have embryonic or somatic stem cell properties. Therefore it is not surprising that HH signaling pathway also plays an important role in maintaining these cells (45–49). Normally, these cells divide rather slowly, but under certain conditions they can divide and differentiate very. Taken together, these properties also lead to the enormous heterogeneity of cancer (45–47). It is known that HH signaling pathway is involved in embryonic development and that it has there an important role in the formation of lung. It has long been assumed that the HH signaling pathway is inactive in adults. However, some stem cells must be active or reactivated for repair purposes of lung epithelium. Incorrect regulation of the pathway can lead to CSC, but the origin and the biology of these raises some unanswered questions (45,47,48,50). As discussed in previous chapters, NSCLC with its many histological subtypes represents the majority of often therapy- resistant lung cancers. More and more information indicate that CSCs are involved in treatment failure and relapse. Although most of the tumor can be eliminated, very small cell populations are able to survive, pointing to CSC, because these often represent only 0.5% of the total tumor mass. In addition, there are studies on resistant lung cancer that strongly link CSC and HH signaling pathway (47,50). Due to active HH signaling pathway the CSC could build resistance mechanisms. Studies show that they increasingly express ABC- transporters and this can lead to treatment failures. If the HH signaling pathway could be blocked, it is assumed that the cells would lose their stem cell properties and so the platin-based therapy could be reintroduced. A completely new approach for fighting cancer is the targeted destruction of CSC. However, it should be noted that not only the indicated HH signaling plays a role but a variety of other pathways are active in human cancers and also interact with each other (46–50).

1.5.3 GLI proteins

Gli proteins are transcription factors that where first identified in glioblastoma cells. Gli therefore means “glioma-associated”. They belong to the family of zinc finger transcription factors and in vertebrates Gli1, Gli2 and Gli3 are the most present ones (51–53). Gli proteins play a key role in the HH signaling pathway. Each of the 3 proteins contains a C-terminal activator domain. Gli2, as well as Gli3 have an additional N-terminal repressor domain. From this, it can be concluded that Gli1 only acts as activator, Gli2/3 act as both repressor and activator, whereby the main activity of Gli3 is repression. The mode of action of Gli proteins is controlled by phosphorylation and posttranscriptional events, e.g. ligand binding (51,53–56). This complex Gli network can be activated not only via the canonical HH signaling pathway but also via the non-canonical pathway. Furthermore, additional signaling pathways, which are common in cancers, use Gli proteins as effectors, which makes the network even more complex (51,54,55).

As mentioned above, this study focuses on the canonical HH signaling pathway. If the Ligand (SHH) binds to the receptor, a signaling cascade is triggered, the role of which is to activate Gli1/2. In particular, full length Gli1 translocates into the nucleus and fulfils the task as transcription factor. Expression of target genes controlling, for example, proliferation, angiogenesis or stem cell renewal are the final goal. Even genes of the HH signaling pathway are targets which are regulated by Gli transcription factors, so the HH signaling pathway is able to regulate the expression of its own genes, like *ptch* or *gli*. This indicates a positive feedback loop that leads to deregulation of the HH (51,54). Previous lung cancer studies showed deregulated HH signaling pathway and a significant overexpression of Gli proteins in tumor cells. High Gli mRNA levels are accompanied with a very poor prognosis. It is also suspected that the activator Gli2 is strongly linked to often occurring chemoresistance (51,54–57).

If no ligand binds to the receptor, Gli1 is retained in the cytoplasm by SUFU and repressor forms are increased. Expression of Gli genes can also be controlled by miRNAs, as already described (40,53,54,56).

1.5.4 SUFU

Suppressor of fused (SUFU) is a key component of the HH signaling pathway with the function as the main negative regulator of this pathway (58–70). SUFU is a monomer consisting of two globular domains linked by a short linker. It is able to bind and regulate Gli proteins. Gli1 is thereby inhibited in its translocation into the nucleus, and therefore, unable to induce the expression of specific genes. The interaction of SUFU with Gli takes place via the C terminus of SUFU with N terminus of Gli and vice versa. By binding Gli2/3, SUFU promotes the formation of the respective repressor form. SUFU is located mainly in the cytoplasm but is also found in the nucleus. In the cytoplasm the Gli proteins are regulated through binding to SUFU (58–65,67–70). In this case, SUFU competes with importin β1, which transports the Gli proteins into the nucleus upon detection of the nuclear localization signal (NLS). This NLS is covered by SUFU (59,60). Gli proteins also contain another identifier for SUFU, the SYGH motif. If mutations occur at this point, SUFU is no longer able to bind and regulate Gli proteins (59,60). There are alternative splice variants of SUFU. Two are already well described, however, further research is needed to elucidate differences in the functional mechanism. Variant 1 is 54 kDa large and consists of 484 amino acids (aa). This variant is the most common and best described one. Variant 2 is 48 kDa large and is truncated by 19 aa. This deletion takes place at the C-terminus, therefore, it is assumed that variant 2 can only perform regulation in the nucleus. Interestingly, the SUFU locus is on chromosome 10 q24-q25, which is the locus where deletions and mutations are mainly found in glioblastoma, with an associated high level of expressed Gli (59–61,70). Apart from glioblastoma, downregulations and mutations of SUFU are also found in many other tumors. Not every mutation leads to a loss of function, some are silent and preserve the wild type characteristics of SUFU. Even if SUFU is completely intact, there may still be a loss of function in subsequent cancer formation. This speaks for epigenetic changes, as well as for post-translational events, with the aim of increased activation of the HH signaling pathway. SUFU is therefore a notable tumor suppressor, which is of particular importance. Beside its role in cancer, loss of SUFU leads to lethality during embryonic development (58–61,63,66,67). As indicated, SUFU does not only assume its regulatory role in the cytoplasm but also in the nucleus. Nuclear SUFU promotes the export of Gli, on the other hand it recruits the SAP18-

mSin3-HDAC complex. This blocks the binding site of Gli and the result is a reduced expression of target genes (59,60,63–67).

HH signaling pathway is deregulated in cancer cells and as a result an increased degradation of SUFU is observed. Polyubiquitination of K257 of SUFU leads to degradation by the proteasome (59,67). Aberrant regulation of miRNA´s also leads to HH signaling pathway deregulation. SUFU for example is the direct target of miRNA-214, and if high levels of miRNA-214 are expressed, SUFU is downregulated. (59,61,68,69). Examinations of lung cancers showed an upregulation of miRNA-214 whereas a knockdown of this miRNA resulted in an increase of SUFU expression (68).

2. Aims

The aim of the study was to inhibit the HH signaling pathway in cisplatin resistant NSCLC cells by overexpression of the negative regulator SUFU. This should subsequently lead to restrictions in growth and viability of the cancer cells. Furthermore, we wanted to investigate whether the inhibition of the HH signaling pathway increases the sensitivity to cisplatin. Another part deals with co-transfection of NSCLC cells with miR-182-5p and SUFU plasmid, the aim of which was also the inhibition of the HH signaling pathway.

3. Materials and Methods

3.1 General solutions

Table 1. General solution and kits and the respective providers

Acetic acid (glacial)	Merck, Darmstadt, Germany
Acrylamide	Merck, Darmstadt, Germany
Agarose	VWR, Darmstadt, Germany
AlamarBlue®	Thermo Fisher Scientific, Fremont, USA
Amersham ECL™ Prime Western blotting detection reagent,	GE Healthcare, Little Chalfont, GBR
Ampicillin	Sigma Aldrich, Vienna, Austria
β-mercaptoethanol	Sigma Aldrich, Vienna, Austria
Biozym Blue S´Green qPCR Kit	Biozym, Hessisch Oldendorf, Germany
Bromophenol blue	Sigma Aldrich, Vienna, Austria
BCA Protein Assay Kit	Merck, Darmstadt, Germany
CASYton	OMNI Life Science, Bremen, Germany
Cisplatin "Accord" 1 mg/mL	LKH Graz pharmacy
Collagen I, Rat-Tail, 100 mg	Szabo-Scandic HandelsgmbH & Co KG, Vienna, Austria
Color Prestained Protein Standard, Broad Range (11–245 kDa)	New England BioLabs, Ipswich, MA
Crystal violet	Sigma Aldrich, Vienna, Austria
D-(+) Glucose monohydrate	Sigma Aldrich, Vienna, Austria
DMEM High Glucose	Gibco, Paisley, UK
DMEM 1x	Gibco, Paisley, UK
Dimethylsulfoxide (DMSO)	Sigma Aldrich, Vienna, Austria
DPBS	PAN Biotech, Aidenbach, Germany
DNase1	PeqLab Gold
Dual-Luciferase® Reporter Assay System	Promega, Mannheim, Germany
Endo – Free Plasmid DNA Maxi Kit E.Z.N.A.®	Omega Bio-tek, Inc., Norcorss, USA
Ethanol	Merck, Darmstadt, Germany
FastRuler High Range DNA Ladder, ready-to-use	Thermo Fisher Scientific, Fremont, USA
Fetal Calf Serum (FCS)	Biowest, Nuaillé, France
Gel Loading Dye, Purple (6X)	New England BioLabs, Ipswich, MA
GeneRuler 100 bp Plus DNA Ladder	Thermo Fisher Scientific, Fremont, USA
Glacial Acetic Acid	Sigma Aldrich, Vienna, Austria
Glycerol	Sigma Aldrich, Vienna, Austria
Glycine	Sigma Aldrich, Vienna, Austria
Isopropanol	Merck, Darmstadt, Germany

Jet Prime®	Polyplus-transfection, Illkirch-Graffenstaden, France
LB-Medium	Roth, Karlsruhe, Germany
LB-Agar	Roth, Karlsruhe, Germany
L-Glutamine 200 nM (100x), liquid	Gibco, Paisley, UK
MassRuler DNA Ladder Mix, ready-to-use	Thermo Fisher Scientific, Fremont, USA
Methanol	Merck, Darmstadt, Germany
Milk powder	Roth, Karlsruhe, Germany
MinElute® Gel Extraction Kit	Qiagen, Venio, Netherlands
miRCURY LNA™ ExiLENT SYBR-Green master mix	Exiqon, Vedbaek, Denmark
miRCURY LNA™ Universal cDNA synthesis kit II	Exiqon, Vedbaek, Denmark
Monarch DNA Gel Extraction Kit	New England BioLabs, Ipswich, MA
NEBuilder® HiFi DNA Assembly	New England BioLabs, Ipswich, MA
Nitrocellulose Membran	BioRad Industries, Hercules, USA
N,N,N',N'-Tetramethylethylendiamin (TEMED)	Sigma Aldrich, Vienna, Austria
PeqGOLD® Plasmid Miniprep Kit II	Peqlab, Erlangen, Germany
PeqGOLD® Taq-DNA-Polymerase 'all inclusive'	Peqlab, Erlangen, Germany
PeqGOLD® Total RNA Kit	Peqlab, Erlangen, Germany
PeqGreen	VWR, Radnor, USA
Pierce protease inhibitor Minitablest	Thermo Fisher Scientific, Fermont, USA
Polyvinylidene Difluoride Membrane (PVDF)	GE Healthcare, Little Chalfont, UK
Ponceau-S	Merck, Darmstadt, Germany
Protein Marker IV (pre-stained), peqGOLD 10-170 kDA	VWR, Radnor, USA
Q5® High-Fidelity 2X Master Mix	New England BioLabs, Ipswich, MA
Q5® High-Fidelity DNA Polymerase	New England BioLabs, Ipswich, MA
qScript™ cDNA Synthesis Kit	Quanta Biosciences, Beverly, USA
Restore PLUS Western Blot Stripping Buffer	Thermo Fisher Scientific, Fremont, USA
RIPA Buffer	Sigma Aldrich, Vienna Austria
RLT Lysis Buffer	Peqlab, Erlangen, Germany
RNase	Thermo Fisher Scientific, Fremont, USA
RPMI 1640	Gibco, Paisley, UK
SOC Outgrowth Medium	New England BioLabs, Ipswitch,USA
Sodium Chloride	Roth, Karlsruhe, Germany
Skim Milk	Roth, Karlsruhe, Germany
Sodium Dodecyl Sulfate	Sigma Aldrich, Vienna, Austria
SuperSignal Western Femto Chemiluminescent Substrate	Thermo Fisher Scientific, Fremont, USA
SuperSignal Western Pico Chemiluminescent Substrate	Thermo Fisher Scientific, Fremont, USA

TAE	LKH Graz Apotheke, Graz, Austria
Trizma Base	Sigma Aldrich, Vienna, Austria
Trizma HCl	Sigma Aldrich, Vienna, Austria
Trypan blue	Sigma Aldrich, Vienna, Austria
Trypsin	Gibco, Paisley, UK
Tween 20	Sigma Aldrich, Vienna, Austria
Vectashield® Mounting Medium for Fuores-cence with DAPI	Vector Laboratories, Burlingame, CA
0.025% Trypsin-EDTA	Gibco, Paisley, UK
1000 U/ml Penicillin	Gibco, Paisley, UK
10 000 µg/ml Streptomycin	Gibco, Paisley, UK

3.2 Buffer and Solutions

Table 2. Western Blot buffers and solutions

10X TBS	31,5 g	Tris HCl
	80 g	NaCl
	1 l	A.D.
	pH 7,5	(with 10 M NaOH)
TBS-T	200 ml	10X TBS
	1800 ml	A.D.
	2000 µl	Tween 20
10X running buffer	30 g	Tris Base
	144 g	Glycine
	100 ml	SDS
	ad to 1l	A.D.
1X running buffer (ready to use) 4°C	100 ml	10X running buffer
	add to 1 l	A.D.
10X transfer buffer	56 g	Trizma Base
	286 g	Glycine
	ad to 2 l	A.D.
1X transfer buffer (ready to use) 4°C	200 ml	10X transfer buffer
	1400 ml	A.D.
	400 ml	MeOH
5% milk solution	5 g	milk powder
	100 ml	TBS-T
5X sample buffer	60 mM	Tris HCl pH 6,8
	2%	SDS
	10%	glycerol
	5%	β-mercaptoethanol
	0.01%	bromphenolblue

10% APS	1 g	APS
	10 ml	A.D.
resolving gel buffer (pH 8,8)	1,5 M	Tris
	0.40%	SDS
stacking gel buffer (pH 6,8)	0.5 M	Tris
	0,40%	SDS
5X sample buffer (Lämmli buffer)	60 mM	Tris HCL (pH 6,8)
	2%	SDS
	10%	glycerol
	5%	ß-mercaptoethanol
	0.01%	bromephenolblue

Table 3. Agarose gel components.

100 ml x % agarose Gel			
x g	agarose		
100 ml	1X TAE (Tris-Acetate-EDTA) buffer	40 nM	Tris Acetat
		1 nM	EDTA- Na2
		pH 8.5	
10 µl	PeqGreen		

50X TAE buffer is used as running buffer

3.3 Primer and gBLOCKs

Table 4. gBLOCKs for Gibson Assembly and Primers for sequencing. gBLOCK sequences can divided to the overhang to the psiCHECK 2 vector were the sequence is shown in small letters. Capital letters clarify the sequence of the 3´UTR of Gli2. Nucleotides in bold and underlined letters are the seed sequence, one as wildtype and one mutated.

	Name	**Sequence 5´ → 3`**
gBLOCKs	Gli2_WT	tggagcgcgtgctgaagaacgagcagtaattct aggcgatcgctcgagCACACACCCCAAA CCTTTTCATGGGGAATGTGTGGCAA CCT**<u>TGCCAAA</u>**CAGCACCACTCAGAG TGTGACTgcggccgctggccgcaataaaata tctttatt
	Gli2_mut2_compl2	tggagcgcgtgctgaagaacgagcagtaattct aggcgatcgctcgagCACACACCCCAAA CCTTTTCATGGGGAATGTGTGGCAA CCT**<u>CTAAGGG</u>**CAGCACCACTCAGA GTGTGACTgcggccgctggccgcaataaaa tatctttatt

gBLOCK Primer / sequencing primer	Primer FWD Gli2_mut_total	TGGAGCGCGTGCTGAAGAAC
	Primer_RV_Gli2_mut_total	AATAAAGATATTTTATTGCGGCCAGCGG

Table 5. Primes for the HH signaling pathway Panel for qPCR analysis

Primername	**Sequence 5´ → 3´**
h_IHH_f	AGG CCG GCT TTG ACT GGG TGT ATT
h_IHH_r	GCG GCC GAG TGC TCG GAC TT
h_SHH_f	CCG GCT TCG ACT GGG TGT ACT A
h_SHH_r	CGC CAC CGA GTT CTC TGC TTT
h_DHH_f	CCG GCT TCG ACT GGG TCT ACT AC
h_DHH_r	GAC CGC CAG TGA GTT ATC AGC TTT
h_HHAT_f	CCT GGA TGC TGG CCT ATG TCT T
h_HHAT_r	GCT CCT GCT GCT GCA TCT GTT
h_DISP1_f	ACT TCT CTG ATC CAT TGC TGG GTT
h_DISP1_r	GAC CAA TCT CTG GCC TAT TGC TGT
h_DISP2_f	TGT GCA GCA CCA TGT GGT CA
h_DISP2_r	AGC AAT CAG CTG GGA ATA GCT CTT
h_PTCH1_f	CCC CTG TAC GAA GTG GAC ACT CTC
h_PTCH1_r	AAG GAA GAT CAC CAC TAC CTT GGC T
h_PTCH2_f	GAT GGG GCC ATC TCC ACA TT
h_PTCH2_r	CGC CGC AAA GAA GTA CCT TAC A
h_SMO_f	GCT ACT TCC TCA TCC GAG GAG TCA
h_SMO_r	GGC GCA GCA TGG TCT CGT T
h_HHIP_f	GGG CGC CTG GAG AAT AAG ATA TTT
h_HHIP_r	GTGGAGAGCAAAGTGCACATTTGA
h_GAS1_f	CGT CAT TGA GGA CAT GCT GGC TAT
h_GAS1_r	TTC TCC TTG ACC GAC TCG CAG AT
h_RAB23_f	GAA AGT AGT AGC CGA AGT GGG AGA
h_RAB23_r	AGT GCC TCA GCT TCC TCA TTC TT
h_KIF7_f	GTC CCA GTG CGA GAT GAA CCT
h_KIF7_r	CGG AGC GTC ACC ACC TTG T
h_KIF27_f	AGC TTG CCT GAG TCC TGT TGA GAT TA
h_KIF27_r	GCT TCT CGC AAA TTC ACC ACC TTA
h_STK36_f	ACC CCA GAT TGT GAA CGA GCA T
h_STK36_r	CAT TGT CAC TGT CTG GCT CCT CAT
h_SUFU_f	GCT GCT GAC AGA GGA CCC ACA
h_SUFU_r	GTG CAG ACA CCA ACG ATC TGG A
h_BTRC_f	GTC TAC GGA CCC TTG TGG AGC AT
h_BTRC_r	GGG CAG CTG GAT CAT TTA GGA AGT
h_GLI1_f	CCA ACT CCA CAG GCA TAC AGG AT
h_GLI1_r	CAC AGA TTC AGG CTC ACG CTT C

h_GLI2_f	AAG TCA CTC AAG GAT TCC TGC TCA
h_GLI2_r	GTT TTC CAG GAT GGA GCC ACT T
h_GLI3_f	CGC GAC TGA ACC CCA TTC TAC
h_GLI3_r	GTG TTG TTG GAC TGT GTG CCA TT
h_GLI4_f	CCA TGG GCA TCA ACA TGG CT
h_GLI4_r	TCC TCT ACG TCT TGG AGA TCC AGG T
h_GLIS1_f	CCC AGC CCA CAA GGT TAC CA
h_GLIS1_r	CAT CCG GTA GCA GTC GCC ATA
h_GLIS2_f	GTG TCG CTG GGC CAA GTG TAA
h_GLIS2_r	CGG GCT TGA CAT GGT AAT CGT T
h_MTSS1_f	CTG CGG CCA GTG ATT GAA GAA
h_MTSS1_r	GGG CAG TTT GTG AGG GTC CAT
h_FOXE1_f	GCG CTG GGA GCC TGC TAC AA
h_FOXE1_r	TGG CGG ACA CGA ACC GAT CTA T
h_FOXA2_f	TGG GAG CGG TGA AGA TGG AA
h_FOXA2_r	GAG GAG TAG CCC TCG GGC TCT
h_FOXM1_f	GGG AGA CCT GTG CAG ATG GTG A
h_FOXM1_r	TCG AAG CCA CTG GAT GTT GGA T
h_SPP1_f	TCG CAG ACC TGA CAT CCA GTA CC
h_SPP1_r	CCA TTC AAC TCC TCG CTT TCC AT
h_OSF_f	GTC CTA ATT CCT GAT TCT GCC AAA
h_OSF_r	GGG CCA CAA GAT CCG TGA A
h_IGF2_f	CGA CCG TGC TTC CGG ACA AC
h_IGF2_r	AGG CGC TGG GTG GAC TGC TT
h_CCND2_f	GCT GTC TCT CTG ATC CGC AAG CAT
h_CCND2_r	GGC AAA CTT AAA GTC GGT GGC A
h_PTHR1_f	ACA ACA GGA CGT GGG CCA ACT AC
h_PTHR1_r	CGG TCA AAC ACC TCC CGT TCA
h_MKI67_f	ATT GAA CCT GCG GAA GAG CTG A
h_MKI67_r	GGA GCG CAG GGA TAT TCC CTT A
h_RPS3_f	AAC TGG TAA GAT TGG CCC TAA GAA G
h_RPS3_r	TGT TAT GCT GTG GGG ACT GG
h_IL6_f	AGA CAG CCA CTC ACC TCT TCA G
h_IL6_r	TTC TGC CAG TGC CTC TTT GCT G
h_MUC5AC_f	CCA CTG GTT CTA TGG CAA CAC C
h_MUC5AC_r	GCC GAA GTC CAG GCT GTG CG
h_CTNNB1_f	ATT GTC CAC GCT GGA TTT TC
h_CTNNB1_r	TCG AGG ACG GTC GGA CT
h_CDH1_f	ACA GCC CCG CCT TAT GAT T
h_CDH1_r	TCG GAA CCG CTT CCT TCA

Table 6. Primers for the SUFU sequencing

Primer Name	Sequence 5´ → 3´
h_SUFU-var1_f	ATCAAGCTTATGGCGGAGCTGCGGCCTA
h_SUFU-var1_r	AATGGATTCCTAGTGTAGCGGACTGTCGAACAC
h_SUFU-var2_r	AATGGATTCTCAGAGTTGTAACCAGGGTCCATGAG
SUFU_int 1	ATGCAGCCCGTGCAGAC
SUFU_int 2	GAGCCGCAAAGACAGCCTGG
T7 Primer	TAATACGACTCACTATAGGG
SP6 Primer	CATTTAGGTGACACTATAG

Table 7. miRNA primers for SUFU overexpression qPCR experiments

Name	Target sequence	Product number	sequence reference
hsa-miR-214-3p	UGCCUGUCUACACUUGCUGUGC	YP00204510	MIMAT0004564
hsa-miR-378a-5p	CUCCUGACUCCAGGUCCUGUGU	YP00304347	MIMAT0000731
hsa-miR-423-5p	UGAGGGGCAGAGAGCGAGACUUU	YP00205624	MIMAT0004748
hsa-miR-16-5p	UAGCAGCACGUAAAUAUUGGCG	YP00205702	MIMAT0000069
hsa-miR-92a-3p	UAUUGCACUUGUCCCGGCCUGU	YP00204258	MIMAT0000092
hsa-miR-93-5p	CAAAGUGCUGUUCGUGCAGGUAG	YP00204715	MIMAT0000093

3.4 Cell culture

For this work mainly one cell line, the cisplatin resistant H460 (H460-CisR) was used. To determine the most appropriate cell line for this study, initial screenings were performed in parallel with parental and cisplatin resistant H460 (H460-Par / H460-CisR) and the parental and cisplatin resistant A549 cell lines (A549-Par / A549-CisR). The human embryonic kidney cell line (HEK293) was also used to end the previous research project. This previous project was also the aim to carry out this project.

The HEK293 cell line was provided by ZMF Core Facility-Cell culture. The Human H460-Par and H460-CisR adenocarcinoma cell lines, as well as the A549-Par and A549-CisR adenocarcinoma cell lines, where obtained from Dr. Martin Barr (Thoracic Oncology, Institute of Molecular Medicine, Trinity Centre for Health Sciences St. James's Hospital & Trinity College Dublin, Ireland) (71).

3.4.1 Cell cultivation

Cells were passaged twice a week in order to keep them in monolayer culture. Additionally, every second day the media was removed and fresh one was added to ensure good growth and nutrient supply. The cisplatin resistant cell lines were treated with cisplatin every 2 months to maintain the resistance property. The maintenance concentration for H460-CisR was 6.6 µM cisplatin and 11.62 µM for A549-CisR. For passaging, complete RPMI for the H460 cell lines and complete DMEM-F12 for the A549 and HEK293 cell lines, as well as trypsin and DPBS were used. All solutions were pre-heated to 37°C in a water bath. Additives for the culture media are listed in Table 8.

Table 8. Cell line specific media and their preparation

Cell line	media	complete media (500 ml)	starvation media (50 ml)
H460	RPMI	440 ml RPMI	49.5 ml RPMI
	10% fetal bovine serum (FBS)	50 ml heat inactivated FBS	
	1% penicilin/ streptomycin (P/S)	5 ml P/S	0.5 ml P/S
	1% L-Glutamin (L-Gln)	5 ml L-Gln	
A549/ HEK293	DMEM-F12	440 ml DMEM- F12	
	10% fetal bovine serum (FBS)	50 ml heat inactivated FBS	
	1% penicilin/ streptomycin (P/S)	5 ml P/S	
	1% L-Glutamin (L-Gln)	5 ml L-Gln	

When using 75 cm² cell culture flask first step for passaging the cells was to remove the old media, wash the cells once with 5 ml PBS and then incubate with 2 ml trypsin-EDTA for 5 min at 37°C. HEK293 cells are not that adherent, so they just needed 1 min at 37°C. After incubation time, 5 ml of the cell line specific complete culture media was added to stop the trypsin reaction. After collecting the suspension in a fresh 15 ml tube, it was centrifugated 5 min at 400 x g. The supernatant was removed and the

pellet was resuspended in a small volume of complete media. Meanwhile in a new 75 cm² cell culture flask, 10 ml of complete medium was aliquoted, and a small amount of cell suspension was added.

For the HEK293, it was necessary to coat the cell culture flask with collagen type I for 30 min at room temperature, to ensure cell adherence.

3.4.2 Starvation and non-starvation conditions

Some cell lines show a low transfection rate, which can be improved by using so-called starvation media (see Table 8). One day after culturing the cells, the complete media was removed, cells were washed twice with pre-heated DPBS and then incubated 4 h with pre-heated starvation media. After 4 h cells were transfected and complete media was added. Starvation method was used only in the initial phase of the study (RT-qPCR and Western Blot analysis), cells suffered to much under starvation conditions for phenotypical investigation studies.

3.4.3 Cell counting and plate out

In chapter 3.4.1 the passaging of cells was described. For cell culture experiments it is necessary to work with a defined number of cells, therefore, cell counting is essential. Until the centrifugation step, the handling was identical to the passaging, but after removing the supernatant, resuspension of the pellet with 10 ml of the provided media was necessary. By taking a 50 µl aliquot and mixing it with 10 ml Casytone, a 1:200 dilution was generated. Cell number measurement was done by using the CASY® cell counter (Innovatis, Reutlingen, Germany) and the output included the total cell number, living cell number, viability rate and aggregation factor. The aggregation factor shouldn´t be higher than 2 for a reliable result. For culturing the cells, only the number of living cells was taken into account and the viability rate was over 90% to ensure that the cells were doing well. The total cell number was experiment-dependent, as indicated in Table 9.

Table 9. Number of cells plated out according to cell line, experimenal design and associated end volume.

	Cell line	Cell number	Plate	Media/ well
RNA harvest	H460-Par/ CisR	150.000	12-well	1 ml
RNA harvest	A549-Par/ CisR	60.000	12-well	1 ml
Protein harvest	H460-CisR	300.000	6-well	2 ml
Colony forming assay	H460-CisR	50.000 / 500	12-well / 6-well	1 ml / 2 ml
Scratch assay	H460-CisR	150.000	12-well	1 ml
Alamar assay	H460-CisR	5.000	96-well	0.1 ml
Immunofluorescence	H460-CisR	10.000	8-chamber slide	0.5 ml
Luciferase assay	HEK 293	30.000	48-well	0.2 ml

3.4.4 Transfection methods and protocols

There are various possibilities to get nucleic acid in cells. Physical methods such as electroporation or microinjection are one possibility, however, these are somewhat crude methods. The other possibility is the transfection with chemical reagents which are more gentle (72,73).

By using jetPRIME transfection reagent (Polyplus chemicals), the more gentle method of transfection was chosen for this study.

The chemical method is essentially based on 3 steps. The complexation, were the negatively charged nucleic acid forms a complex with the cationic transfection reagent. The formation of the now positively charged complex can be absorbed by the cell through endocytosis. Last step the nucleic acid is released from the endocytotic vesicles and can perform its function in the cytoplasm or after entering the nucleus, which is necessary in the case of plasmid transfection (73).

In this study only plasmid transfections were performed, with different approaches. By performing the standard transfection method, the cells were seeded and grown until a confluency of 60% - 80%. At day 2 the transfection was done. DNA and jetPRIME buffer were mixed according to the manufactures protocol at a certain ratio followed by 10 s vortexing and spinning down. The second step was adding the jetPRIME reagent, followed by vortexing for 10 s and spinning down before the transfection mix was incubated for 10 min at RT. This is necessary for the formation of the positively charged complex. After this procedure the transfection mix was added dropwise to the cells. Important to note is that the mix is applied well distributed, as it can lead to local toxic effects if it is supplied only in one place. Twenty-four h after transfection the medium was changed again.

Performing the reverse transfection method, the transfection step and the seeding step were proceeded simultaneously. First, the transfection mix was prepared the same way as described above. Then the mix was added to the empty wells before adding the cell suspension.

The third application used was co-transfection. This can be done in both ways, normal and reverse. The only difference is that not only one plasmid but several plasmids are used simultaneously. It should be noted that the final amount of DNA to be introduced is not exaggerated in order to avoid toxicity. For every plate format a different amount of buffer, reagent, cells and media was used, as listed in Table 10.

Table 10. Transfection protocol for different experimental designs. Information given below relates to 1 well or 1 chamber.

Plate	Media	Cells	Buffer	Reagent	Plasmid DNA
6-well	1.8 ml	300.000 (H460-CisR)	200 µl	4 µl	x µg/ml
12-well	0.9 ml	150.000 (H460-CisR)	100 µl	2 µl	x µg/ml
8-chamber slide	180 µl	10.000 (H460-CisR)	20 µl	0.4 µl	x µg/ml
48-well	180 µl	30.000 (HEK293)	20 µl	0.4 µl	x µg/ml
96 well	90 µl	5.000 (H460CisR)	10 µl	0.2 µl	x µg/ml

3.5 RNA analysis

3.5.1 RNA harvesting

The first step of RNA isolation was cell harvesting. The medium in the 12- well plates was first thoroughly aspirated and cells were washed with 1 ml of warm DPBS. After removing DPBS, 350 µl RNA Lysis Buffer T was added to the cells. RNA Lysis Buffer T is part of the peqGOLD Total-RNA Kit (74). The lysate was collected by circular movement using a pipette tip and transferred to a 1.5 ml reaction tube. Sample were immediately processed or frozen at -20°C until further use. This is especially useful if samples after different time points upon transfection are used for RNA isolation. In this study, 24 h, 48 h and 72 h post transfection where chosen. For 48 h and 72 h treatment the medium was renewed 24 h after transfection.

3.5.1.1 mRNA and miRNA isolation and measurement

When working with RNA it is important that the workplace is cleaned thoroughly to prevent any contamination. An RNase Zap ™ RNase Decontamination Solution was used (75). Surfaces and all utensils needed for isolation were cleaned with this solution.

The entire cell lysate was transferred to a DNA removing column and centrifuged for 1 min at 12.000 x g. The flow-through was mixed with the same volume of 70% EtOH. The RNA was isolated according to the producer´s protocol (74). Optimization steps were involved in the washing step. On the one hand the DNase I digestion was done, to ensuring a higher quality of RNA and removal of co-isolated gDNA, which can influence further steps. On the other hand, the washing step with RNA Wash Buffer II was done twice. For miRNA isolation, 100% isopropanol instead of 70% EtOH was used. The remaining steps were the same as for mRNA isolation (74).

The Thermo Scientific™ NanoDrop™ 2000 UV-Vis Spectrophotometer was used to determine the amount, as well as the quality and purity of isolated RNA (76). The blank was measured with the same water that was used for RNA elution. 260 / 280 ratio of approximately 2 and 260 / 230 ratio of approximately 1.8 – 2.2 indicate pure RNA (77).

3.5.2 cDNA Synthesis

3.5.2.1 mRNA

Quanta Biosciences´ qScript cDNA Synthesis Kit was used to reversely transcribe mRNA to cDNA. Provided that the amount of isolated RNA was sufficient, 1000 ng of the isolated RNA were used for synthesis. Four µl qScript reaction mix and 1 µl reverse transcriptase were used per sample. A mastermix was created to minimize pipetting failure. The mastermix was prepared for the number of samples needed for reverse transcription, plus a surplus and a non- template control (NTC). The NTC is a control sample, containing only mastermix and water. A second control sample was the so-called RT (-) control, where the reverse transcriptase was replaced by 1 µl of water. Each cDNA synthesis reaction was performed in a total volume of 20 µl.

The temperature profile for cDNA synthesis can be found in Table 11. Thermocyclers used the synthesis were the “MyCycler thermocycler” and the “C100Touch™ Thermal Cycler with 96- well FastReaction Module” from Biorad.

Table 11. Temperature profile for cDNA synthesis after mRNA isolation.

temperature profile	22°C	5 min
	42°C	30 min
	85°C	5 min
	4°C	∞

3.5.2.2 miRNA-based cDNA synthesis

The miCURY LNA™ Universal RT microRNA PCR Kit was used for miRNA-based cDNA synthesis. The miRNA samples were first diluted to 5 ng/µl. Then a mastermix was created, containing 2 µl of 5X reaction buffer, 1 µl enzyme mix and 5 µl H_2O per each sample. When creating the mastermix, a volume for NTC and an excess volume was included. After aliquoting the mastermix, 2 µl of the diluted miRNA sample was added. A RT(-) control sample was also done. The total volume per sample was 10 µl. Incubation was done by using the “C100Touch™ Thermal Cycler with 96-well FastReaction Module” with the temperature profile listed in Table 12.

Table 12. Temperature profile for cDNA synthesis after miRNA isolation.

temperature profile	42°C	60 min
	95°C	5 min
	4°C	∞

3.5.3 RT-qPCR

The RT-qPCR is an excellent and highly sensitive method to determine which genes are expressed in particular cells and to determine changes in the expression pattern upon transfection experiments.

3.5.3.1 RT-qPCR for mRNA expression level

For determining mRNA levels, the Blue S'Green qPCR mix, a clear 384 well plate and the LightCycler 480 from Roche was used.

Primers listed in Table 5 were used for screening the mRNA expression levels of Hedgehog signaling pathway (HH) genes in different cell lines and to examine the expression level of targeted genes after SUFU overexpression. The primers, which have already been dissolved to a stock concentration of 100 pmol/µl, were diluted 1:10 and the respective primer pairs (forward and reverse) were mixed. After cDNA synthesis, an amount of 50 ng/µl was obtained. This was followed by a 1:8 dilution based on experiences of the research group. This dilution varies among cell lines, 1:8 was the optimal dilution for H460 cell line, for A549 a 1:4 dilution was more adequate. In Table 13 the reaction mix composition as well as the temperature profile for the RT-qPCR are listed.

In these experiments, duplicates were always applied in order to achieve a higher precision in the subsequent data analysis.

Table 13. Used reaction mix and temperature profile for the qPCR to detect mRNA expression level.

reaction mix per primer pair	5 µl	Blue S'Green qPCR mix	
	1 µl	Primer Mix (1:10)	
	4 µl	diluted cDNA	
	Total 10 µl --> --> 4 µl total mix per well (4 µl duplicate in next well)		
temperatur profile	1X	95°C	2 min
	40X	95°C	5 sec
		60°C	30 sec
additional parameters	Ramp rate: 4.8°C/s (95°C) and 2.5°C/s (65°C) optical read melting curve analyses SYBR Green/HRMDye format		

3.5.3.2 RT-qPCR for miRNA expression level

For detecting miRNA expression level, the miRCURY LNA™ Universal RT microRNA PCR kit was used. For this type of RT-qPCR the cDNA has to be diluted 1:80, as recommended by producer. Primers used for this test are listed in Table 7. The device used was the LightCycler 480 from Roche, and white 384-well plates were needed. Reaction mix and temperature profile can be seen in Table 14.

Table 14. Reaction mix and temperature profile for the RT-qPCR used to detect miRNA expression level.

reaction mix per primer	5 µl	PCR Mastermix	
	1 µl	Primer	
	4 µl	cDNA template (1:80)	
	Total--> 10 µl/well		
temperatur profile	1X	95°C	10 min
	45X	95°C	10 sec
		60°C	1 min
additional parameters	Ramp-rate: 4.8°C/s (95°C) and 2.5°C/s (60°C), optical read melting curve analyses SYBR Green/HRMDye Format		

3.5.3.3 Analysis of the RT-qPCR data

Cycle threshold (Ct)-value and melting temperature (Tm) are required for correct data interpretation. The LightCycler Calculation Software calculated these values from the row data of the instrument. The Ct-value was calculated by selecting the 2nd derivate method. As soon as the fluorescent signal exceeds a certain threshold, this is documented and reflects the number of used cycles. A Ct-value of 37 was set as maximum, everything above was defined as negative. The Tm values, as well as the melting curves, confirm the technical quality of the experiment. Since the experiments were performed in duplicates, the mean value and the standard deviation of Ct-value and of Tm were calculated. If the standard deviation was 1 or higher, the entire sample was excluded from the analysis. Further calculations were done with the mean values.

By using the ΔΔCt method, the expression profile was analysed. A housekeeping gene was included in every run. In this study, the housekeeping gene for mRNA analysis was ß2-microglobulin (ß2MG) and for miRNA analysis that was hsa-miR-16-5p. This is particularly important in order to normalize the data for comparison between different samples/ treatments. The Ct-value of the housekeeping gene minus the Ct-value of the gene of interest results in the ΔCt value. ΔCt from the treated samples minus the ΔCt of untreated samples, gives the ΔΔCt-value. Untreated samples were transfected with empty plasmid (pcDNA3.1(+)). The differences in expression were quantified and interpreted.

3.6 DNA analysis

In order to transfect the cells, recombinant plasmids were generated by using various cloning methods.

3.6.1 Cloning

3.6.1.1 *In silico* cloning, restriction cloning and ligation for preparing the SUFU plasmid

In order to generate a SUFU plasmid, the SUFU sequence had to be obtained first. With the help of the NCBI database, the SUFU sequence with the accession number NM_016169.3 was used (78). This reflects the SUFU variant I, the standard variant. Also the sequence of the shorter SUFU variant II, because of alternative splicing, with the accession number NM_001178133.1 was used (79). The sequences were loaded into the SnapGene cloning program and specific primers, which are listed in Table 6, were designed.

In silico cloning was done using SnapGene software. pcDNA3.1(+) (Figure 30) was selected as the cloning and transfection vector. Unique restriction sites can be listed by selecting single cutters in SnapGene. These were checked for their absence in the SUFU sequence. The decision was made for BamHI and HindIII restriction enzymes. These two restriction sites were considered in the primer design in order to achieve a targeted cloning. The entire cloning was virtually tested using SnapGene (Figure 7).

To start the practical work, the SUFU sequence was amplified. A RT-qPCR screening showed that A549-Par cells had the highest SUFU level among the cell lines which were tested. Thus, cDNA from A549-Par was used for a PCR amplification with corresponding primers. The device used was the thermocycler peqSTAR (VWR, peqLab). The associated reaction mix and the temperature profile can be found in Table 15.

*Table 15. Reaction mix and temperature profile for the SUFU amplification. * second approach with h_SUFU-var2_r to generate the shorter SUFU variant SUFU Var II.*

reaction mix	12.5 µl	Q5® High-Fidelity 2X Master Mix (New England Biolabs)		
	1.25 µl	h_SUFU-var1_f		
	1.25 µl	h_SUFU-var1_r*		
	3.5 µl	cDNA (50ng/µl)		
	6.5 µl	H_2O		
temperature profile	denaturation	98°C	30 s	
	denaturation	98°C	10 s	33X
	annealing	70°C	20 s	
	elongation	72°C	50 s	
	final elongation	72°C	2 min	
	hold	4°C	∞	

A 1% agarose gel (Table 3) was made to analyse the specific PCR product. The samples were mixed with the 6X Loading Dye and loaded onto the gel. Five µl of FastRuler High Range DNA Ladder was used as standard. Settings for electrophoresis were 100 V for 40 min. Bands were cut out from the gel, cleaned with the Monarch DNA Gel Extraction Kit and then measured on the Nanodrop.

The amplified and already sequenced insert (SUFU) and the cloning vector (pcDNA3.1(+)) undergo a restriction cut (Table 16). Since the restriction enzymes were from NewEngland Biolabs the right buffer was determined using an online tool (NEBcloner) (80). The restriction was performed for at least 1 h at 37°C and was then inactivated for 5 min at 80°C.

Table 16. Restriction approach for insert and vector.

x µl	DNA (1000 ng)
2 µl	2.1 Buffer (10X)
0.5 µl	BamHI
0.5 µl	HindIII
x µl	H_2O
20 µl	Total

Ligation was done with the T4 DNA Ligase and the associated T4 DNA Ligase Buffer (10X) from New England Biolabs. For a total volume of 20 µl, 1 µl of the enzyme and 2 µl of the buffer (10X) were used. The insert and the vector volume were calculated according the formula below. The molar ratio was generally assumed to be 3:1 for insert : vector. The rest of the ligation mix was filled with water up to 20 µl and incubated for 30 min at RT before termination for 10 min at 65°C.

$$\frac{bp\ insert}{bp\ vector} \times \frac{3}{1} \times ng\ vector = ng\ insert$$

E. coli DH5α competent cells from New England BioLabs were used for transformation. Thirty µl aliquots of the competent cells were thawed on ice. Two µl of the ligation mix were added. After incubation for 30 min on ice, a heat shock for 40 s at 42°C was performed. Followed by a 2 min incubation on ice, 900 µl SOC medium were added and mixed gently. Next to 1 h incubation at 37°C, 100 µl of the transformation mix were plated out on LB-Amp agar plates. Producing 500 ml of LB agar, 500 µl of ampicillin (100 mg/µl) were added after autoclaving and cooling.

The rest of the transformation mix was centrifuged 5 min at 5000 x g, the supernatant was discarded, the pellet was resuspended in 100 µl SOC media and plated as well. Twenty-four h after incubation at 37°C, single colonies were chosen for sequencing. If sequences were correct, a Maxiprep was performed to ensure a high amount of plasmid for further approaches.

3.6.1.2 *In silico* cloning and Gibson assembly – Preparation of the Gli2 plasmids

Earlier studies in the group showed that there is an interaction between Gli2 and miR-182-5p. For that the miR-182-5p sequence had already been successfully cloned into the pcDNA3.1(+) vector as well as the 3´UTR of Gli2 (Gli2 wild type- WT) was also

already cloned successfully into the psiCHECK-2 vector. Plasmid maps are listed in the supplementary (Figure 32, Figure 33 and Figure 34). However, to prove whether Gli2 is a direct target of miR-182-5p a luciferase assay with the wild type and a mutant version of the 3`UTR seed sequence of Gli2 must be performed.

An overhang, which is identical to the psiCHECK-2 vector, was attached to the 3´UTR sequence of Gli2. To get a mutant version of Gli2, the 3`UTR containing the miRNA seed sequence was mutated at multiple sites. These steps were first *performed in-silico* by using SnapGene. The created sequences (Table 4) were ordered as gBLOCK from Integrated DNA Technologies, IDT (Iowa, USA).

These overhangs are necessary for Gibson assembly. After the gBLOCKs arrived, they were dissolved in water according to the manufacturer´s instruction. The assembly was performed by using NEBuilder® HiFi DNA Assembly form New England BioLabs. A 2:1 ratio of insert : vector, regarding the total amount in ng, was used for this approach. The vector was already cut previously. The total volume of 20 µl consists of 10 µl NEBuilder HiFi DNA Assembly mix, the calculated amount of vector and insert and water. This mix was incubated 15 min at 50°C. Transformation was performed as described above.

3.6.2 DNA isolation methods and sequencing

Five ml of LB- Medium (+ 100 mg/µl Ampicillin) were inoculated by single colonies. After incubation over night at 37°C, 500 µl for a glycerol stock were put aside and DNA was isolated from the rest. The PeqGOLD® Plasmid Miniprep Kit II was used according to manufacturer´s protocol. In order to analyze the miniprep DNA, a restriction analysis was performed, this indicating whether the insert was present or not. Sequencing was done for a precise control. Miniprep samples and primers were therefore sent to a sequencing company (Eurofins Genomics). Sequencing results were checked by alignment to the original sequence by using SnapGene.

If the sequences matched, the 500 µl for the glycerol stock were mixed with 500 µl 50% glycerol and stored at -80°C.

In order to obtain plasmids that can be used in cell culture, maxiprep DNA isolation was performed. This is important to remove bacterial endotoxins and also to get a sufficient amount of plasmid DNA. Five ml LB/ Amp medium was inoculated from the glycerol stock. After an incubation phase of 6 h at 37°C, the total amount was transferred to a cultivation bottle, filled with 200 ml LB Amp. After overnight incubation, the maxiprep was done according to the protocol of Endo – Free Plasmid DNA Maxi Kit E.Z.N.A®. Finally, the concentration was measured on Nanodrop.

3.7 Protein analysis

In order to verify data from experiments on RNA level, analysis at protein level were performed.

3.7.1 Protein harvesting and isolation

For working with proteins, it is crucial to keep the samples on ice and use cooled reagents to avoid denaturation. After removing the medium from previously transfected cells, described in chapter 3.4.3 and chapter 3.4.4, cells were washed with cold DBPS. This was removed again and 100 µl of RIPA buffer were added. The RIPA Buffer is a lysis buffer appropriate for extraction of proteins. It causes cell lysis and promotes solubility of the proteins (81). By using a cell scraper, the buffer was immediately distributed and the cells were scraped off and transferred into a 1.5 ml reaction tube. The collected samples were next sonicated to improve cell lysis. An ultrasound processor (Ultraschall-Desintegrator UP50H ROTH, Carl Roth GMbH+Co.KG Karlsruhe, Germany) was used for this approach. With the settings of cycle 1 and amplitude 80%, each sample was sonicated twice for 5 s. All this was done on ice. Using a pre-cooled centrifuge, the homogenate was centrifuged for 10 min at 4°C and 13000 rpm. The supernatant was transferred into a new reaction tube. The pellet containing insoluble components was discarded, the supernatant consists of soluble protein.

3.7.2 BCA

To determine the total protein content, a BCA (Bicinchoninic acid assay) was performed. This is a colorimetric detection method based on the reduction of Cu^{2+} to Cu^{+}, which is mainly performed by peptide bonds. After adding the reagent solution, a colour change is observed which can be measured photometrically at 562 nm.

This assay was done by using a 96-well plate. The first two columns were used for the standard series. Twenty-five µl of RIPA buffer were placed in these wells, then 25 µl of a 2 mg/ml BSA solution were added (starting concentration of 2 µg/µl), which results in a 1:1 dilution and a concentration of 1 mg/ml. After thorough mixing, 25 µl were removed from this well and pipetted into the next one. This continued until the penultimate well. After mixing, 25 µl were discarded from the penultimate well. The last well served as blank and contains only RIPA buffer. The previous isolated samples were applied to the rest of the plate as duplicates in a 1:5 dilution (20 µl RIPA buffer + 5 µl sample). Final step was the addition of 200 µl reagent solution in each well. This consisted of BCA-solution and cooper sulphate in a 1:50 ratio. After 30 min incubation at 37°C, the measurement was done by using the SpectramaxPlus 384 (Molecular Devices, Orleans Drive Sunnyvale, CA) or the CLARIOstar microplate reader (BMG LABTECH GmbH, Ortenberg, Germany). The absolute concentration was recalculated due to the 1:5 dilution.

3.7.3 SDS Page

The BCA Assay described above was performed in order to use the same amount of total protein in the subsequent SDS PAGE. This is important for a better comparison and a precise interpretation of differences in protein level for further analysis.

This electrophoresis separates the proteins based on their molecular weight. The used gel consists of a stacking gel and a resolving gel. The task of the stacking gel is to collect and concentrate the protein samples which then can be separated in the resolving gel based on their molecular size. The stacking gel always has the same concentration and is freshly prepared. The concentration of the resolving gel varies

depending on the size of the target protein and can be prepared a few days before the electrophoresis is done. The components and associated volumes for the composition of the specific gels can be found in Table 17. The compilation of the individual buffers and solutions are listed in Table 2.

Table 17. Amounts of reagents to be used for the corresponding concentration for gel preparation.

Resolving gel		6%	8%	10%	12%	15%
Millipore water	[ml]	10.4	9.2	9.75	6.4	4.4
Acrylamid stock 30%	[ml]	4	5.2	6.65	8	10
Resolving gel buffer	[ml]	5.2	5.2	5	5.2	5.3
SDS (10%)	[µl]	200	200	200	200	200
APS (10%)	[µl]	200	200	200	200	200
Temed	[µl]	16	16	16	16	16

Stacking gel		Always 4,5%
Millipore water	[ml]	4.1
Acrylamid stock 30%	[ml]	0.75
Stacking gel buffer	[ml]	1
SDS (10%)	[µl]	60
APS (10%)	[µl]	60
Temed	[µl]	6
Bromphenolblue	[µl]	10

Protein samples were prepared in a way that the same amount of protein was used in each experiment. Then 5X Lämmli Buffer was added, e.g. for a total volume of 30 µl 6 µl Lämmli buffer were used. The rest was supplemented with RIPA buffer to the final volume. After spinning down the samples, they were heated 10 min at 95°C and spinned down again.

While the samples were prepared, the gel was mounted in the provided holder and placed into the electrophoresis chamber. A running buffer was used to check that the assembly was completely sealed. If this was the case, the sample application was started. A suitable protein marker was applied. The electrophoresis was done at 180 V until the colour front reached the lower limit of the gel.

3.7.4 Western Blot

Next step was the transfer of the separated proteins from the gel to a nitrocellulose membrane in order to be able to analyse them. When assembling the so-called sandwich transfer, make sure that all components, e.g. sponges, filter paper and the cut to size membrane, are soaked with transfer buffer. When building up the sandwich, a specific order of assembly is necessary, as well as removal of air bubbles, otherwise the transfer is impaired. After inserting the blotting chamber, ice-cold transfer buffer was added. It is also advisable to perform the entire experiment on ice. The transfer was done by 400 mA for about 2 h (transfer time is directly proportional to the molecular size of target proteins).

To check whether the transfer worked, the membrane was stained with Ponceau-S-red. This makes all protein bands visible. Destaining was done by using H_2O.

Antibodies were used to examine the desired protein bands. In order to prevent non-specific antibody binding, membrane blocking for 1 h with a 5% skim-milk solution, made from 5 g skim-milk powder and 100 ml TBST, was done. For that, about 30 ml 5% M-TBST is needed per membrane. The dilution of the antibody was done using 1% M-TBST according to experience or manufacturer´s instructions. The membrane was transferred to a 50 ml sample tube, then covered with 5 ml of the antibody solution and incubated overnight in a cold room on a rotator. The next day, the antibody solution was collected, frozen and reused for another run. The membrane was washed 3x with TBST for 10 min. Then the secondary antibody, again in a proper dilution, was applied to the membrane for 1 h at RT. The secondary antibody solution was then discarded and the membrane was washed 3x for 15 min with TBST. The secondary antibody was linked to horse-radish peroxidase (HRP) and by using Western Blot Detection Kits from Amersham ECL Prime Western Blotting Detection Reagent (GE Healthcare Bio-Sciences, Pittsburgh, USA) and SuperSignal® West Pico Chemiluminescent Substrate from Thermo Fisher Science (Fremont, USA) the specific signal was detected after a 5 min incubation in the dark. Detection was done by the ChemiDoc ™ Touch Imaging System (BioRad Industries, Hercules, USA). Used antibodies, associated dilutions and detection kits are listed in Table 18.

Table 18. Primary and secondary antibody dilution from different companies and specific detection kits for Western Blot experiments.

1st AB	Host	Dilution	Cat. Nr	Company	2nd AB	Detection kit
SUFU	mouse	1:1000	sc-137014	Santa Cruz Biotechnology, Inc., Dallas, USA	1:2000	West Pico
Gli1	mouse	1:1000	sc-515751	Santa Cruz Biotechnology, Inc., Dallas, USA	1:2000	ECL Prime
Gli1	rabbit	1:1000	PA5-23411	Thermo Fisher Scientific, Fremont, USA	1:2000	ECL Prime
Gli1	rabbit	1:500	ab49314	Abcam, Cambridge, UK	1:2000	ECL Prime
Gli2	mouse	1:1000	sc-271786	Santa Cruz Biotechnology, Inc., Dallas, USA	1:2000	ECL Prime
Gli2	rabbit	1:500	NB600-874	Novus Biologicals, Colorado, USA	1:2000	ECL Prime
Gli3	mouse	1:1000	sc-74478	Santa Cruz Biotechnology, Inc., Dallas, USA	1:2000	ECL Prime
Gli3	rabbit	1:1000	PA5-28029	Thermo Fisher Scientific, Fremont, USA	1:2000	ECL Prime
ß- Actin	mouse	1:5000	sc-47778	Santa Cruz Biotechnology, Inc., Dallas, USA	1:5000	West Pico
Vinculin	mouse	1:1000	sc-25336	Santa Cruz Biotechnology, Inc., Dallas, USA	1:2000	West Pico

To analyse housekeeping proteins or additional proteins, the membrane can be stripped using restore PLUS Western Blot stripping buffer (Thermo Fisher Scientific, Fremont, USA). This will remove the bound antibodies and proteins from blocking solutions. For this, the membrane was washed twice with TBST and then incubated for 10 min with the stripping buffer, then washed 2x 5 min with PBS. The membrane was then incubated with 5% skim-milk solution before another primary antibody was applied.

3.7.5 Immunofluorescence

To visualize differences between cells treated with specific DNA or control, as well as to draw conclusions about the localisation of the proteins or protein interactions, immunofluorescence was used.

For this, the cells in the 8-chamber slide were washed 2x with DPBS to remove the medium and then carefully fixed with 4% formaldehyde for 10 minutes. After washing twice for 5 min with DPBS, it was incubated with 0.5% Triton X100 for 5 min. This makes the cells and the cell nuclei more accessible to the antibodies. After washing 3 times, the actual staining took place. For this purpose, 10 µl of the primary antibody with the required dilution were used per well. Incubation was performed for 1 h at RT in the dark. Since a relatively small volume was used, the wells were covered with parafilm so that the antibody solution actually covered the entire well. Then it was washed 3x 5 min in a staining container with PBS. In the case of double staining, another primary antibody was applied with the same parameters. The used secondary antibodies were marked with a fluorophore. From here on it was important to work in the dark as far as possible. In the case of double staining, the application was also carried out one after the other. In Table 19 the used primary and secondary antibodies are listed. Last step was to cover up the slide with mounting medium with DAPI and sealing with nail polish. By using DAPI the cell nuclei were stained. Microscopy was done on the Nikon A1R+ confocal microscope.

Table 19: Primary and secondary antibody dilutions for immunofluorescence experiments.

1st antibody	**dilution**	**host**	**2nd antibody**	**dilution**
SUFU (Santa Cruz)	1:200	mouse	donkey anti mouse (H+L) Alexa Fluor 555 (Invitrogen)	1:400
Gli1 (Thermo Fisher)	1:100	rabbit	donkey anti rabbit (H+L) Alexa Fluor 488 (Invitrogen)	1:400
Gli1 (Abcam)	1:100	rabbit	donkey anti rabbit (H+L) Alexa Fluor 488 (Invitrogen)	1:400
Gli2 (Novus)	1:100	rabbit	donkey anti rabbit (H+L) Alexa Fluor 488 (Invitrogen)	1:400

3.8 Phenotypical assays

3.8.1 Colony Forming Assay

Tumorigenic ability of transfected and treated cells was determined by performing a Colony Forming Assay. 50.000 cells were first plated and transfected in one well of a 12-well plate. After 2 days, these cells were harvested, the cell number was determined and then 5.000 cells per well were plated in a 6-well plate. Cisplatin treatment was performed one day later. The cisplatin treatment was done for 3 days before switching back to pure medium. In total, the cells were left in the 6-well plates for 10 days, regardless of whether they are treated with cisplatin or not. On the 10^{th} day the cells were fixed with MetOH : glacial acetic acid (3 : 1 ratio). Fixation took place at RT for 10 min. Before staining, it must be ensured that residues of the fixation solution have evaporated. Staining was carried out with 0.4% crystal violet solution for 10 minutes at RT. Then it was washed with water until there was no more decoloration. The number of colonies was counted manually. The size of the colonies and thus the occupied area by the colonies in one well were evaluated using a plugin (colony area) from ImageJ.

3.8.2 AlamarBlue Assay

To determine viability and metabolic rate of transfected cells and cells treated with cisplatin an AlamarBlue® assay was performed. Measurements were carried out 24 h, 48 h and 72 h after transfection or cisplatin treatment. The assay was done in black 96-well plates in a total volume of 100 µl/well. To start the assay, 10 µl AlamarBlue reagent was added into a well and then incubated for 2 h at 37°C. The principle of this assay is the metabolism of resazurin. Living and metabolically active cells reduce resazurin to resorufin. Fluorescence can then be measured at 520 nm and emission at 590 nm (82). The CLARIOstar Plus (BMG LABTECH GmbH, Ortenberg, Germany) was used for the measurement.

3.8.3 Scratch Assay

To determine the mobility and the ability for invasion a scratch assay was performed. 150.000 cells were plated and transfected in a well of a 12 well plate. Two days later, after a monolayer of cells had formed, a continuous scratch was done with a pipette tip (100 µl pipette tip). Then it was washed in order to remove all floating cells and then medium was added again. From this time point, light microscopy images were recorded after a defined time and these were then compared and analysed using the ImageJ plug-in: MRI wound healing. Evaluation provides information about cell proliferation and mobility after transfection.

3.9 Interaction assays

3.9.1 Luciferase assay

A luciferase assay was used to analyse whether a miRNA actually interacts with its target gene sequence. From previous cloning (see 2.6.1.2), plasmids for Gli2-WT and Gli2-mut2, as well as a miR-182-5p plasmid were used for a co-transfection.

To carry out this assay, a 48-well plate was first coated with collagen type I for 30 minutes. This was important because the HEK293 cells used for this experiment due to their good transfection efficiency can otherwise not adhere. 30.000 HEK293 cells were seeded per well and co-transfected the next day. Co-transfection were performed with psiCHECK-2/Gli2-WT and pcDNA3.1(+)/miR-182-5p or with psiCHECK-2/Gli2-mut2 and pcDNA3.1(+)/miR-182-5p. Two days after transfection, the medium was removed thoroughly and cells were washed with DPBS. The PBL lysis buffer provided with the used Dual-Luciferase® Reporter Assay System (DLR™ Assay System; Promega) was diluted according to the manufacturer's instructions and then 30 µl were applied to the cells. In order to obtain better lysis, cells were shaken for 20 min at RT at 550 rpm and the plate was then transferred to -80°C. The lysed cells were scraped off very thoroughly and 20 µl were transferred to a white 96-well plate. The final measurement was a chemiluminescence-based. This was done with the CLARIOstar Plus (BMG LABTECH GmbH, Ortenberg, Germany). Two solutions that were also

included in the DLR™ Assay System were prepared and placed in the device like the plate to be measured. After setting the reagents on the CLARIOstar, the solutions were pipetted into the wells and the reactions was measured. The principle behind this measurement method is that two luciferase activities and luminescence levels are measured. The first signal comes from Firefly, which is measured at 600 nm and is used for normalization. The second luciferase activity originates from Renilla after adding the second reagent. The luminescence can be measured at 450 nm and if the miRNA is able to bind to its target sequence, the signal is reduced.

3.10 Statistical analysis

The statistical data analysis was done by using the statistic software GraphPad Prism 7. One-way ANOVA and two-way ANOVA were used for multiple comparison. RT-qPCR data were normalized using housekeeping genes and analyzed using the $\Delta\Delta$Ct method. Comparisons were made with control cell lines that were always treated in the same way and transfected with equivalent amounts of empty plasmid.

Experiments for which a statistical evaluation was done were repeated at least 3 times. A p-value of 0.05 was chosen for the significance difference and the p value style was chosen with $p>0.05$ (n.s), $p<0.05$ (*), $p<0.01$(**), $p<0.001$ (***) and $p<0.0001$(****).

4. Results

4.1 H460-CisR was chosen as working cell line

To examine the functionality of the HH signaling pathway primer panel, which are listed in Table 5, and to investigate the activity of the HH signaling pathway in different cell lines a RT-qPCR was performed. After cDNA synthesis based on total RNA from H460-CisR, H460-Par, A549-CisR and A540-Par cells, the RT-qPCR was performed with settings listed in Table 13. The HH signaling pathway primer panel test was done twice for each cell line. After normalizing to the housekeeping gene, ß2-microglobuin (ß2MG) was chosen, the CP value (crossing point) was directly comparable through the mean values of the two runs for each cell line and gene. As can be seen in Figure 5 A, the HH signaling pathway genes show highest expression in H460-CisR cells, reflected in the low CP values (high expression level) for almost all analyzed genes. In Figure 5 B key players of the HH signaling pathway were selected and compared directly with one another. Here the aforementioned trend was confirmed again. Detection of SUFU in the H460 cell lines was unclear, and invited to further investigation.

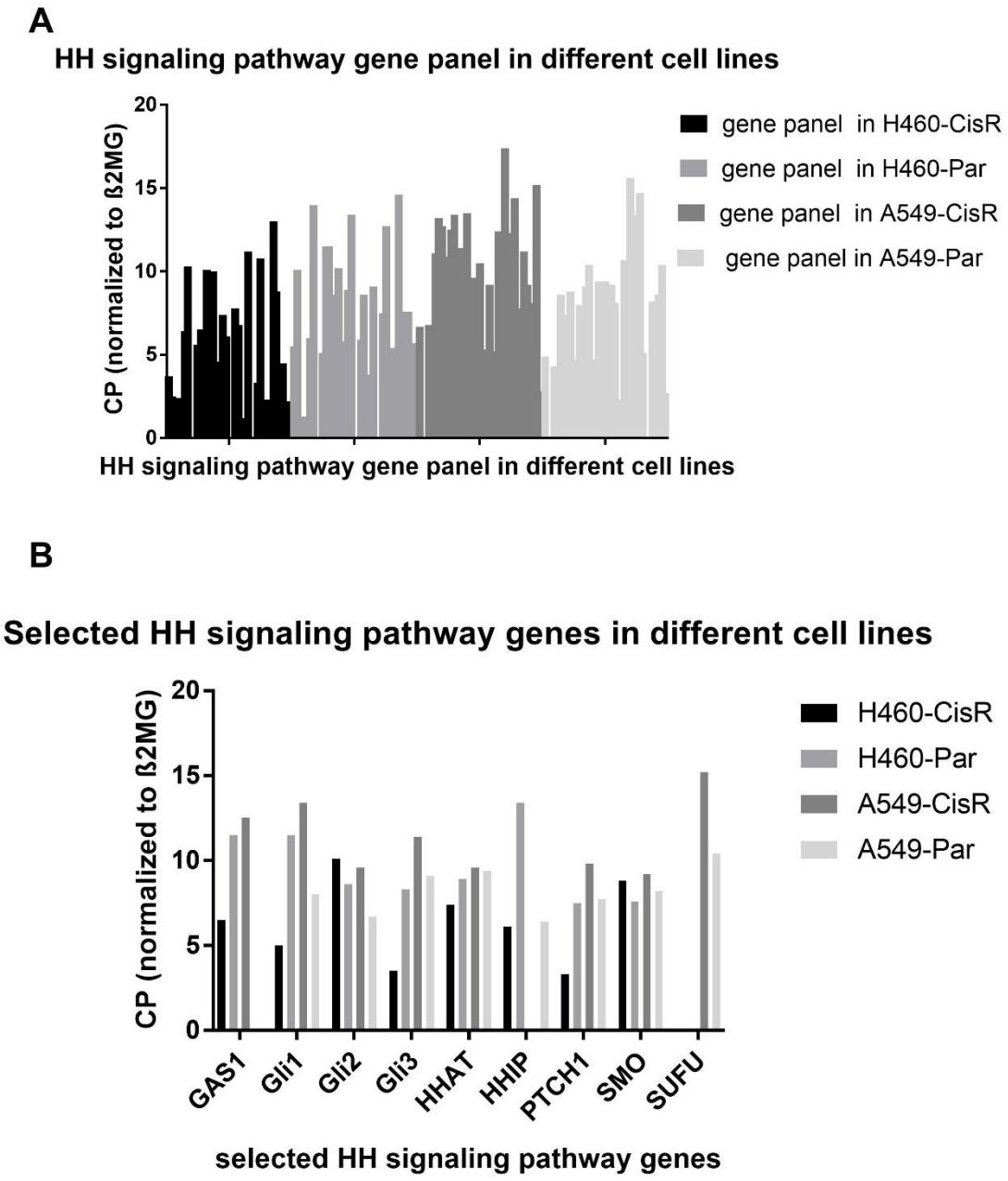

Figure 5. RT-qPCR analysis of HH signaling pathway gene expression in different NSCLC cell lines *(A) HH signaling pathway gene expression profile in H460-CisR, H460-Par, A549-Cis and A549-Par cell lines. Data has been already normalized to the housekeeping gene (ß2MG). H460-CisR cell line shows the lowest CP values over the entire range. (B) Prominent genes of the HH signaling pathway were compared to get a better overview of the expression profile. This also reflects that the HH signaling pathway is most active in H460-CisR cell line. The negative regulator of HH signaling pathway, SUFU, could not be detected at all in the H460 cell lines.*

4.2 SUFU gene amplification and restriction cloning into transfection vector

As can be seen in Figure 5 B SUFU could not be detected in the H460 cell lines. Therefore, as described in chapter 3.6.1.1, SUFU DNA was amplified from A549-Par cDNA, as this cell line showed the highest SUFU expression. Figure 6 shows the agarose gel electrophoresis which was performed after the PCR amplification. After separation, bands at desired height were observed according to the sequence data. Sequence data, as well as sequence length, were determined by NCBI with the reference number NM_016169.3 for SUFU Var I and NM_001178133.1 for SUFU Var II. The bands at the intended heigh were carefully cut out of the gel and the DNA fragments were purified using Monarch DNA Gel Extraction Kit.

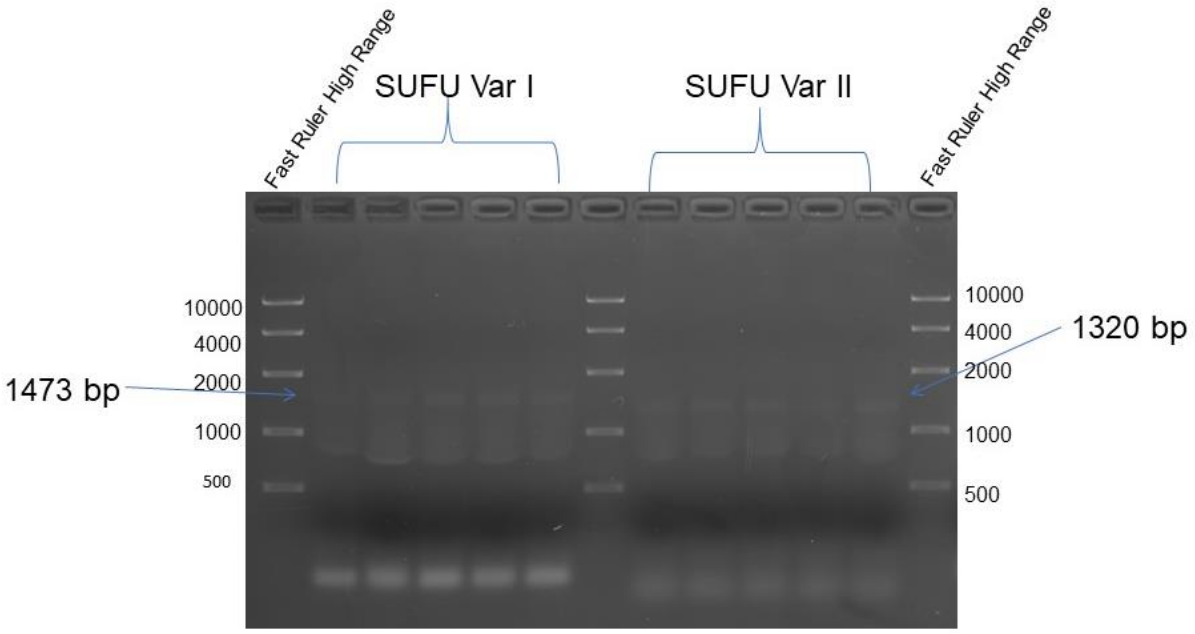

***Figure 6. Agarose gel electrophoresis of the SUFU DNA amplification out of A549-Par cDNA**. A 1% agarose gel was used for seperation. Five µl of the DNA ladder (Fast Ruler high range) and 20 µl PCR product were used per well. Seperation was done at 100 V for 40 min. Propper DNA fragments are labeld with arrows.*

After purification, a restriction digestion of the inserts (SUFU Var I and SUFU Var II) and the expression vector (pcDNA3.1(+); expression vector map is listed in the supplemental information Figure 30) was performed with the restriction enzymes HindIII and BamHI (described in chapter 3.6.1.1) followed by subsequent ligation

(chapter 3.6.1.1). The *in silico* cloned expression vector, by using the SnapGene software, is shown in Figure 7. Experiments were performed with pcDNA3.1(+)/SUFU Var I, since the sequence does not have any alternative splicing forms.

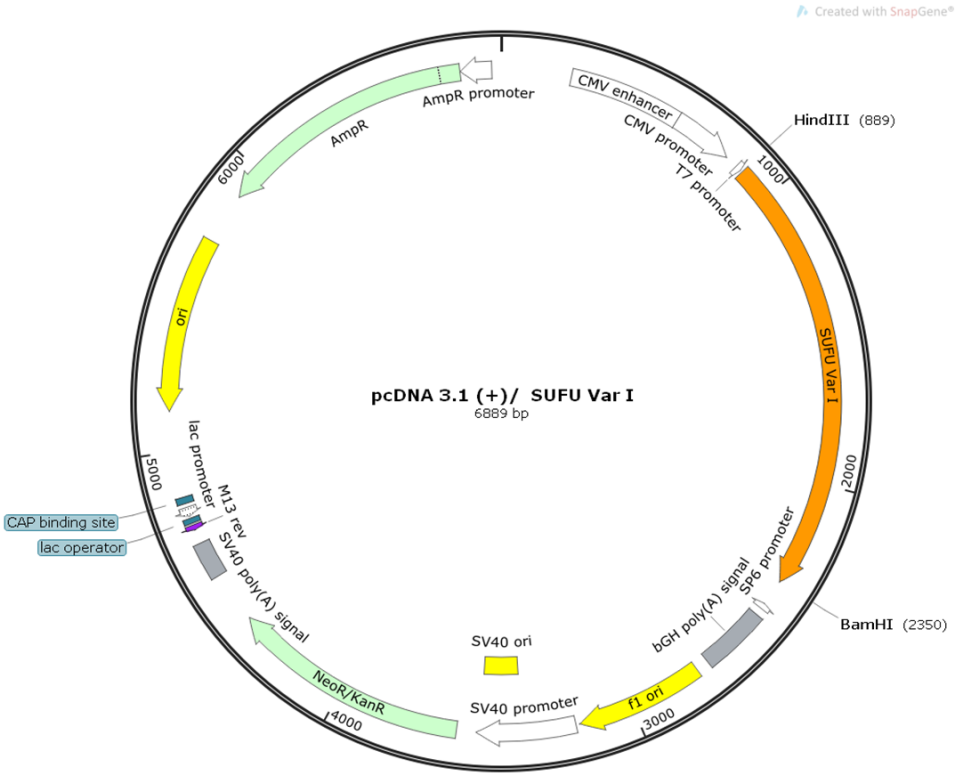

Figure 7. In silico construction of the expression vector pcDNA3.1(+)/SUFU Var I. *For a better illustration only the most important features and the used unique restriction enzymes are listed. In silico experimentes were done by using SnapGene 5.2.3.*

In order to check the correctness and the completeness of the cloned insert sequence, sequencing and subsequent alignment of the sequence with the original sequence from NCBI were done. Sequencing was performed using sequencing primers (Table 6) by “Eurofins Genomics” and SnapGene was used for the alignment as shown in Figure 8.

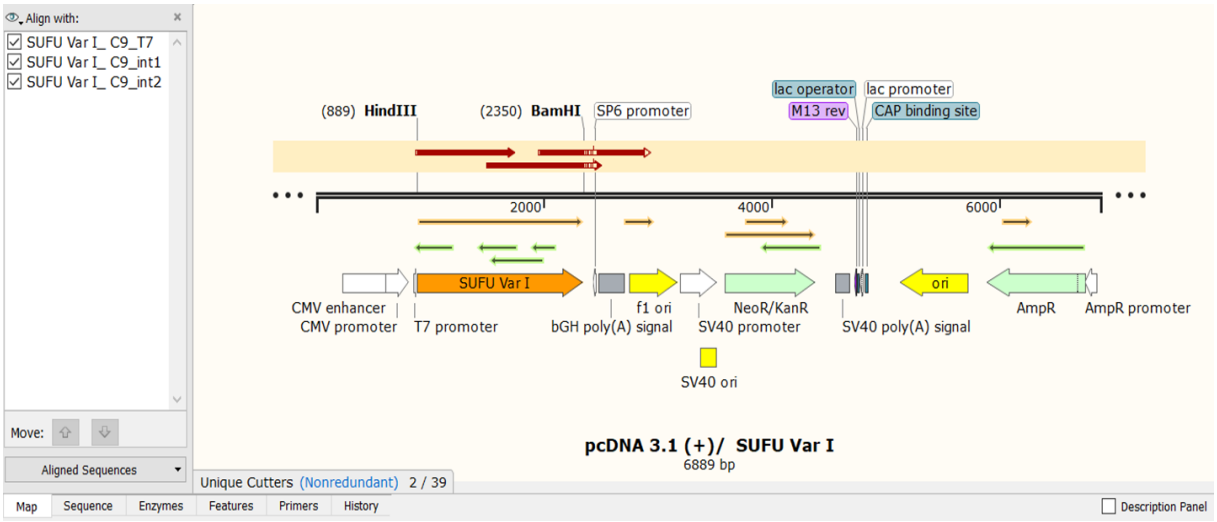

***Figure 8. Overview of the SUFU alignment**. Clone 9 shows a consistent error-free reading frame, indicated by the small orange arrow. The big orange arrow reflects the original sequence which was inserted in in silico cloning. The red arrows reflects the individual sequencing by the specific primers. By overlaying them, the error-free reading frame was obtained.*

4.3 Testing SUFU plasmid overexpression with different DNA amounts at certain time

After preparatory work, amplification, cloning and sequencing, the intended pcDNA3.1(+)/SUFU Var I overexpression in H460-CisR was performed.

In order to be able to plan further experiments, the amount of plasmid used for transfected was validated in order to achieve a solid overexpression. As can be seen in Figure 9, starvation has considerably influenced reproducibility. It can be seen that an amount of 0.35 µg/ml pcDNA3.1(+)/SUFU Var I lead to a completely exaggerated high fold change. This huge overexpression could lead to unspecific effects in cell metabolism. An amount of 0.25 µg/ml was sufficient for further experiments and the risk of unspecific effects was lower. A dilution effect of SUFU overexpression was observed over time. As control, cells transfected with empty plasmid (pcDNA3.1(+)) were used.

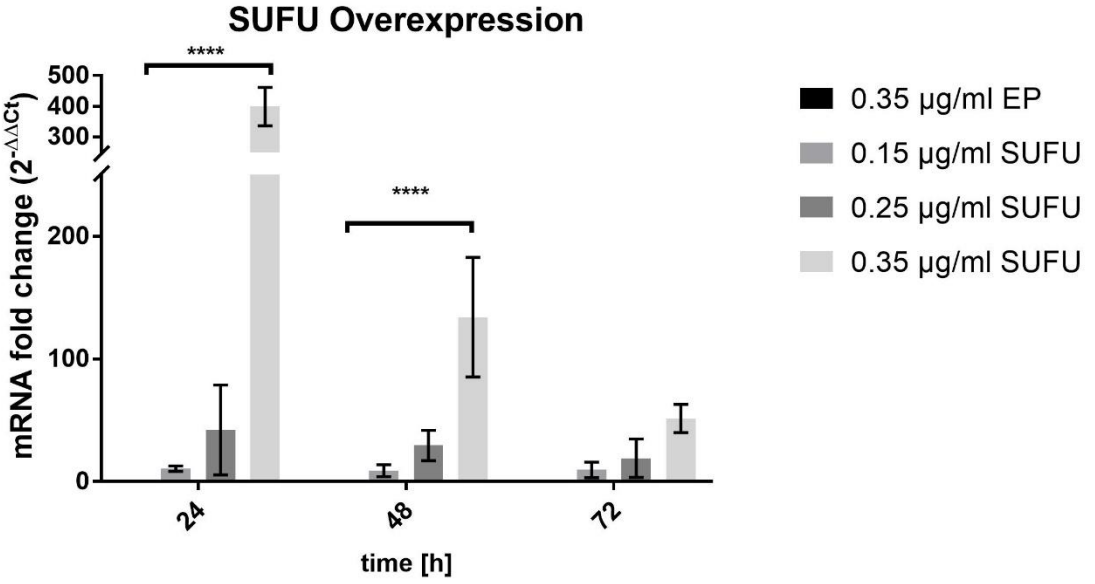

Figure 9. RT-qPCR analysis of SUFU gene expression in H460-CisR cells with different amounts of pcDNA3.1(+)/SUFU Var I plasmid*. Data were normalized using the housekeeping gene ß2MG and the fold change is calculated under the assumption that the empty plasmid (EP) represents the "untreated" cells and is set to 1 in the graphic representation. SUFU = pcDNA3.1(+)/SUFU Var I; EP = pcDNA3.1(+). n=3*

To further check the SUFU expression rate on protein level a Western Blot was performed. For this approach, the same amounts of the pcDNA3.1(+)/SUFU Var I and pcDNA3.1(+), like in the RT-qPCR analyses, were used. The results show that the overexpression worked in a reliable manner. Given the information in Figure 10, it can be assumed that the transfection with 0.35 µg/ml pcDNA3.1(+)/SUFU Var I lead to a very high SUFU expression, which reflects the RT-qPCR data. The amount of 0.25 µg/ml of SUFU plasmid also showed reliable results. However, a rapid decrease in SUFU expression over time could also be identified. Vinculin (124 kDa) served as loading control.

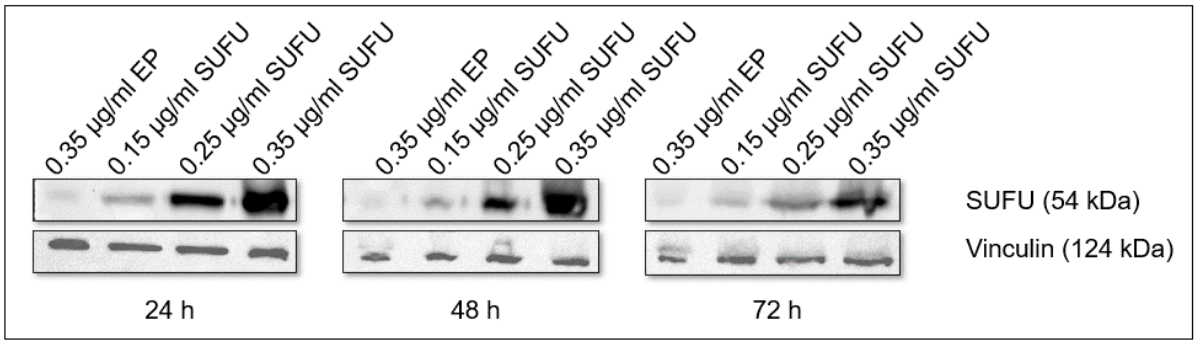

Figure 10. Western Blot analysis of SUFU expression after cell transfection with different amounts of SUFU plasmid in comparison to the EP transfection*. Protein harvest was done 24 h, 48 h and 72 h after transfection. Vinculin was used as loading control. Gel conentration was 8%. Six µl of peqGOLD Protein Marker IV (pre stained, 10-170 kDa) were used and detection kit was West pico. SUFU was detected at ~ 54 kDa. SUFU = pcDNA3.1(+)/SUFU Var I. EP = pcDNA3.1(+).*

4.4 SUFU plasmid overexpression in H460-CisR influences expression of Gli transcription factors

We also investigated whether the SUFU overexpression has an influence on the expression on other genes of the HH signaling pathway. Above all, the Gli genes were investigated because, according to literature, they can interact with SUFU. As shown in Figure 11, no clear up or down regulation of these genes was identified by analyzing the RT-qPCR. Gli expression was initially slightly downregulated, but the expression differences disappeared very quickly over time.

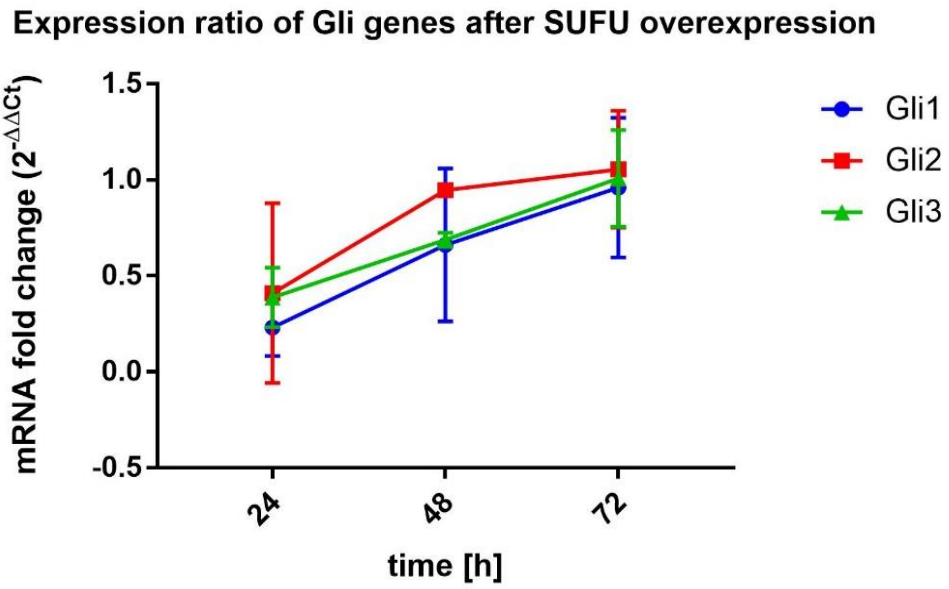

Figure 11. Investigation of expression level of Gli genes after cell transfection with 0.25 µg/ml pcDNA3.1(+)/SUFU Var I in H460-CisR cell line*. RNA isolation was done 24 h, 48 h, 72 h after cell transfection. Housekeeping gene for normalization was ß2MG, and control sample was transfected with EP = pcDNA3.1(+) and was set to 1. n=3.*

As before, an examination on protein level was also performed. Interestingly, these data do not really reflect the RT-qPCR data. Slight overexpression of the Gli proteins was observed, especially with the Gli1 antibody from Thermo Fisher and the Gli2 antibody from Novus (Figure 12).

Transfection with control plasmid has no effects on expression. For this reason, Gli investigation was performed after transfection with 0.25 µg/ml SUFU and 0.35 µg/ml EP. In general, Gli protein detection proves to be extremely tricky. Therefore, several Gli antibodies that were predicted to work on Western Blot, were tested. The Novus antibody showed more specific Gli2 results, Gli3 could not be detected at all and for Gli1 both antibodies showed specific signals.

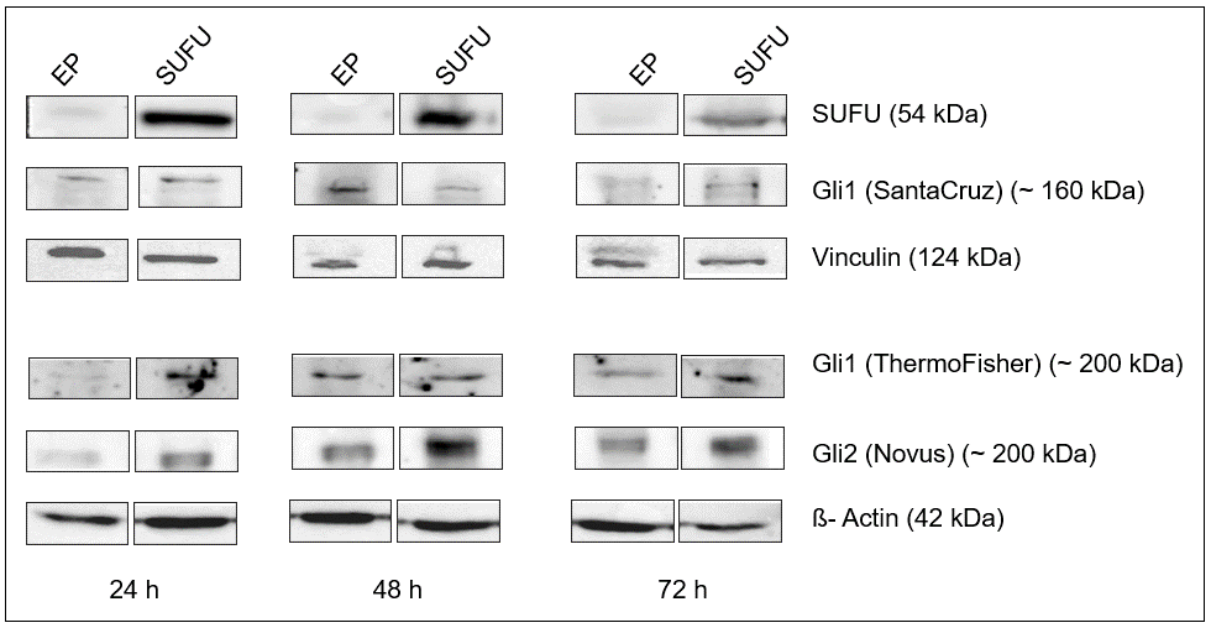

Figure 12. Western Blot analysis of SUFU, Gli1 and Gli2 after SUFU plasmid overexpression*. Gel concentration was 8%. Protein marker for Gli Western Blot was 6 µl color prestained protein standard, Broad range (11-245 kDa), and for SUFU Western Blot 6 µl peqGOLD Protein Marker IV (pre stained, 10-170 kDa) were used. As loading control Vinculin for the SUFU and ß-Actin for the Gli Western Blot were used. Detection kit for SUFU was West Pico and Gli detection was done with ECL prime. SUFU = pcDNA3.1(+)/SUFU Var I. EP = pcDNA3.1(+).*

4.5 SUFU overexpression influences the localisation of Gli proteins

Immunofluorescence was done to visualize the SUFU overexpression as well as to check the localisation of SUFU and Gli proteins in transfected cells. We wanted to determine whether SUFU overexpression has an influence on Gli localisation and whether there are signs of a direct interaction. However, the direct interaction could not be proven as can be seen in Figures 13, 14, 15 and 16. If there would be a direct interaction and thus a colocalization of the proteins, a yellow signal would be visible in the merged image due to the selection of different labelled secondary antibodies. For SUFU and Gli detection a donkey anti mouse (H+L) Alexa Fluor 555 (Invitrogen) and donkey anti rabbit (H+L) Alexa Fluor 488 (Invitrogen) were used, respectively.

Cells were analysed 48 h and 72 h after transfection. First, 24 h after transfection the cell number was too low for reliable results. Second, the fixation of the cells proved to be very tricky, as cells are impaired after transfection that leads to a decrease in the adherence to the glass slides during fixation.

Figure 13 shows the SUFU and Gli1 staining 48 h after cell transfection. SUFU overexpression was clearly observed. Comparing cells transfected with SUFU plasmid and transfected with EP, it was clear that SUFU overexpression has an impact on Gli1 expression and at the location. In the SUFU transfected cells less Gli1 was in the nucleus. As expected, 72 h after transfection, SUFU overexpression was still detectable (Figure 14) but reduced. Gli1 proteins were still less present in the nucleus due to the SUFU transfection after 72 h.

Figure 15 displays the SUFU and Gli2 labelling 48 h after SUFU and EP transfection. SUFU overexpression was clearly seen again. Gli2 showed nearly the same signal in both, however, interpretation was difficult and was not directly comparable due to the relatively low density of fixed cells (Figure 15 B). Looking at the enlarged picture it could be assumed that in the SUFU transfected cells (Figure 15 C) less Gli2 was found in the nucleus. As can be seen in Figure 16, the SUFU overexpression was still seen 72 h after transfection. In addition, it seems that Gli2 was increasingly retained in the cytoplasm by the SUFU overexpression.

Individual color channels of the 4X enlargement are found in the supplemental information (Figure 26, Figure 27, Figure 28 and Figure 29).

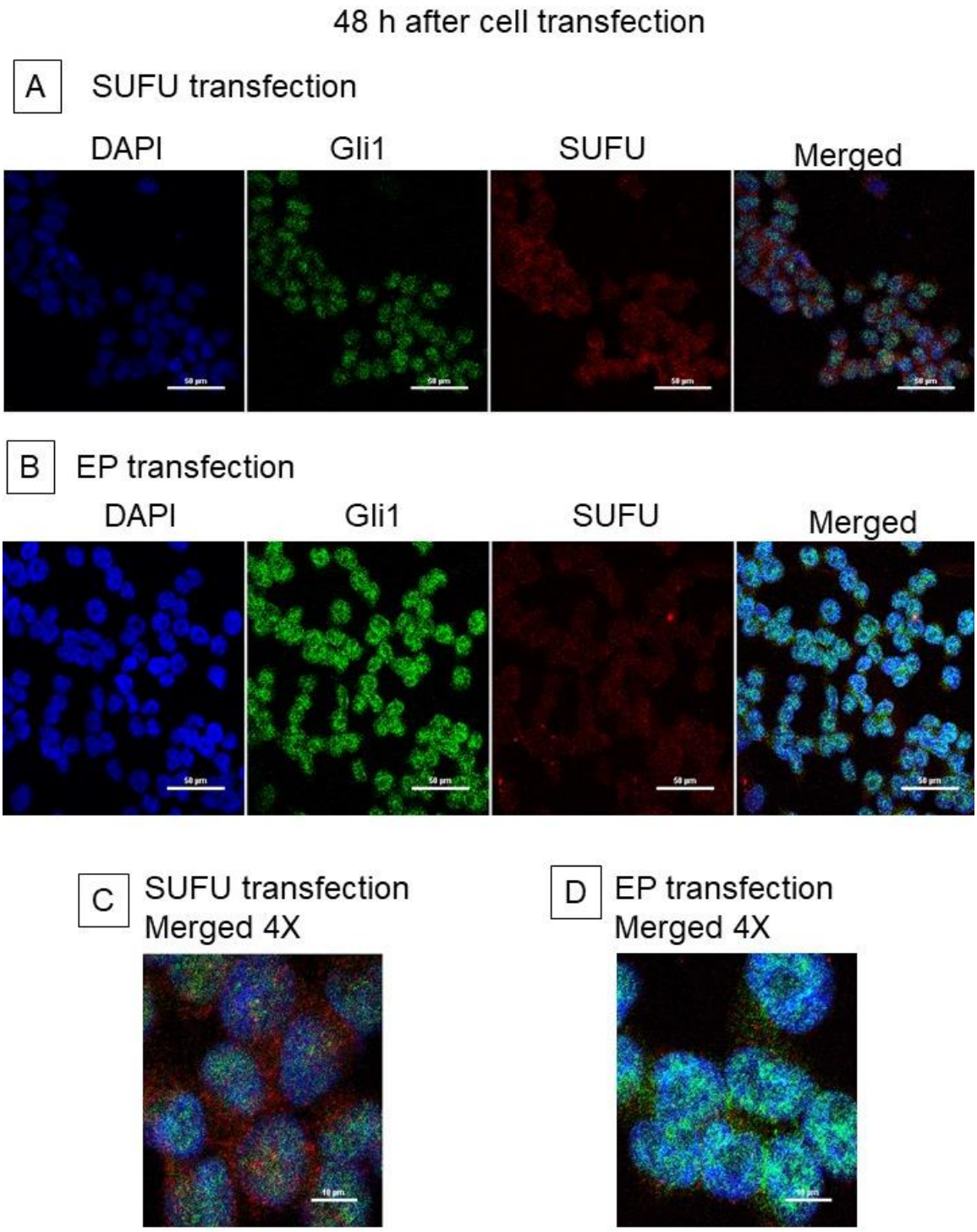

Figure 13. Immunofluorescence 48 h after transfection of H460-CisR cells with SUFU plasmid. *A: Staining after cell transfection with SUFU. B: Staining cell transfection with EP. C: 4X enlargement of SUFU transfected cells. D: 4X enlargment of EP transfected cells. Blue: DAPI stained nuclei, Green: Gli1 (abcam antibody) specific secondary donkey anti rabbit (H+L) Alexa Fluor 488 (Invitrogen) antibody, Red: SUFU specific secondary donkey anti mouse (H+L) Alexa Fluor 555 (Invitrogen) antibody, Merged: image channels overlayed. SUFU = 0.25 µg/ml pcDNA3.1(+)/SUFU Var I. EP = 0.25 µg/ml pcDNA3.1(+)*

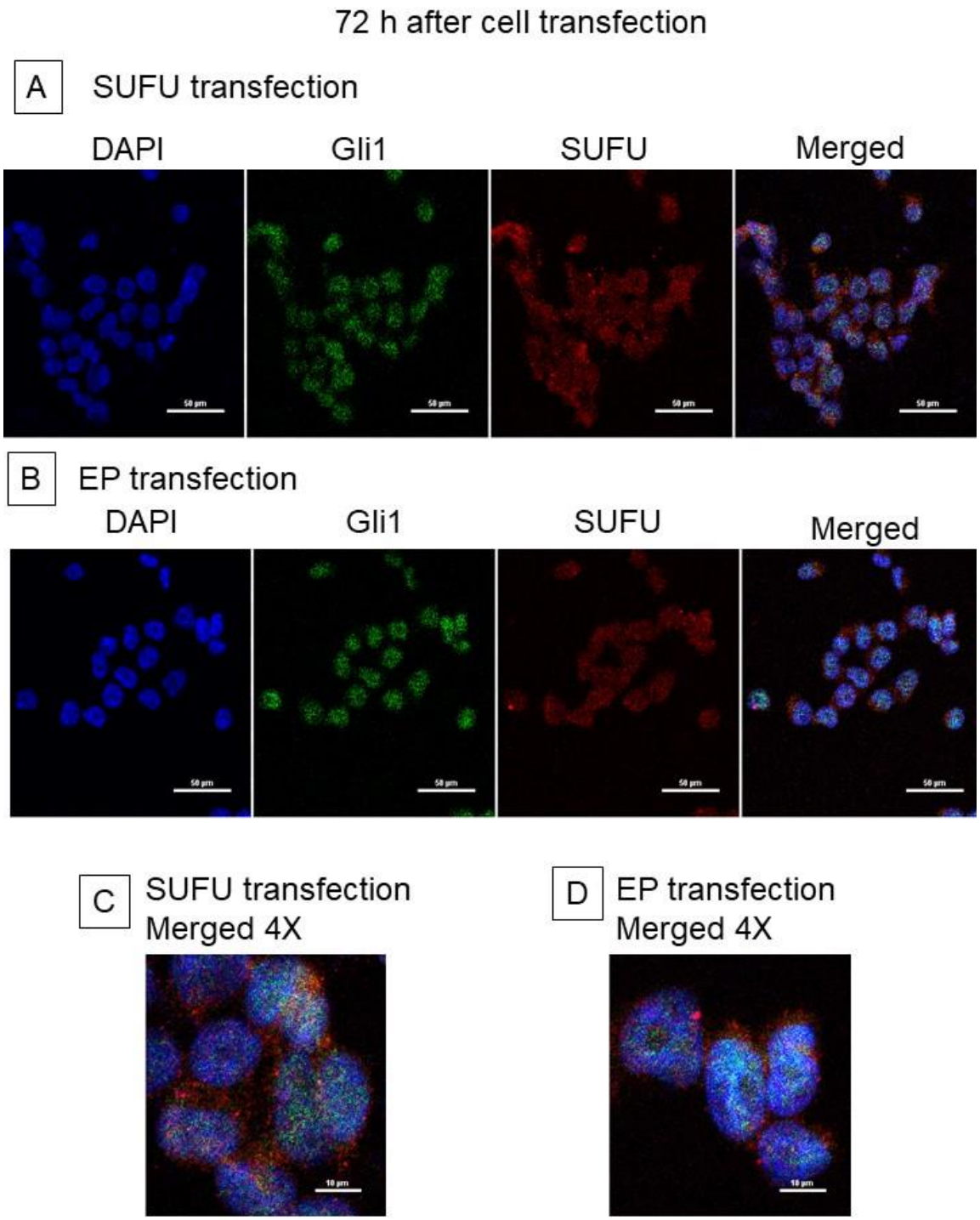

Figure 14. Immunofluorescence 72 h after transfection of H460-CisR cells with SUFU plasmid. *A: Staining after cell transfection with SUFU. B: Staining cell transfection with EP. C: 4X enlargement of SUFU transfected cells. D: 4X enlargment of EP transfected cells. Blue: DAPI stained nuclei, Green: Gli1 (abcam antibody) specific secondary donkey anti rabbit (H+L) Alexa Fluor 488 (Invitrogen) antibody, Red: SUFU specific secondary donkey anti mouse (H+L) Alexa Fluor 555 (Invitrogen) antibody, Merged: image channels overlayed. SUFU = 0.25 µg/ml pcDNA3.1(+)/SUFU Var I. EP = 0.25 µg/ml pcDNA3.1(+).*

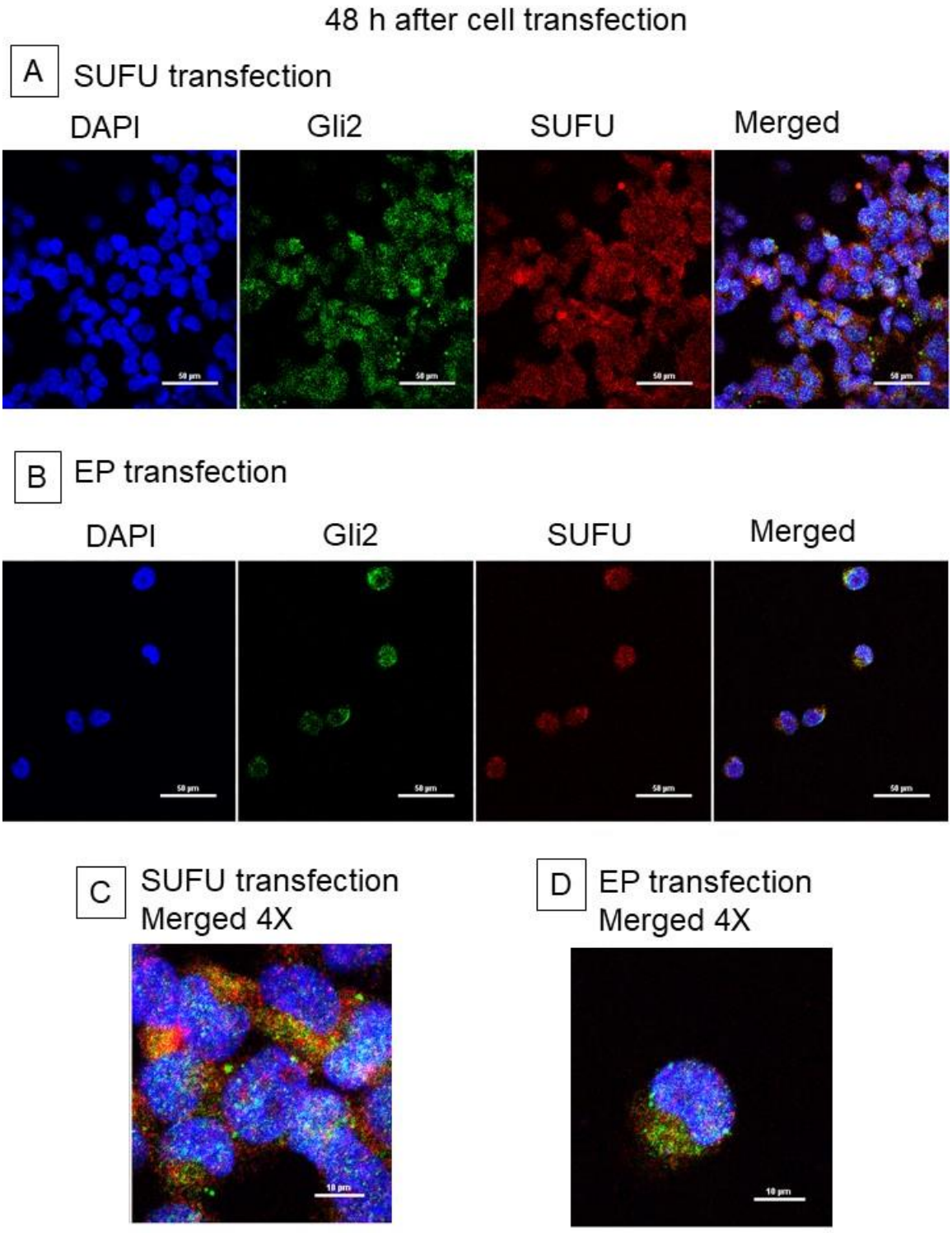

Figure 15. Immunofluorescence 48 h after transfection of H460-CisR cells with SUFU plasmid. *A: Staining after cell transfection with SUFU. B: Staining cell transfection with EP. C: 4X enlargement of SUFU transfected cells. D: 4X enlargment of EP transfected cells. Blue: DAPI stained nuclei, Green: Gli2 specific secondary donkey anti rabbit (H+L) Alexa Fluor 488 (Invitrogen) antibody, Red: SUFU specific secondary donkey anti mouse (H+L) Alexa Fluor 555 (Invitrogen) antibody, Merged: image channels overlayed. SUFU = 0.25 µg/ml pcDNA3.1(+)/SUFU Var I. EP = 0.25 µg/ml pcDNA3.1(+)*

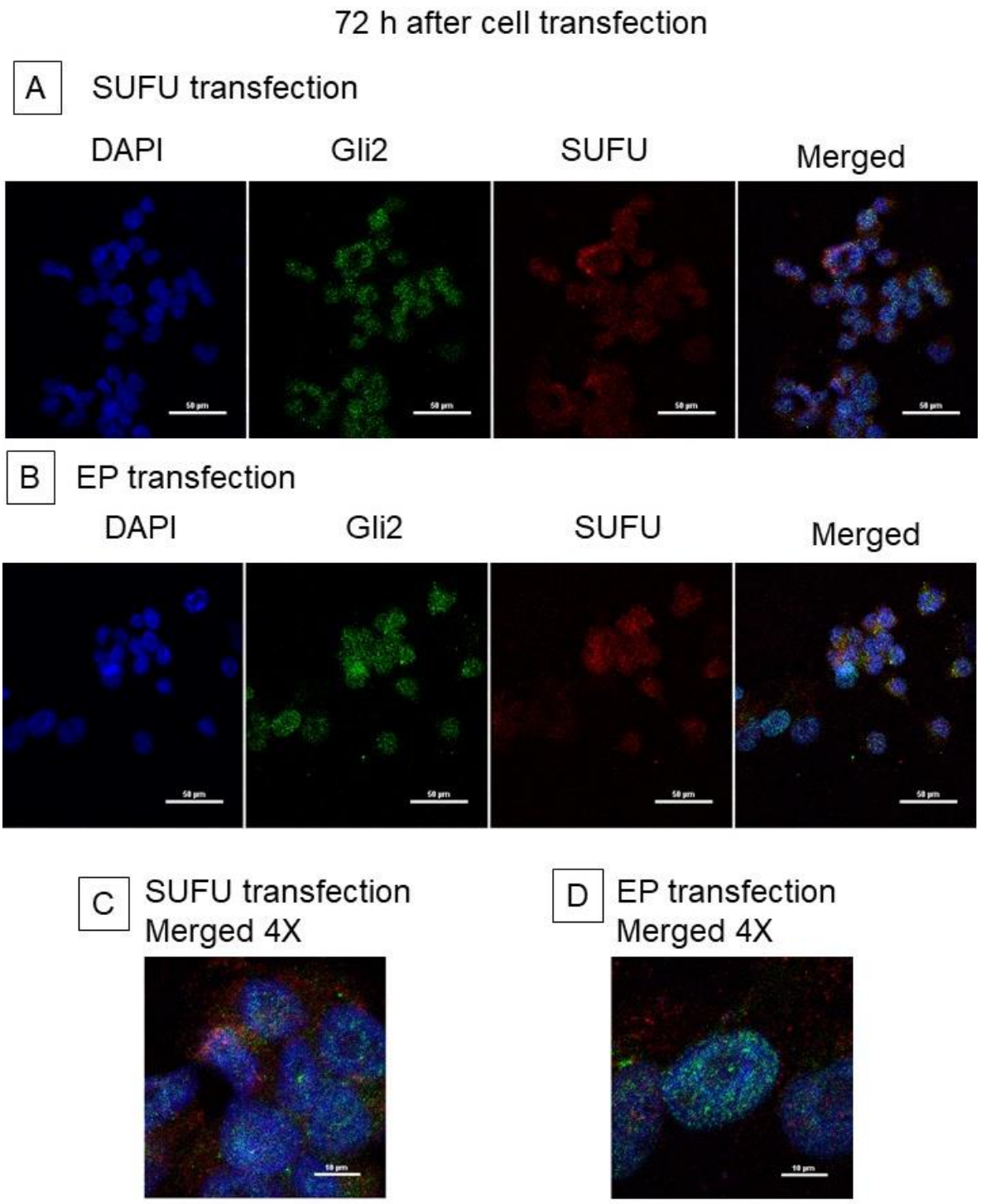

Figure 16. Immunofluorescence 72 h after transfection of H460-CisR cells with SUFU plasmid. *A: Staining after cell transfection with SUFU. B: Staining cell transfection with EP. C: 4X enlargement of SUFU transfected cells. D: 4X enlargment of EP transfected cells. Blue: DAPI stained nuclei, Green: Gli2 specific secondary donkey anti rabbit (H+L) Alexa Fluor 488 (Invitrogen) antibody, Red: SUFU specific secondary donkey anti mouse (H+L) Alexa Fluor 555 (Invitrogen) antibody, Merged: image channels overlayed. SUFU = 0.25 µg/ml pcDNA3.1(+)/SUFU Var I. EP = 0.25 µg/ml pcDNA3.1(+)*

4.6 SUFU overexpression influences the colony forming ability upon cisplatin treatment

To compare changes in the colony forming ability of H460-CisR cells upon SUFU overexpression and cisplatin treatment, a colony forming assay was performed.

By counting the colonies, it was found that the overexpression of SUFU, without administration of cisplatin, leads to a significant reduction of colony forming ability. Not only the number but also the size of colonies was limited by the SUFU overexpression, as the data in Figure 17 A and B show. This trend continues with the treatment of cisplatin, but an improvement due to the cisplatin treatment was not seen. Effects that lead to changes in the colony forming ability due to SUFU overexpression were already recognized in the crystal violet staining of the colonies, as can be seen in Figure 17 C.

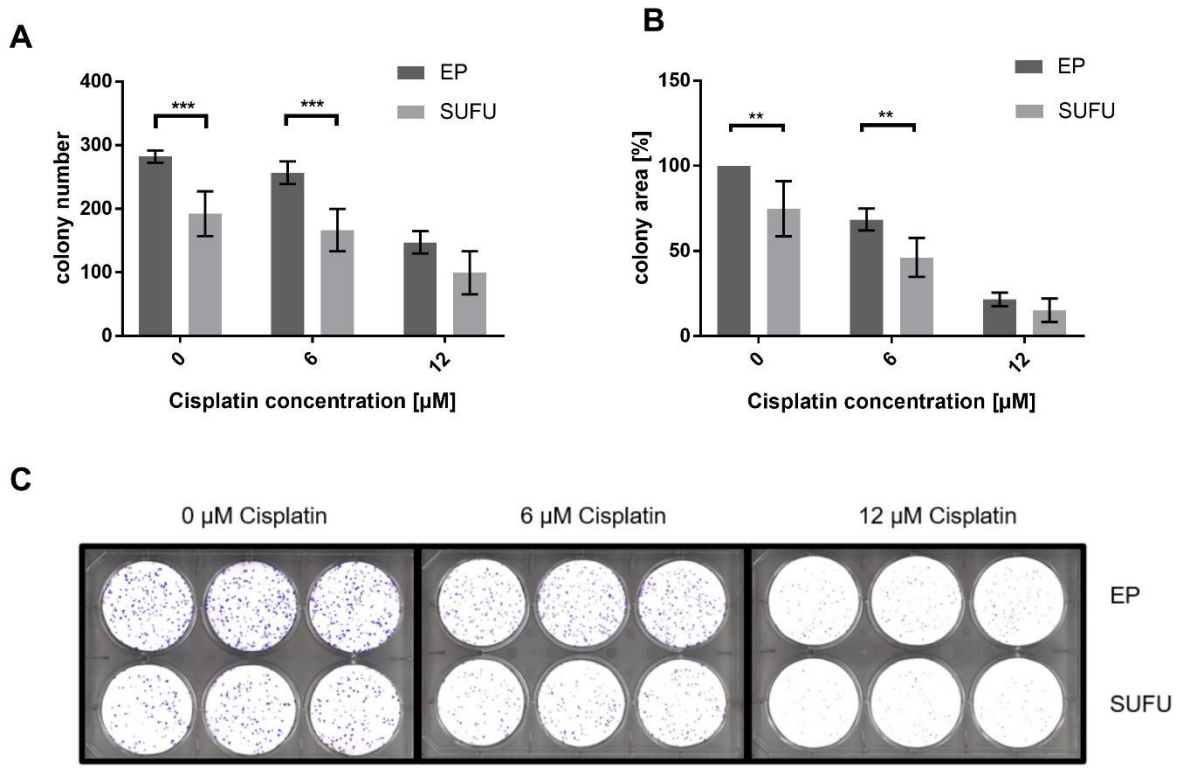

Figure 17. Colony forming ability of H460-CisR cells after SUFU overexpression and cisplatin treatment. *A: Counted colonies were compared to control cells. B: Colony areas were compared. Area occupied by colonies of the untreated control cells was set to 100% C: Crystal violet staining of H460-CisR colonies after SUFU transfection and after cisplatin treatment. Scan of crystal violet staining 8 days after transfection and 5 days after cisplatin treatment over 3 days. SUFU = pcDNA3.1(+)/SUFU Var I. EP = pcDNA3.1(+). n=4*

4.7 SUFU overexpression has an effect at the cell viability of cisplatin resistant H460 cells

To examine the viability of H460-CisR cells after transfection with different amount of SUFU plasmid-DNA, a viability assay was performed. In Figure 18 the cell viability upon transfection with indicated amounts of plasmid and at certain time points is shown. The experimental design in a 96-well plate allowed investigation of different plasmid concentrations in parallel. A decrease in cell viability based on SUFU overexpression can be observed over the entire time period.

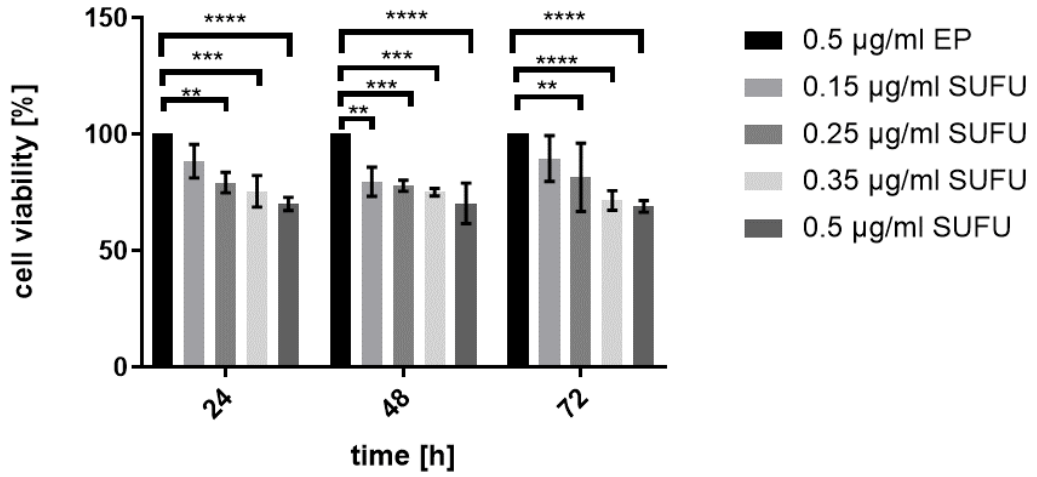

Figure 18. Cell viability measurement of H460-CisR cell lines after transfection with different amounts of SUFU plasmid. *Cell viability of control cells were set to 100% per time point after transfection. SUFU = pcDNA3.1(+)/SUFU Var I. EP = pcDNA3.1(+). n=3*

In order to find out whether the reduced cell viability due to the SUFU overexpression was further reduced by additional treatment with cisplatin, another assay was performed. Therefore, H460-CisR cells were transfected with 0.25 µg/ml SUFU plasmid, but treated with different cisplatin concentrations. As seen in Figure 19, the decrease in cell viability after treatment with cisplatin was not improved.

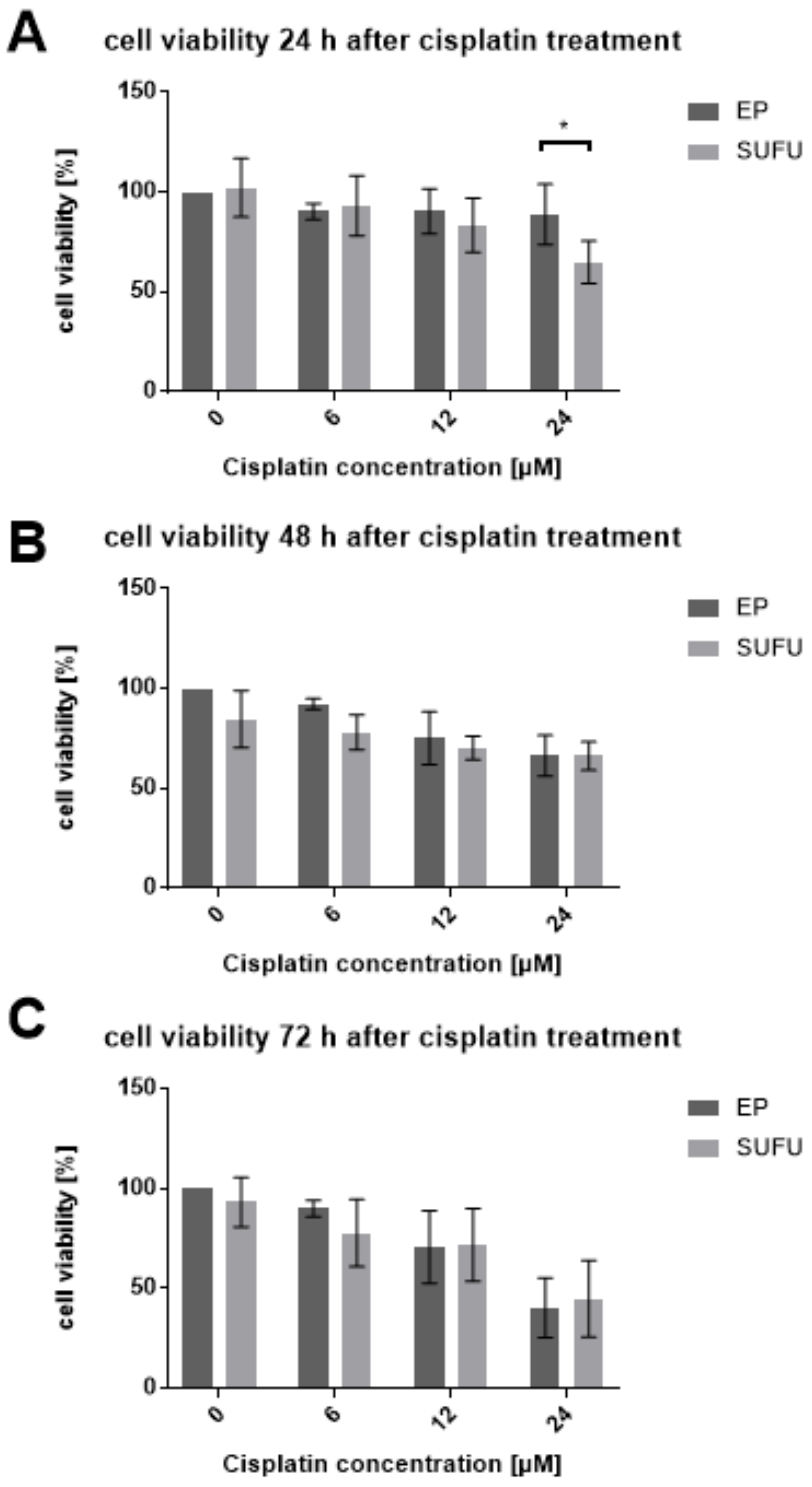

Figure 19. Cell viability measurement of SUFU plasmid transfected H460-CisR cells after cisplatin treatment*. A: Cisplatin treatment for 24 h. n=5. B: Cisplatin treatment for 48h. n=4. C: Cisplatin treatment for. n=6. H460-CisR cells transfected with EP were set to 100% for each time point. SUFU = 0.25 µg/ml pcDNA3.1(+)/SUFU Var I. EP = 0.25 µg/ml pcDNA3.1(+).*

4.8 Proliferation and migration of H460-CisR cells are not influenced by SUFU overexpression

To determine the proliferation and motility of the H460-CisR cells after transfection with SUFU and EP, we performed a scratch assay. Figure 20 A shows the data analysis of the scratch assay by measuring the closed scratch area. No meaningful changes between SUFU transfected cells and control cells were detected. Different concentrations of SUFU plasmid also showed no significant differences from one another. Figure 20 B shows an example of the microscopic snapshot used for data analysis.

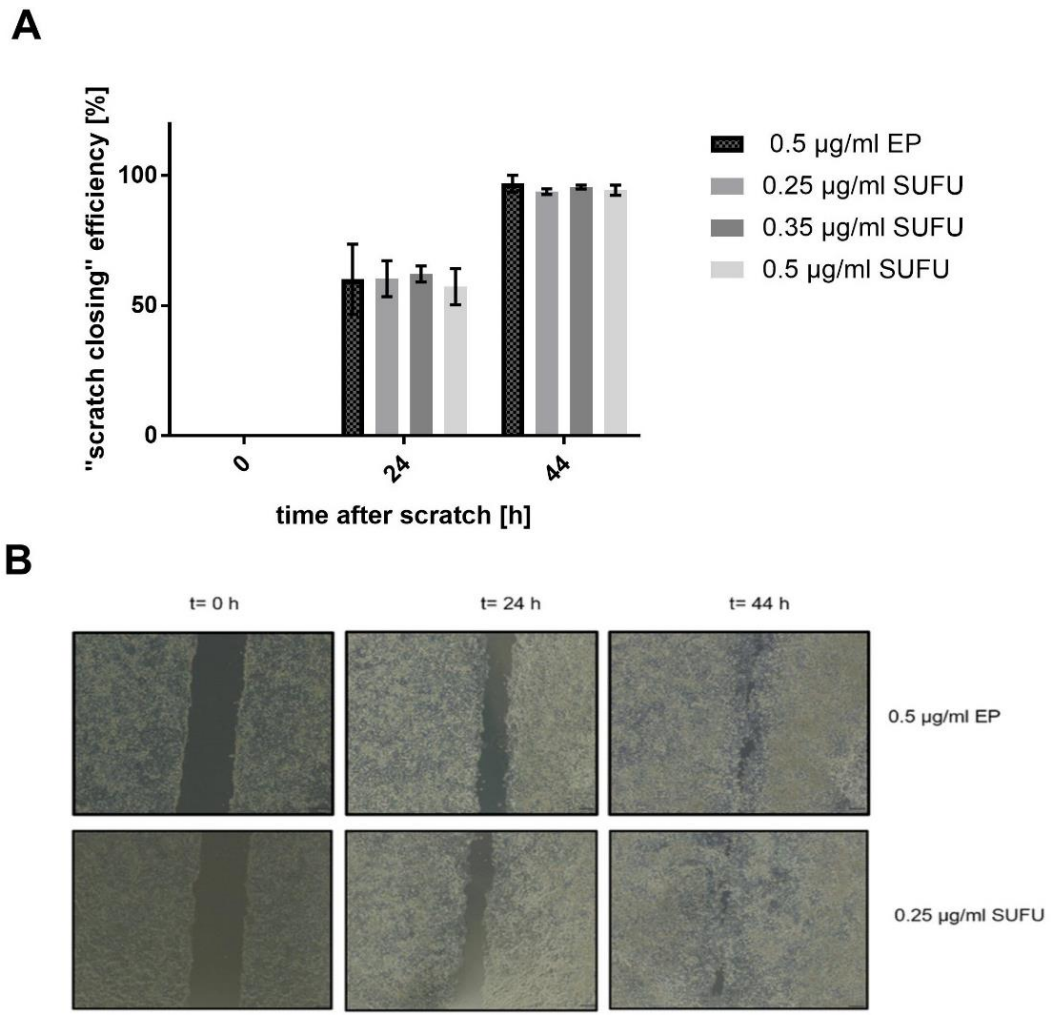

Figure 20. Scratch assay with H460-CisR cells transfected with different amounts of SUFU plasmid*. A: Time of doing the scratch is 0 and was set to 100% because the scratch was maximally open. Data analysis were performed by using ImageJ plug-in "wound healing", which calculates the area of the scratch. Data were collected at 24 h and 44 h. B: Microscopic snapshots of the scratch assay of transfected H460-CisR cells at t= 0 h, 24 h and 44 h. SUFU = pcDNA3.1(+)/SUFU Var I. EP = pcDNA3.1(+). n=3*

4.9 Co-transfection experiments of H460-CisR cells with SUFU and miR-182-5p plasmid

4.9.1 Gli2-mut2 plasmid preparation by using Gibson Assembly

Based on data from previous studies of our group, Gli2 was validated as direct target of miR-182-5p. In order to confirm this finding, a luciferase assay with wild-type 3´UTR in comparison to mutant- type 3´UTR of Gli2 was necessary. psiCHECK-2/Gli2-WT plasmid as well as pcDNA3.1(+)/miR-182-5p plasmid was already previously created by our group (Figure 32-34). psiCHECK-2/Gli2_mut2 (Figure 21) was generated by Gibson Assembly using a psiCHECK-2 vector and a gBLOCK (Chapter 3.3).

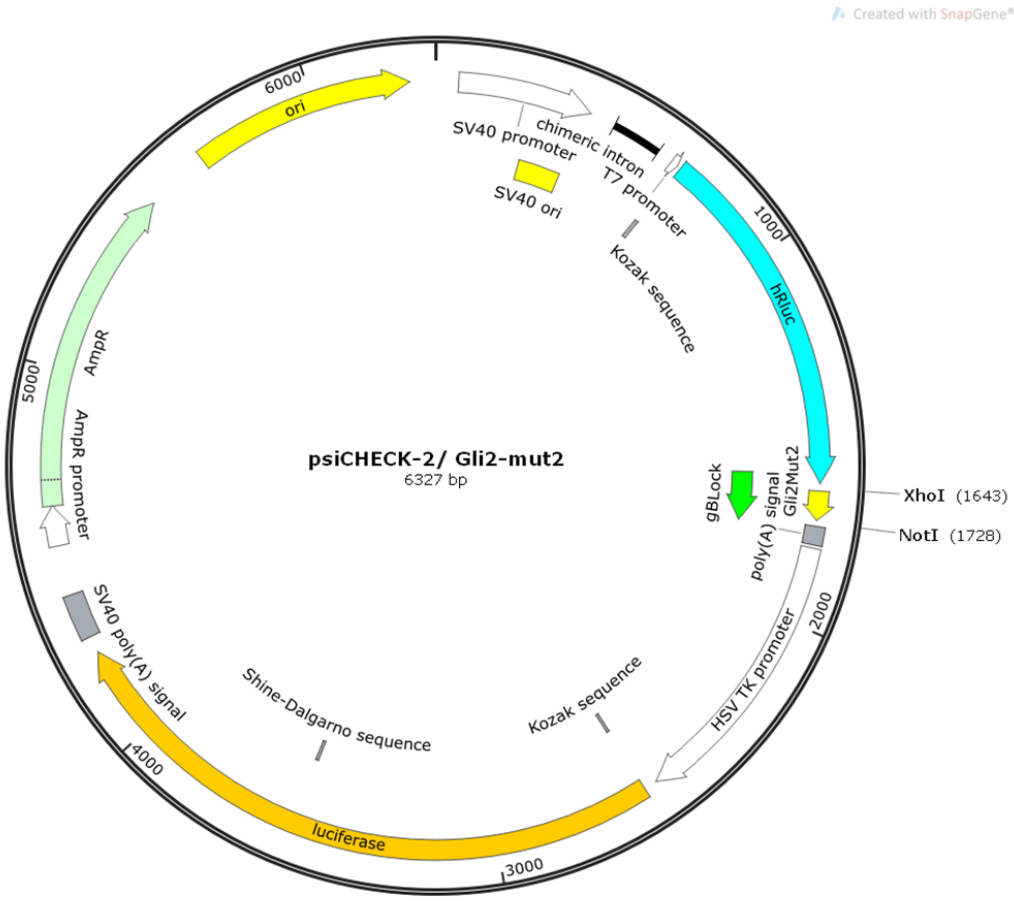

Figure 21. In silico cloning of psiCECK-2/Gli2_mut2 vector. *gBLOCK was inserted via Gibson assembly. Used single cutter restriction enzymes are listed. With these, the size of the fragment was checked in a restriction digest and a subsequent separation in an agarose gel.*

4.9.2 Gli2 3´UTR is a direct target of miR-182-5p

As described above, a luciferase assay was performed to actually determine whether Gli2 3`UTR is a direct target of miR-182-5p. Namely, the mutant version is expected to diminish the effect of miR-182-5p on Gli2. To determine this, co-transfection was performed with pcDNA3.1(+)/miR-182-5p and the psiCHECK-2/Gli2_mut2, as well as with pcDNA3.1(+)/miR-182-5p and psiCHECK-2/Gli2_WT.

As can be seen in Figure 22, the signal of the co-transfection with miR-182-5p plasmid and Gli2-WT plasmid was reduced. In the co-transfection with Gli2_mut2 this reduction was not seen, which confirmed that Gli2 is a direct target of miR-182-5p and that the target site of miR-182-5p was successfully mutated.

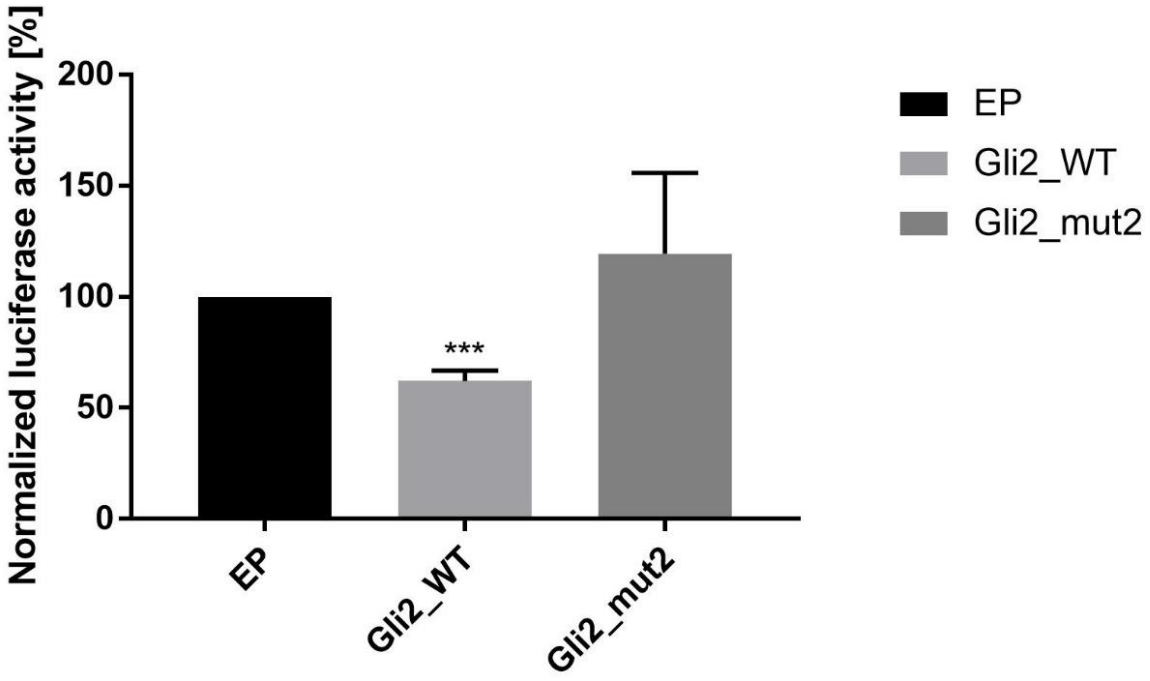

Figure 22. Dual luciferase assay with Gli2_WT and Gli2_mut2. *HEK293 transfected with EP served as control and was set to 100%. Co-transfection with Gli2_WT and miR-182-5p plasmid show signal reduction and by co transfection of miR-182-5p plasmid and Gli2_mut2 plasmid the effect got lost, indicating that Gli2-UTR is a direct target of miR-182-5p. EP = pcDNA3.1(+). Gli2_WT = psiCHECK-2/Gli2_WT. Gli2_mut2 = psiCHECK-2/Gli2_mut2. n=3*

4.9.3 Co-transfection showed mild effects on SUFU and Gli2 protein level

To find out whether the co-transfection of SUFU and miR-182-5p plasmid has an influence on the protein level, especially on SUFU and Gli2 proteins, a Western Blot was performed. In order to elucidate all effects, co-transfections with EP + SUFU as well as EP + miR-182-5p plasmids were performed next to the usual co-transfection of SUFU + miR-182-5p plasmid. EP was used as control. The total amount of transfected plasmids (0.7 µg/ml) was consistent through all the experiments, 0.5 µg/ml miR-182-5p plasmid was used in order to reproduce previous experiments.

As can be seen in Figure 23, despite the co-transfection, SUFU overexpression decreases over time. Looking at signals from Gli2, it can be concluded that the transfection with miR-182-5p causes a lower Gli2 expression, which can be seen especially after 48 h. After 72 h, these effects diminished.

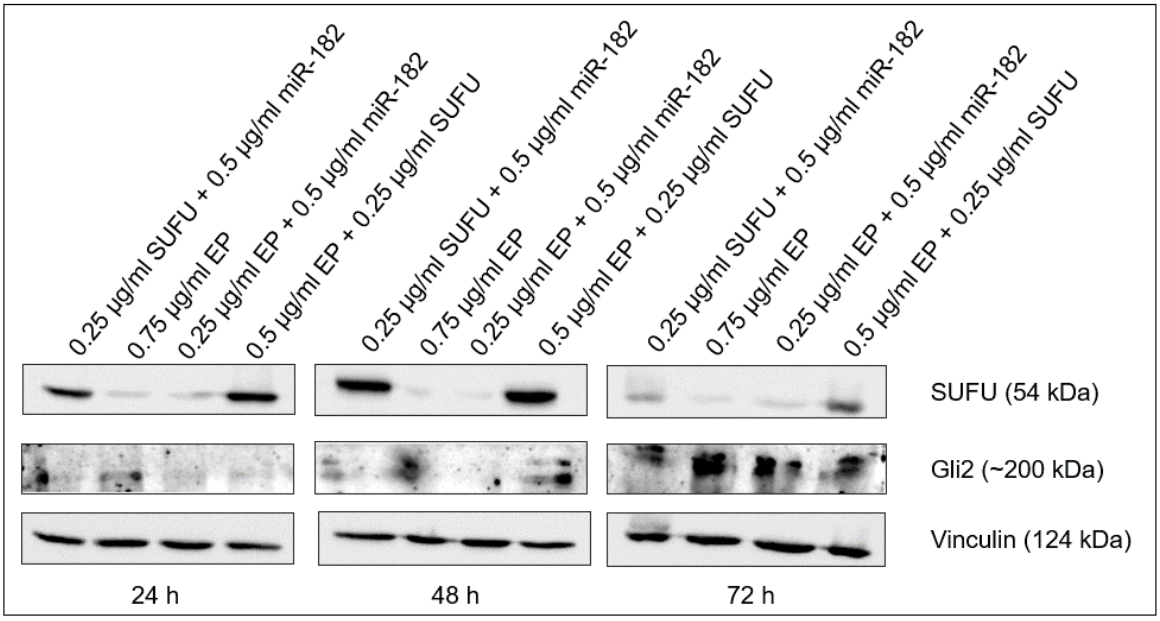

Figure 23. Western Blot analysis of the H460-CisR cells co-transfeced with SUFU and miR-182-5p plasmid*. Protein samples were collected over 3 days. Gel concentration was 8%, used detection kits were West Pico for SUFU and Vinculin and ECL Prime for Gli2. Vinculin was used as loading control. SUFU = pcDNA3.1(+)/SUFU Var I. miR-182 = pcDNA3.1(+)/miR182-5p. EP = pcDNA3.1(+).*

4.9.4 Cell viability of H460-CisR is only negligibly affected after co-transfection and cisplatin treatment.

An AlamarBlue® assay was performed in order to investigate phenotypic differences in cell viability due to the co-transfection of SUFU and miR-182-5p plasmid and subsequent cisplatin treatment. Different plasmid compositions, but the same total amount of plasmid DNA, were transfected in order to identify phenotypic effects between different conditions. EP transfection, without cisplatin treatment, serves as control and was set to 100%. Treatment with cisplatin was performed 24 h after reverse transfection. Quantifications are shown in Figure 24. According to our data, co-transfection did not show the desired effect and cell viability was more likely stabilized. However, 24 h after transfection SUFU overexpression alone caused significant limited cell viability without cisplatin treatment (Figure 24 A).

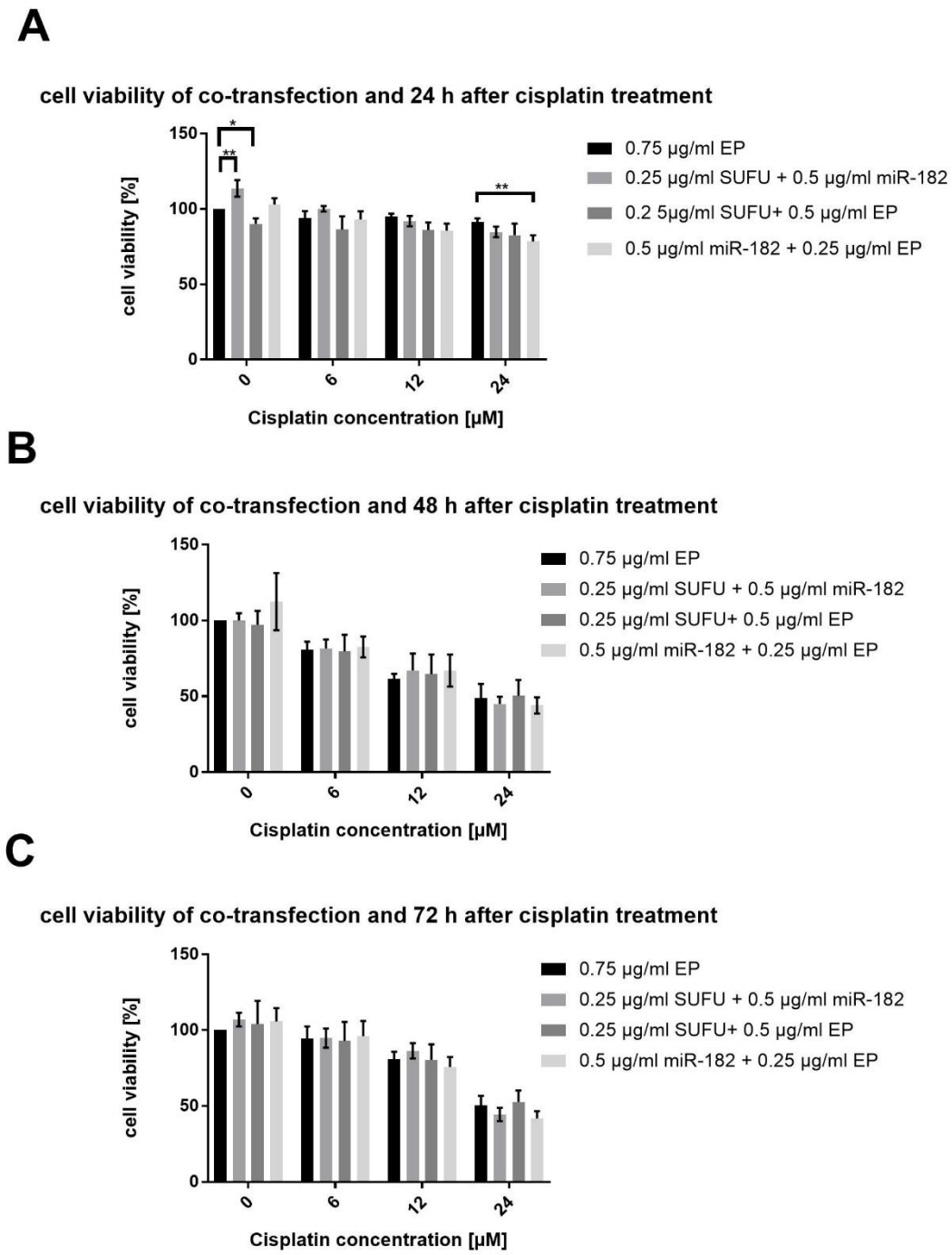

Figure 24. Cell viability assay of co-transfected and cisplatin-treated H460-CisR cells. *Cisplatin treatment occured 24 h after reverse transfection. EP transfection and no cisplatin treatment were set to 100% in each time point. A: 24 h after cisplatin treatment. B: 48 h after cisplatin treatment. C: 72 h after cisplatin treatment. n=3 for each experiment. SUFU = pcDNA3.1(+)/SUFU Var I. miR-182 = pcDNA3.1(+)/miR-182-5p. EP = pcDNA3.1(+).*

4.9.5 Co-transfection and cisplatin treatment has less effects on colony forming ability as SUFU overexpression alone

To investigate differences in the colony forming ability between the co-transfection of SUFU and miR-182-5p and the SUFU overexpression alone, a colony forming assay was performed. Different combinations of co-transfections, with the same total amount of plasmid DNA, were done to find the most suitable conditions and to better assess differences. Single EP transfection was used for comparison and quantifications. In Figure 25, the counted colonies as well as the occupied area from the colonies are shown. H460-CisR cells transfected with SUFU + EP showed the best results regard to a decrease in colony forming ability.

Figure 25 C shows one representative colony forming experiment of the co-transfected cells. Clear differences between the different transfections cannot be recognized by visual analysis of the stained colonies.

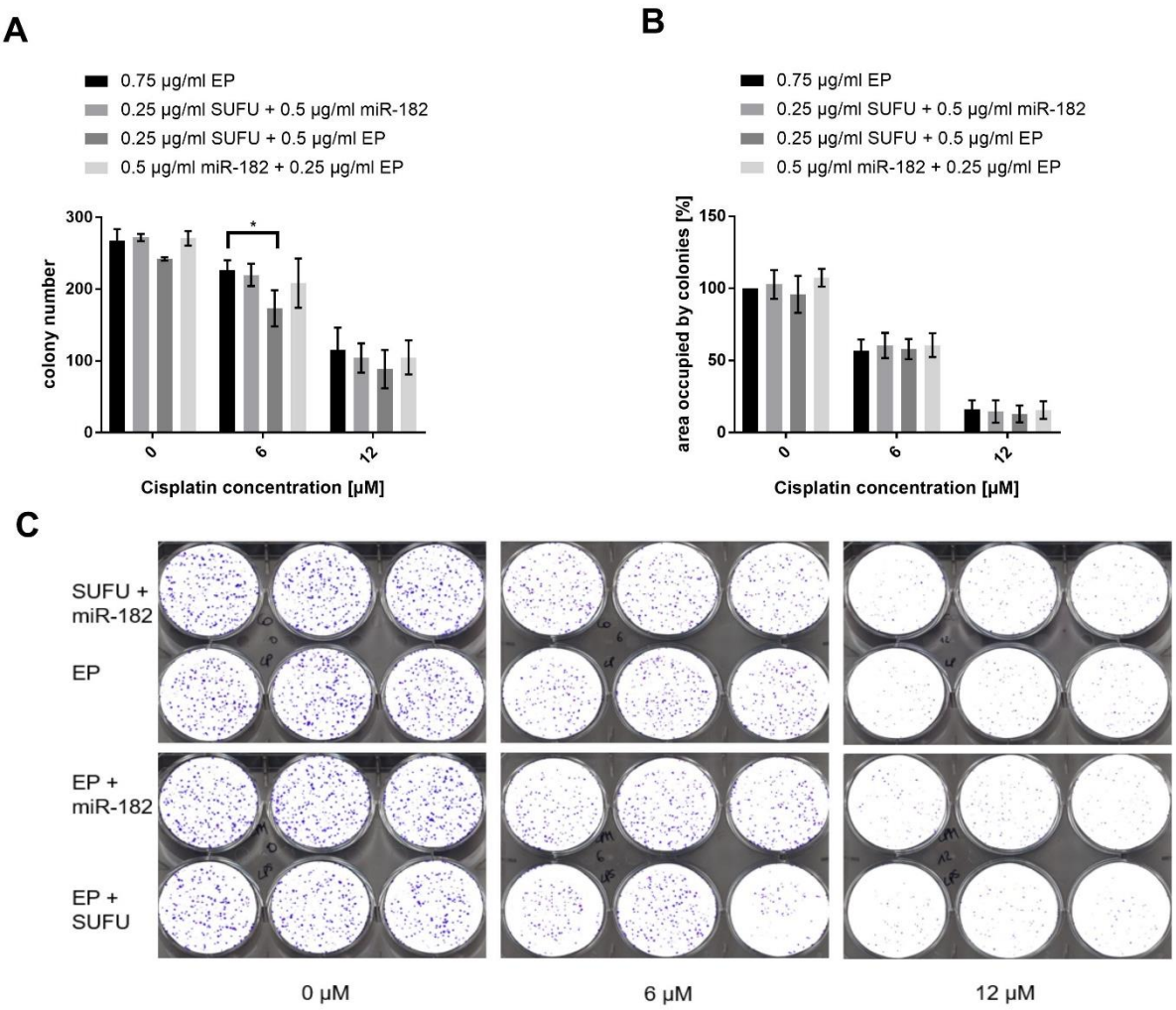

Figure 25. Colony forming ability of co-transfected and cisplatin treated H460-CisR cells*. Cisplatin treatment occur 24 h after seeding 500 transfected cells and was performed for additional 72 h A: number of counted colonies compared to EP transfected H460-CisR cells. B: Occupied area of EP transfected cells were set to 100%. C: Scan of crystal violet staining of the colony forming assay from the co-transfected H460-CisR cells. SUFU = pcDNA3.1(+)/SUFU Var I. miR-182 = pcDNA3.1(+)/miR-182-5p. EP = pcDNA3.1(+). n=3.*

5. Discussion

Globally, cancer is the second leading cause of death after cardiovascular diseases. Lung cancer is one of the most common cancers and also takes the first place among cancer associated deaths (83–85). Despite intensive research and new insights on molecular biological level, lung cancer is still associated with extremely poor prognosis. The poor prognosis is also because cancer is often recognized at a later stage. Different genetic mutations, e.g. mutations in EGFR, KRAS, BRAF or ALK, as well as deregulated signal transduction pathways have been implicated in lung cancer. As a result of these findings, there are increasing numbers of clinical trial studies (9,86).

One of the major problems in cancer treatment is the development of resistance against the treatment itself. One signaling pathway that is frequently associated with resistance mechanisms is the Hedgehog (HH) signaling pathway, especially the Sonic Hedgehog (SHH) signaling pathway due to its role in lung development (46–48,55). It is strongly suspected that cancer stem cells (CSC) lead to development of resistance. Since CSC have similar properties to embryonic stem cells and the Hedgehog signaling pathway plays a major role in embryonic development, this pathway is often associated with CSC (46,47,55).

Since it is known that the HH signaling pathway is active in NSCLC (55), we screened the HH signaling pathway genes in different NSCLC cell lines (H460-CisR/ H460-Par and A549-CisR/ A549-Par). Our results indicated that the pathway is active in every cell line, showing highest activity in the H460-CisR cell line.

Research that links the HH signaling pathway with cancer has been around for long time. Therefore, it is not surprising that there are already various approaches in clinical trials with the aim of inhibiting this pathway. Gli, as well as Smo inhibitors, are between the most popular representatives of these studies (54,87). In addition to the canonical pathway, the non-canonical pathway must be also observed. The non-canonical pathway is able to transcribe HH signaling pathway target genes by activating Gli transcription factors via other mechanisms or signaling pathways. Due to the possible presence of this non-canonical pathway, the Smo inhibitors are ineffective because Gli

transcription factors are regulated independently of the Smo signal transmission (50,54,88).

Therefore, an approach was sought to inhibit the HH signaling pathway independently of canonical and non-canonical activation. For this purpose, the Gli proteins should be prevented from functioning as transcription activator. SUFU, the negative regulator of the pathway, can play a decisive role through its ability to inhibit the function of the Gli proteins by holding them back in the cytoplasm or occupying the Gli binding site in the nucleus (45).

In our screening of HH signaling pathway genes, SUFU was only detected in the A549 cell lines with a low expression, whereas in H460 cell lines it wasn´t detected. For this reason, SUFU was amplified from A459-Par cDNA, cloned into a transfection vector and then overexpressed in the selected working cell line, H460-CisR. In parallel, a shorter alternatively spliced variant of SUFU (SUFU Var II), was also amplified and cloned. This was performed to check in further studies if effects observed through overexpression of standard SUFU (SUFU Var I) are also observed by working with the shorter variant. However, due to the limited time, the focus of this work was on standard SUFU.

By performing a transient transfection, a decrease of SUFU mRNA, as well as protein, was clearly observed. Corresponding effects, because of the transient SUFU overexpression, are also only temporary (89). Despite the rapid decrease of expression, 0.25 µg/ml of recombinant plasmid was chosen as working concentration for transfections because atypical physiological effects due to massive overexpression should be prevented or reduced. Atypical effects are e.g., an altered cell metabolism, which arises from the fact that many resources are used for the production of the overexpressed protein. Thus, we wanted to avoid secondary effects, which are not directly related to SUFU overexpression (90–92).

The SUFU overexpression should keep more Gli proteins in the cytoplasm and thereby inhibit the expression of specific target genes. So Gli expression should also be downregulated because Gli target genes include the Gli genes themselves (43–45,52,54). This trend was not confirmed by checking the mRNA and protein expression level of the Gli1 and Gli2. On the contrary, a trend towards induction was identified at

protein expression level of the Gli1 and Gli2 proteins. However, the higher Gli protein level normalizes again with the decrease of SUFU. These results could indicate that high SUFU level has an effect on the Gli expression. This could mean that more Gli proteins could be produced or stabilized in order to counteract SUFU overexpression effects. If this claim is correct, the Hedgehog signaling pathway, with a special view at the Gli signaling, which can be also controlled via several signaling pathways (51,52,54), is common in tumor cells. However, in order to make precise statements, further research overall the HH signaling network is required.

The localisation of the SUFU and Gli proteins was checked by immunostaining and the overexpression of SUFU was confirmed. In addition, we observed that due to the SUFU overexpression the Gli proteins accumulate in the cytoplasm. A direct binding of SUFU and Gli proteins (45,52,54,60,70) couldn´t be confirmed by the immunofluorescence experiment. To determine if there is a direct interaction between these two proteins, or if an additional protein is involved in this complex, an protein interaction assay has to be performed.

SUFU overexpression showed particular effects on phenotypical level. We clearly showed significantly decreased colony forming ability due to the SUFU overexpression. These effects were present without cisplatin treatment and were not increased upon cells treatment with 6 µM cisplatin. This indicates that the restricted colony forming ability caused by SUFU overexpression was independent of cisplatin treatment. When treated with 12 µM cisplatin, all cells, with and without SUFU overexpression, were restricted in their colony forming ability. Therefore, the effect that SUFU transfected cells show higher sensitivity to cisplatin, could have not been demonstrated. Not only the number of colonies was interesting, but also the area occupied by colonies. One could assume that more colonies simply take up more space, but even macroscopically differences in the size of single colonies was observed. SUFU overexpressing cells showed colonies with a smaller size. From these data we can conclude, that the SUFU overexpression leads to a decrease in colony forming ability and an additional cisplatin treatment does not significantly improve this reduction.

Cell viability was also influenced by SUFU overexpression. We showed that the SUFU overexpression reduces viability of H460-CisR cells. The most prominent results were observed with the 0.5 µg/ml SUFU plasmid-DNA overexpression. However, due to possible negative effects of excessive overexpression, this concentration can be counterproductive. The selected working concentration of recombinant plasmid (0.25 µg/ml) showed also significantly reduced cell viability. In an additional experiment 0.25 µg/ml SUFU transfected H460-CisR cells were treated with cisplatin. The additional treatment showed not a significant reduction in cell viability compared to the SUFU transfection alone. However, this additional step compromised reproducibility in this experiment. Cisplatin treatment 24 h after transfection is an additional stress factor for cells. This assumption is made because in the colony forming experiment the effects from SUFU transfection are only marginally influenced by cisplatin treatment. One difference between these two experiments is that in the colony forming experiment cisplatin was added 3 days after transfection. A stable transfection could thereby eliminate a stress factor and thus possibly lead to more stable and meaningful values.

By performing a scratch assay, no influence on motility due to SUFU overexpression was detected. However, it is difficult to make a clear statement because the H460 cell line was less suitable for this approach. They tend to grow in smaller groups or nests and, thus, less effectively form a continuous monolayer. In some areas there were still cell free places, whereas in others cell groups were very dense and started growing in multiple layers. After performing the scratch, despite washing steps and media exchange, cells were increasingly detached from the cell cluster and settled down somewhere, this being the case also in the scratch. Due to this cluster formation, an exact motility and invasion efficiency of the cell line could have not been assessed. A cell line that forms a continuous monolayer would be more effective for this assay. A method based on live cell imaging might be an advantage and might enable making statements that are more specific.

Earlier research by the laboratory team focused on the overexpression of miR-182-5p in the H460-CisR cell line. There were significant differences in the overexpression of the miRNA with regard to increased sensitivity to cisplatin (40). Since Gli2 expression correlates with increased cisplatin resistance (55), we wanted to determine, by use of a luciferase assay, whether Gli2 is a direct target of miR-182-5p. miR-182-5p plasmid

and Gli2-WT plasmid were created earlier in our group. To confirm whether Gli2 is a real target, a Gli2-mut2 version was created. This construct has a mutated seed sequence. As a result, it was to expect that miR-182-5p will no longer be able to bind Gli2 and signal suppression will be rescued. We showed that, compared to a reduction of about 40% by wild-type transfection, the luciferase signal upon mutant transfection went back to 100%. These data clearly confirmed that Gli2 is a direct target of miR-182-5p (40).

By co-transfection of miR-182-5p and SUFU, we investigated whether the above-mentioned effects regarding cell viability, colony forming ability and cisplatin sensitivity were improved or stabilized. At protein level a slight reduction of Gli2 was detected upon cell transfection with miR-182-5p. SUFU overexpression remained at a high level, therefore, it can be assumed that the co-transfection did not adversely affect each other. Investigations of cell viability as well as the colony forming assay didn´t show the expected effect of improvement, since there should now be less Gli2 and thus the HH signaling pathway should be even more inactive. But similar results were observed due to the sole SUFU overexpression. A reduction in colony forming ability, reduced cell viability or an increased cisplatin sensitivity were not observed due to the co-transfection with miR-182-5p and SUFU.

It might be that a total amount of 0.75 µg/ml plasmid DNA was too high. Under these circumstances, it could be possible that the stressed cells switch on another pathway in order to survive. Another explanation could be that these two transfections hinder each other in signal transduction, since both interact with the HH signaling pathway. Although speculative, it could be that the general signaling network of the cell was influenced due to the co-transfection and, at least at this timepoint, some unknown secondary metabolic effects occurred.

For future investigation on SUFU effects, a stable cell line with permanent SUFU overexpression should be considered. From our results it can be seen that the SUFU overexpression decreases relatively fast. It is possible that such a rapid decrease is caused by some miRNA, especially by miR-214, which has been described to directly target SUFU (68). An investigation of miR-214 expression profile in dependence of

SUFU overexpression was not described in this work due to limited time. In order to better and easier examine and assess the expression profile of various miRNAs with regards to SUFU overexpression, a stable cell line would again provide advantages. Stable transfection would further remove experimental obstacles. With stable SUFU overexpression it might be easier to assess more precisely whether the cell sensitivity to cisplatin is influenced. In our colony forming experiments, cisplatin treatment was done 3 days after transfection. However, we also observed that the SUFU overexpression had already decreased at this time point. Therefore, it would be interesting to show how a stable cell line behaves and whether there is an increased sensitivity to cisplatin. Long-term effects with regard to cell viability after cisplatin treatment and SUFU overexpression would also be interesting.

Since upon SUFU overexpression Gli2 was retained in the cytoplasm, an increased sensitivity to cisplatin was expected. Gli2 is known to be an essential factor in different mechanisms of resistance (55). To our surprise, co-transfection with SUFU and miR-182-5p did not lead to increased sensitivity to cisplatin. Therefore, it should be further investigated if other signaling pathways, e.g. Notch or Wnt, are more affected by SUFU overexpression und, thus, regulate genes involved in cell growth, proliferation and chemoresistance (47,48,50,87).

It is not surprising that the HH signaling pathway had moved into the focus of cancer research. Although drugs that can obstruct the pathway are already in clinical trials, e.g. Smo inhibitors, one should always keep in mind that there is also a non-canonical pathway in addition to the canonical one (48,87), which might also affect the treatment. Thus, further research on SUFU could provide valuable knowledge and elucidate new approaches for treatment options in lung cancer.

In summary, SUFU has a central role in the HH signaling pathway. Its overexpression affects growth and viability, however, an increased sensitivity to cisplatin cannot be clearly proven. It should be considered to generate a stable SUFU overexpression cell line. This would allow to investigate (I) how other proteins, especially the Gli proteins, behave, (II) whether SUFU overexpression leads to changes in the miRNA signaling, (III) if the HH signaling pathway is self- repressing and, therefore, the cell is stimulating

another pathway in order to survive and hold the tumorigenicity, (IV) if SUFU influences the sensitivity to cisplatin. These questions need further intensive research.

6. References

1. Lüllmann-Rauch R, Asan E. Taschenbuch Histologie. 5., vollständig überarbeitete Auflage. Stuttgart New York: Georg Thieme Verlag; 2015. 726 p.

2. Hartmann M, editor. Zytologie, Histologie und mikroskopische Anatomie: licht- und elektronenmikroskopischer Bildatlas ; inkl. Übungs-DVD. 5., überarb. Aufl. Wien: Facultas.wuv; 2011. 139 p.

3. SMART [Internet]. Servier Medical Art. [cited 2019 Sep 22]. Available from: https://smart.servier.com/

4. Weinberg RA. The biology of cancer. Second edition. New York: Garland Science, Taylor & Francis Group; 2014. 876 p.

5. Travis WD, Brambilla E, Noguchi M, Nicholson AG, Geisinger KR, Yatabe Y, et al. International Association for the Study of Lung Cancer/American Thoracic Society/European Respiratory Society International Multidisciplinary Classification of Lung Adenocarcinoma. Journal of Thoracic Oncology. 2011 Feb;6(2):244–85.

6. Bishop JA, Benjamin H, Cholakh H, Chajut A, Clark DP, Westra WH. Accurate Classification of Non-Small Cell Lung Carcinoma Using a Novel MicroRNA-Based Approach. Clinical Cancer Research. 2010 Jan 15;16(2):610–9.

7. Wood SL, Pernemalm M, Crosbie PA, Whetton AD. Molecular histology of lung cancer: From targets to treatments. Cancer Treatment Reviews. 2015 Apr;41(4):361–75.

8. Kitamura H, Yazawa T, Okudela K, Shimoyamada H, Sato H. Molecular and Genetic Pathogenesis of Lung Cancer: Differences Between Small-Cell and Non-Small-Cell Carcinomas. TOPATJ. 2008 Oct 30;2(1):106–14.

9. Lemjabbar-Alaoui H, Hassan OU, Yang Y-W, Buchanan P. Lung cancer: Biology and treatment options. Biochimica et Biophysica Acta (BBA) - Reviews on Cancer. 2015 Dec;1856(2):189–210.

10. Duma N, Santana-Davila R, Molina JR. Non–Small Cell Lung Cancer: Epidemiology, Screening, Diagnosis, and Treatment. Mayo Clinic Proceedings. 2019 Aug;94(8):1623–40.

11. Duruisseaux M, Esteller M. Lung cancer epigenetics: From knowledge to applications. Seminars in Cancer Biology. 2018 Aug;51:116–28.

12. Hanahan D, Weinberg RA. Hallmarks of Cancer: The Next Generation. Cell. 2011 Mar;144(5):646–74.

13. Dasari S, Bernard Tchounwou P. Cisplatin in cancer therapy: Molecular mechanisms of action. European Journal of Pharmacology. 2014 Oct;740:364–78.

14. Eljack ND, Ma H-YM, Drucker J, Shen C, Hambley TW, New EJ, et al. Mechanisms of cell uptake and toxicity of the anticancer drug cisplatin. Metallomics. 2014;6(11):2126–33.

15. Ishida S, Lee J, Thiele DJ, Herskowitz I. Uptake of the anticancer drug cisplatin mediated by the copper transporter Ctr1 in yeast and mammals. Proceedings of the National Academy of Sciences. 2002 Oct 29;99(22):14298–302.

16. Galluzzi L, Senovilla L, Vitale I, Michels J, Martins I, Kepp O, et al. Molecular mechanisms of cisplatin resistance. Oncogene. 2012 Apr;31(15):1869–83.

17. Chen HHW, Kuo MT. Role of Glutathione in the Regulation of Cisplatin Resistance in Cancer Chemotherapy. Metal-Based Drugs. 2010;2010:1–7.

18. Su F, Hu X, Jia W, Gong C, Song E, Hamar P. Glutathion s transferase π indicates chemotherapy resistance in breast cancer. Journal of Surgical Research. 2003 Jul;113(1):102–8.

19. Bowden NA. Nucleotide excision repair: Why is it not used to predict response to platinum-based chemotherapy? Cancer Letters. 2014 May;346(2):163–71.

20. MSH2 mutS homolog 2 [Homo sapiens (human)] - Gene - NCBI [Internet]. [cited 2021 Jan 28]. Available from: https://www.ncbi.nlm.nih.gov/gene/4436

21. MLH1 mutL homolog 1 [Homo sapiens (human)] - Gene - NCBI [Internet]. [cited 2021 Jan 28]. Available from: https://www.ncbi.nlm.nih.gov/gene/4292

22. Taft RJ, Pang KC, Mercer TR, Dinger M, Mattick JS. Non-coding RNAs: regulators of disease. J Pathol. 2010 Jan;220(2):126–39.

23. Lee RC, Feinbaum RL, Ambros V. The C. elegans heterochronic gene lin-4 encodes small RNAs with antisense complementarity to lin-14. Cell. 1993 Dec 3;75(5):843–54.

24. Lee R, Feinbaum R, Ambros V. A short history of a short RNA. Cell. 2004 Jan;116:S89–92.

25. Berezikov E, Cuppen E, Plasterk RHA. Approaches to microRNA discovery. Nat Genet. 2006 Jun;38(S6):S2–7.

26. O'Brien J, Hayder H, Zayed Y, Peng C. Overview of MicroRNA Biogenesis, Mechanisms of Actions, and Circulation. Front Endocrinol. 2018 Aug 3;9:402.

27. Wahid F, Shehzad A, Khan T, Kim YY. MicroRNAs: Synthesis, mechanism, function, and recent clinical trials. Biochimica et Biophysica Acta (BBA) - Molecular Cell Research. 2010 Nov;1803(11):1231–43.

28. Li N, You X, Chen T, Mackowiak SD, Friedländer MR, Weigt M, et al. Global profiling of miRNAs and the hairpin precursors: insights into miRNA processing and novel miRNA discovery. Nucleic Acids Research. 2013 Apr;41(6):3619–34.

29. Bohnsack MT. Exportin 5 is a RanGTP-dependent dsRNA-binding protein that mediates nuclear export of pre-miRNAs. RNA. 2004 Feb 1;10(2):185–91.

30. Wang X, Xu X, Ma Z, Huo Y, Xiao Z, Li Y, et al. Dynamic mechanisms for pre-miRNA binding and export by Exportin-5. RNA. 2011 Aug 1;17(8):1511–28.

31. Wu K, He J, Pu W, Peng Y. The Role of Exportin-5 in MicroRNA Biogenesis and Cancer. Genomics, Proteomics & Bioinformatics. 2018 Apr;16(2):120–6.

32. Lund E. Nuclear Export of MicroRNA Precursors. Science. 2004 Jan 2;303(5654):95–8.

33. Melo SA, Moutinho C, Ropero S, Calin GA, Rossi S, Spizzo R, et al. A Genetic Defect in Exportin-5 Traps Precursor MicroRNAs in the Nucleus of Cancer Cells. Cancer Cell. 2010 Oct;18(4):303–15.

34. Fabian MR, Sonenberg N. The mechanics of miRNA-mediated gene silencing: a look under the hood of miRISC. Nat Struct Mol Biol. 2012 Jun;19(6):586–93.

35. Tran N, Abhyankar V, Nguyen K, Weidanz J, Gao J. MicroRNA dysregulational synergistic network: discovering microRNA dysregulatory modules across subtypes in non-small cell lung cancers. BMC Bioinformatics. 2018 Dec;19(S20):504.

36. Sassen S, Miska EA, Caldas C. MicroRNA—implications for cancer. Virchows Arch. 2008 Jan;452(1):1–10.

37. Visone R, Croce CM. MiRNAs and Cancer. The American Journal of Pathology. 2009 Apr;174(4):1131–8.

38. Jansson MD, Lund AH. MicroRNA and cancer. Molecular Oncology. 2012 Dec;6(6):590–610.

39. Skrzypski M, Dziadziuszko R, Jassem J. MicroRNA in lung cancer diagnostics and treatment. Mutation Research/Fundamental and Molecular Mechanisms of Mutagenesis. 2011 Dec;717(1–2):25–31.

40. Seidl C, Panzitt K, Bertsch A, Brcic L, Schein S, Mack M, et al. MicroRNA-182-5p regulates hedgehog signaling pathway and chemosensitivity of cisplatin-resistant lung adenocarcinoma cells via targeting GLI2. Cancer Letters. 2020 Jan;469:266–76.

41. Fattahi S, Pilehchian Langroudi M, Akhavan-Niaki H. Hedgehog signaling pathway: Epigenetic regulation and role in disease and cancer development. J Cell Physiol. 2018 Aug;233(8):5726–35.

42. Briscoe J, Thérond PP. The mechanisms of Hedgehog signalling and its roles in development and disease. Nat Rev Mol Cell Biol. 2013 Jul;14(7):416–29.

43. Niyaz M, Khan MS, Mudassar S. Hedgehog Signaling: An Achilles' Heel in Cancer. Translational Oncology. 2019 Oct;12(10):1334–44.

44. McMillan R, Matsui W. Molecular Pathways: The Hedgehog Signaling Pathway in Cancer. Clinical Cancer Research. 2012 Sep 15;18(18):4883–8.

45. Skoda AM, Simovic D, Karin V, Kardum V, Vranic S, Serman L. The role of the Hedgehog signaling pathway in cancer: A comprehensive review. Bosn J of Basic Med Sci. 2018 Feb 20;18(1):8–20.

46. Cochrane C, Szczepny A, Watkins D, Cain J. Hedgehog Signaling in the Maintenance of Cancer Stem Cells. Cancers. 2015 Aug 11;7(3):1554–85.

47. Leon G, MacDonagh L, Finn SP, Cuffe S, Barr MP. Cancer stem cells in drug resistant lung cancer: Targeting cell surface markers and signaling pathways. Pharmacology & Therapeutics. 2016 Feb;158:71–90.

48. Sari IN, Phi LTH, Jun N, Wijaya YT, Lee S, Kwon HY. Hedgehog Signaling in Cancer: A Prospective Therapeutic Target for Eradicating Cancer Stem Cells. Cells. 2018 Nov 10;7(11):208.

49. Koury J, Zhong L, Hao J. Targeting Signaling Pathways in Cancer Stem Cells for Cancer Treatment. Stem Cells International. 2017;2017:1–10.

50. Giroux-Leprieur E, Costantini A, Ding V, He B. Hedgehog Signaling in Lung Cancer: From Oncogenesis to Cancer Treatment Resistance. IJMS. 2018 Sep 19;19(9):2835.

51. Mastrangelo E, Milani M. Role and inhibition of GLI1 protein in cancer. LCTT. 2018 Mar;Volume 9:35–43.

52. Didiasova M, Schaefer L, Wygrecka M. Targeting GLI Transcription Factors in Cancer. Molecules. 2018 Apr 24;23(5):1003.

53. Stecca B, Ruiz i Altaba A. Context-dependent Regulation of the GLI Code in Cancer by HEDGEHOG and Non-HEDGEHOG Signals. Journal of Molecular Cell Biology. 2010 Apr 1;2(2):84–95.

54. Rimkus T, Carpenter R, Qasem S, Chan M, Lo H-W. Targeting the Sonic Hedgehog Signaling Pathway: Review of Smoothened and GLI Inhibitors. Cancers. 2016 Feb 15;8(2):22.

55. Giroux Leprieur E, Vieira T, Antoine M, Rozensztajn N, Rabbe N, Ruppert A-M, et al. Sonic Hedgehog Pathway Activation Is Associated With Resistance to Platinum-Based Chemotherapy in Advanced Non–Small-Cell Lung Carcinoma. Clinical Lung Cancer. 2016 Jul;17(4):301–8.

56. Abe Y, Tanaka N. The Hedgehog Signaling Networks in Lung Cancer: The Mechanisms and Roles in Tumor Progression and Implications for Cancer Therapy. BioMed Research International. 2016;2016:1–11.

57. Hong Z, Bi A, Chen D, Gao L, Yin Z, Luo L. Activation of Hedgehog Signaling Pathway in Human Non-small Cell Lung Cancers. Pathol Oncol Res. 2014 Oct;20(4):917–22.

58. Urman NM, Mirza A, Atwood SX, Whitson RJ, Sarin KY, Tang JY, et al. Tumor-Derived Suppressor of Fused Mutations Reveal Hedgehog Pathway Interactions. Katoh M, editor. PLoS ONE. 2016 Dec 28;11(12):e0168031.

59. Huang D, Wang Y, Tang J, Luo S. Molecular mechanisms of suppressor of fused in regulating the hedgehog signalling pathway (Review). Oncol Lett [Internet]. 2018 Mar 1 [cited 2020 May 18]; Available from: http://www.spandidos-publications.com/10.3892/ol.2018.8142

60. Dunaeva M, Michelson P, Kogerman P, Toftgard R. Characterization of the Physical Interaction of Gli Proteins with SUFU Proteins. J Biol Chem. 2003 Feb 14;278(7):5116–22.

61. Liu X, Wang X, Du W, Chen L, Wang G, Cui Y, et al. Suppressor of fused (Sufu) represses Gli1 transcription and nuclear accumulation, inhibits glioma cell proliferation, invasion and vasculogenic mimicry, improving glioma chemo-sensitivity and prognosis. Oncotarget. 2014 Nov 30;5(22):11681–94.

62. Xu Q, Gao J, Li Z. Identification of a novel alternative splicing transcript variant of the suppressor of fused: Relationship with lymph node metastasis in pancreatic ductal adenocarcinoma. International Journal of Oncology. 2016 Dec;49(6):2611–9.

63. Zhang Z, Shen L, Law K, Zhang Z, Liu X, Hua H, et al. Suppressor of Fused Chaperones Gli Proteins To Generate Transcriptional Responses to Sonic Hedgehog Signaling. Mol Cell Biol. 2017 Feb 1;37(3):e00421-16, e00421-16.

64. Paces-Fessy M, Boucher D, Petit E, Paute-Briand S, Blanchet-Tournier M-F. The negative regulator of Gli, Suppressor of fused (Sufu), interacts with SAP18, Galectin3 and other nuclear proteins. Biochemical Journal. 2004 Mar 1;378(2):353–62.

65. Cheng SY, Bishop JM. Suppressor of Fused represses Gli-mediated transcription by recruiting the SAP18-mSin3 corepressor complex. Proceedings of the National Academy of Sciences. 2002 Apr 16;99(8):5442–7.

66. Lee Y, Kawagoe R, Sasai K, Li Y, Russell HR, Curran T, et al. Loss of suppressor-of-fused function promotes tumorigenesis. Oncogene. 2007 Sep;26(44):6442–7.

67. Yue S, Chen Y, Cheng SY. Hedgehog signaling promotes the degradation of tumor suppressor Sufu through the ubiquitin–proteasome pathway. Oncogene. 2009 Jan;28(4):492–9.

68. Long H, Wang Z, Chen J, Xiang T, Li Q, Diao X, et al. microRNA-214 promotes epithelial-mesenchymal transition and metastasis in lung adenocarcinoma by targeting the suppressor-of-fused protein (Sufu). Oncotarget. 2015 Nov 17;6(36):38705–18.

69. Ma L, Yang X, Wei R, Ye T, Zhou J-K, Wen M, et al. MicroRNA-214 promotes hepatic stellate cell activation and liver fibrosis by suppressing Sufu expression. Cell Death Dis. 2018 Jul;9(7):718.

70. Stone DM, Murone M, Luoh S, Ye W, Armanini MP, Gurney A, et al. Characterization of the human suppressor of fused, a negative regulator of the zinc-finger transcription factor Gli. J Cell Sci. 1999 Dec;112 (Pt 23):4437–48.

71. Barr MP, Gray SG, Hoffmann AC, Hilger RA, Thomale J, O'Flaherty JD, et al. Generation and Characterisation of Cisplatin-Resistant Non-Small Cell Lung Cancer Cell Lines Displaying a Stem- Like Signature. PLOS ONE. 2013;8(1):19.

72. jetPRIME - DNA / siRNA transfection reagent - Polyplus-transfection [Internet]. Polyplus Transfection. [cited 2019 Nov 23]. Available from: https://www.polyplus-transfection.com/products/jetprime/

73. What is transfection? - Polyplus-transfection [Internet]. Polyplus Transfection. [cited 2019 Nov 23]. Available from: https://www.polyplus-transfection.com/technologies/what-is-transfection/

74. Gesamt-RNA Kit, peqGOLD [Internet]. VWR. [cited 2020 May 30]. Available from: https://at.vwr.com/store/product/16807555/gesamt-rna-kit-peqgold

75. RNase*Zap*™ RNase Decontamination Solution [Internet]. [cited 2020 May 30]. Available from: http://www.thermofisher.com/order/catalog/product/AM9782

76. NanoDrop™ 2000/2000c Spectrophotometers [Internet]. [cited 2020 Jun 2]. Available from: http://www.thermofisher.com/order/catalog/product/ND-2000

77. NanoDrop Nucleic Acid Handbook [Internet]. [cited 2020 Jun 2]. Available from: https://www.thermofisher.com/document-connect/document-connect.html?url=https%3A%2F%2Fassets.thermofisher.com%2FTFS-Assets%2FCAD%2Fmanuals%2Fts-nanodrop-nucleicacid-olv-r2.pdf&title=TmFub0Ryb3AgTnVjbGVpYyBBY2lkIEhhbmRib29r

78. Homo sapiens SUFU negative regulator of hedgehog signaling (SUFU), transcript variant 1, mRNA. 2019 Aug 7 [cited 2020 Jun 3]; Available from: http://www.ncbi.nlm.nih.gov/nuccore/NM_016169.3

79. Homo sapiens SUFU negative regulator of hedgehog signaling (SUFU), transcript variant 2, mRNA. 2019 May 2 [cited 2020 Jun 3]; Available from: http://www.ncbi.nlm.nih.gov/nuccore/NM_001178133.1

80. NEBcloner [Internet]. [cited 2020 Jun 3]. Available from: http://nebcloner.neb.com/#!/redigest

81. RIPA Buffer R0278 [Internet]. Sigma-Aldrich. [cited 2020 Jun 10]. Available from: https://www.sigmaaldrich.com/catalog/product/sigma/r0278

82. alamarBlue™ Cell Viability Reagent [Internet]. [cited 2020 Aug 14]. Available from: https://www.thermofisher.com/order/catalog/product/DAL1025

83. Siegel RL, Miller KD, Jemal A. Cancer statistics, 2020. CA A Cancer J Clin. 2020 Jan;70(1):7–30.

84. Cancer [Internet]. [cited 2020 Dec 18]. Available from: https://www.who.int/westernpacific/health-topics/cancer

85. Cancer [Internet]. [cited 2020 Dec 18]. Available from: https://www.who.int/news-room/fact-sheets/detail/cancer

86. Liu W, Du Y, Wen R, Yang M, Xu J. Drug resistance to targeted therapeutic strategies in non-small cell lung cancer. Pharmacology & Therapeutics. 2020 Feb;206:107438.

87. Dimou A, Bamias A, Gogas H, Syrigos K. Inhibition of the Hedgehog pathway in lung cancer. Lung Cancer. 2019 Jul;133:56–61.

88. Pietrobono S, Gagliardi S, Stecca B. Non-canonical Hedgehog Signaling Pathway in Cancer: Activation of GLI Transcription Factors Beyond Smoothened. Front Genet. 2019 Jun 12;10:556.

89. Types of Transfection - AT [Internet]. [cited 2021 Jan 13]. Available from: //www.thermofisher.com/uk/en/home/references/gibco-cell-culture-basics/transfection-basics/types-of-transfection.html

90. Bolognesi B, Lehner B. Reaching the limit. eLife. 2018 Aug 10;7:e39804.

91. Eguchi Y, Makanae K, Hasunuma T, Ishibashi Y, Kito K, Moriya H. Estimating the protein burden limit of yeast cells by measuring the expression limits of glycolytic proteins. eLife. 2018 Aug 10;7:e34595.

92. Vavouri T, Semple JI, Garcia-Verdugo R, Lehner B. Intrinsic Protein Disorder and Interaction Promiscuity Are Widely Associated with Dosage Sensitivity. Cell. 2009 Jul;138(1):198–208.

93. Seidl C. Masterthesis: Interactions of miR-183 cluster and the hedgehog signaling pathway in cisplatin-resistant NSCLC cells. University of Graz; 2018.

7. Supplemental information

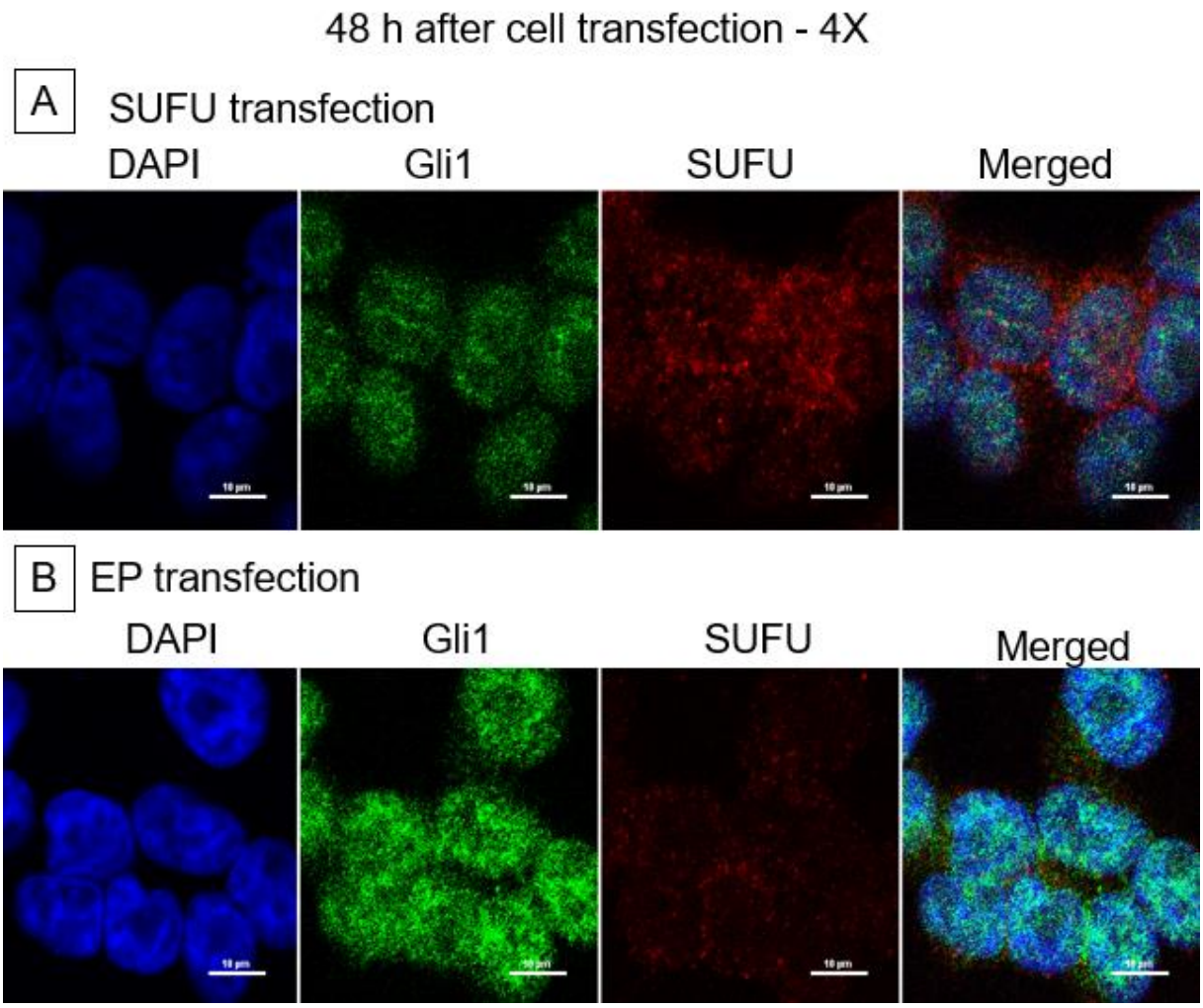

Figure 26. Enlarged images of immunofluorescence analyzes 48 h after transfection of H460-CisR cells with SUFU. *A: Staining after cell transfection with SUFU. B: Staining after cell transfection with EP. Blue: DAPI stained nuclei, Green: Gli1 (abcam antibody) specific secondary donkey anti rabbit (H+L) Alexa Fluor 488 (Invitrogen) antibody, Red: SUFU specific secondary donkey anti mouse (H+L) Alexa Fluor 555 (Invitrogen) antibody, Merged: image channels overlayed. SUFU = 0.25 µg/ml pcDNA3.1(+)/SUFU Var I. EP = 0.25 µg/ml pcDNA3.1(+)*

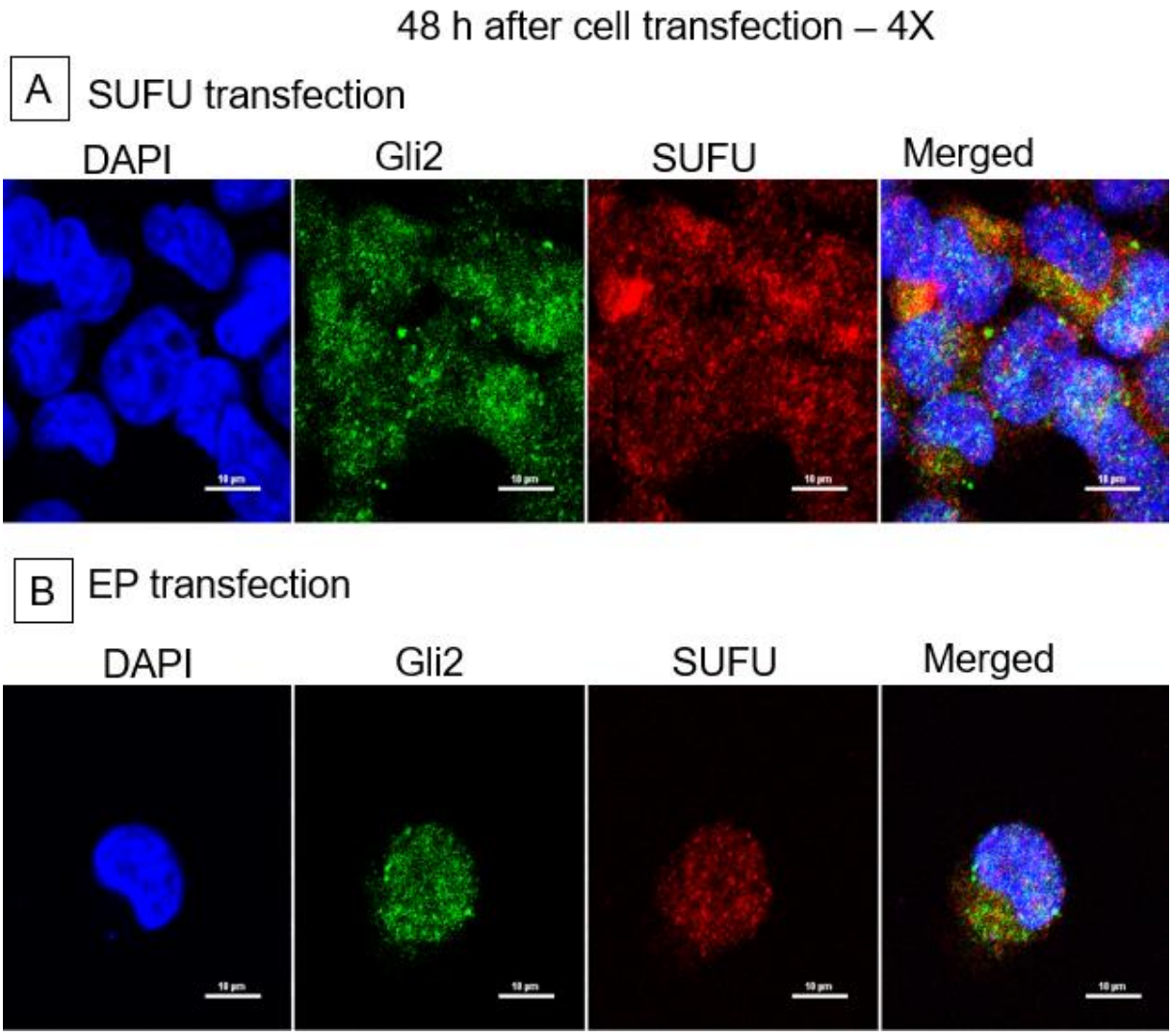

Figure 27. Enlarged images of immunofluorescence analyzes 48 h after transfection of H460-CisR cells with SUFU. *A: Staining after cell transfection with SUFU. B: Staining after cell transfection with EP. Blue: DAPI stained nuclei, Green: Gli2 specific secondary donkey anti rabbit (H+L) Alexa Fluor 488 (Invitrogen) antibody, Red: SUFU specific secondary donkey anti mouse (H+L) Alexa Fluor 555 (Invitrogen) antibody, Merged: image channels overlayed. SUFU = 0.25 µg/ml pcDNA3.1(+)/SUFU Var I. EP = 0.25 µg/ml pcDNA3.1(+)*

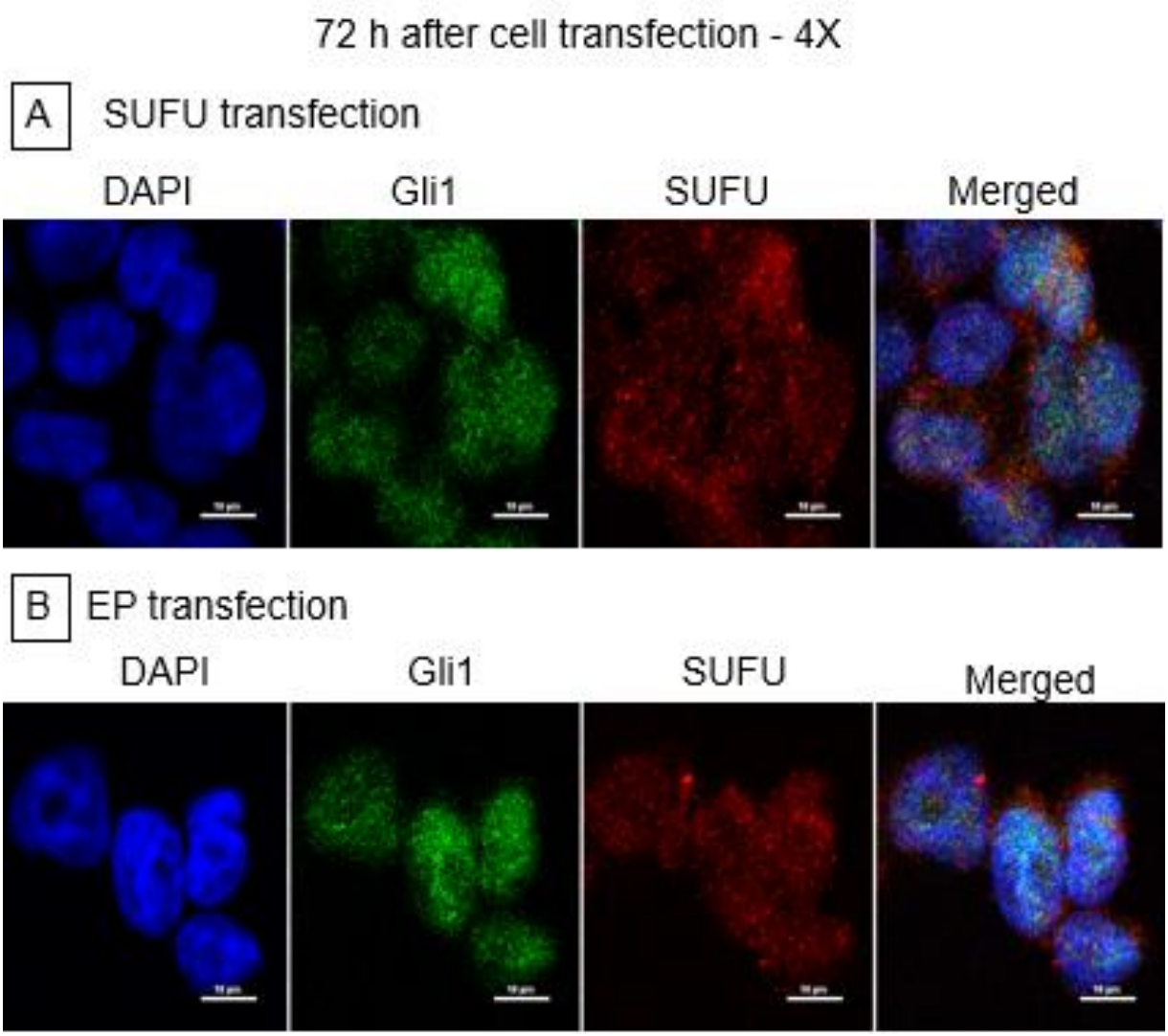

Figure 28. Enlarged images of immunofluorescence analyzes 72 h after transfection of H460-CisR cells with SUFU. *A: Staining after cell transfection with SUFU. B: Staining after cell transfection with EP. Blue: DAPI stained nuclei, Green: Gli1 (abcam antibody) specific secondary donkey anti rabbit (H+L) Alexa Fluor 488 (Invitrogen) antibody, Red: SUFU specific secondary donkey anti mouse (H+L) Alexa Fluor 555 (Invitrogen) antibody, Merged: image channels overlayed. SUFU = 0.25 µg/ml pcDNA3.1(+)/SUFU Var I. EP = 0.25 µg/ml pcDNA3.1(+)*

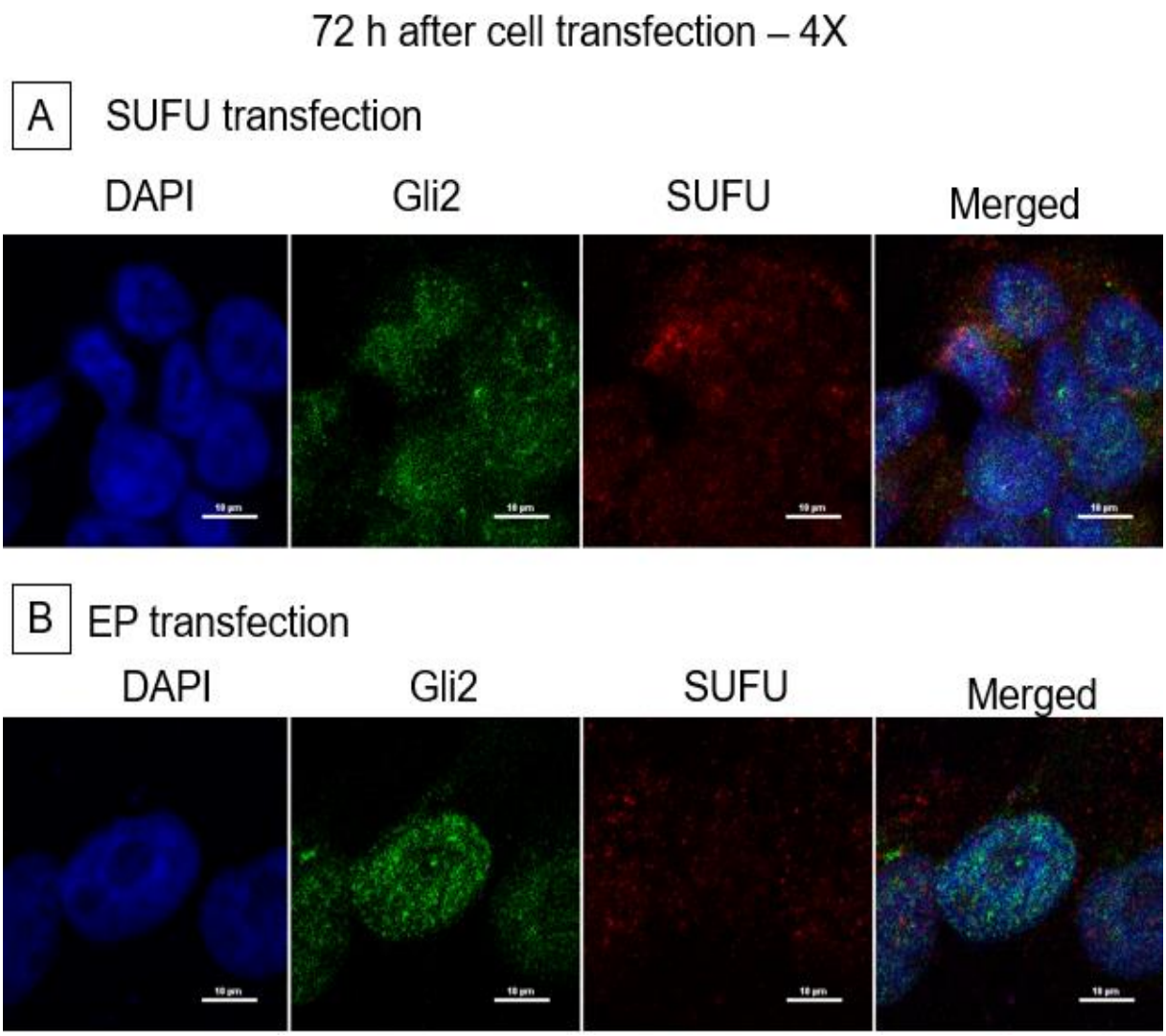

Figure 29. Enlarged images of immunofluorescence analyzes 48 h after transfection of H460-CisR cells with SUFU. *A: Staining after cell transfection with SUFU. B: Staining after cell transfection with EP. Blue: DAPI stained nuclei, Green: Gli2 specific secondary donkey anti rabbit (H+L) Alexa Fluor 488 (Invitrogen) antibody, Red: SUFU specific secondary donkey anti mouse (H+L) Alexa Fluor 555 (Invitrogen) antibody, Merged: image channels overlayed. SUFU = 0.25 µg/ml pcDNA3.1(+)/SUFU Var I. EP = 0.25 µg/ml pcDNA3.1(+)*

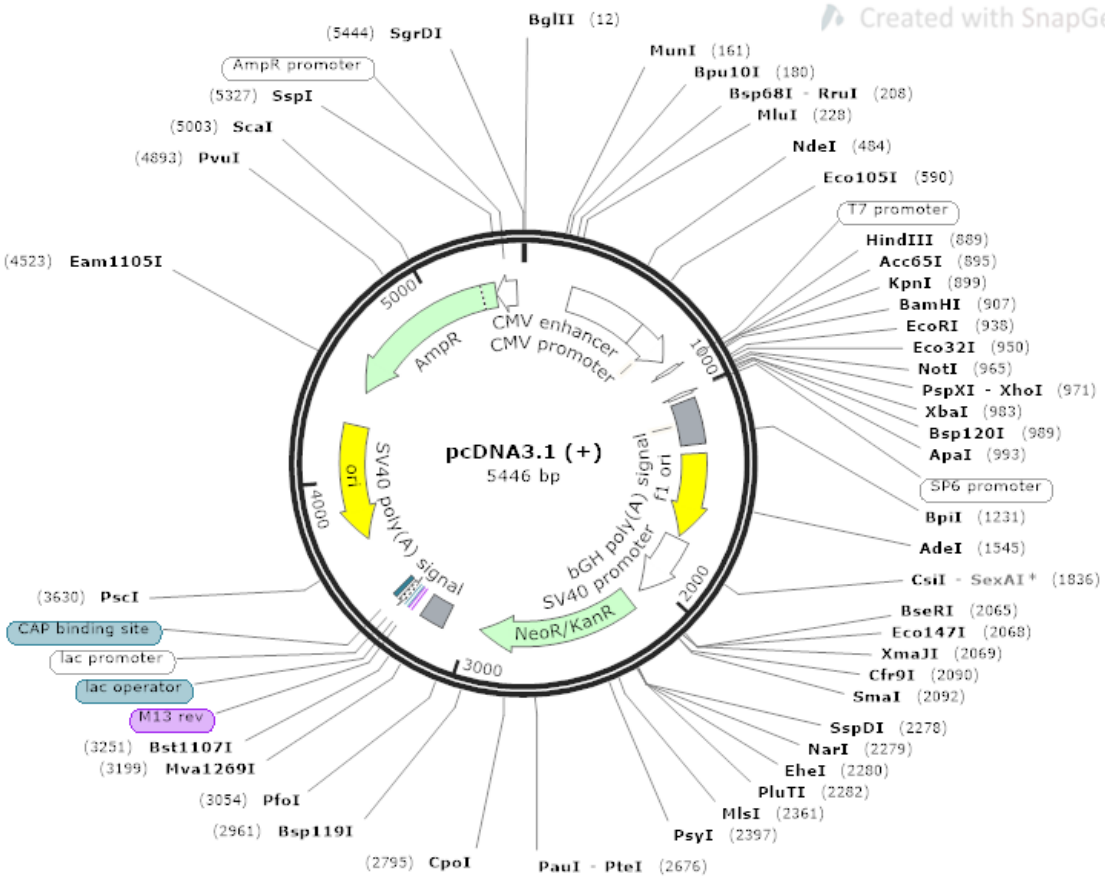

Figure 30. Plasmid map of pcDNA3.1(+). *This plasmid was used as empty vector (EP) as negative control.*

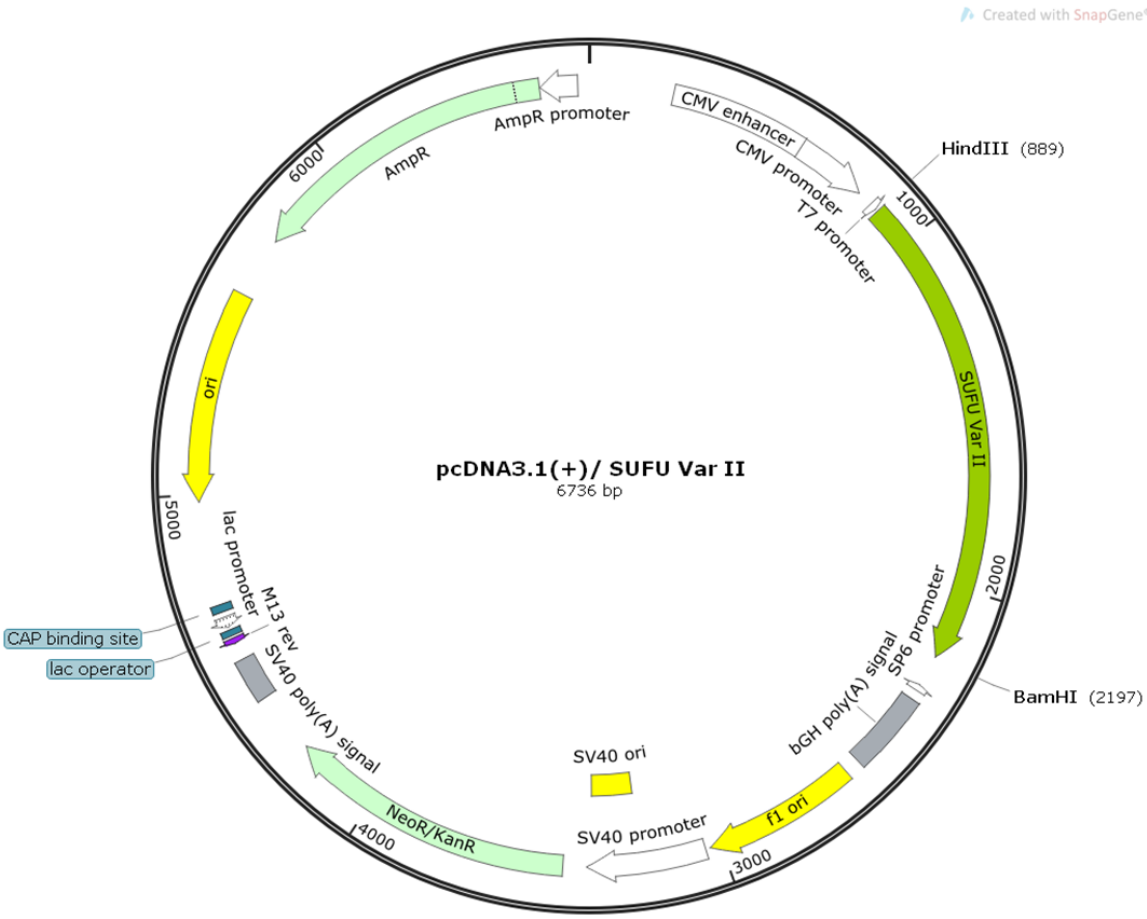

Figure 31. In silico cloned plasmid map of pcDNA3.1(+)/SUFU Var II*. This plasmid was created for further experiments on SUFU Var II overexpression. SUFU Var II is a shorter variant because of alternative splicing.*

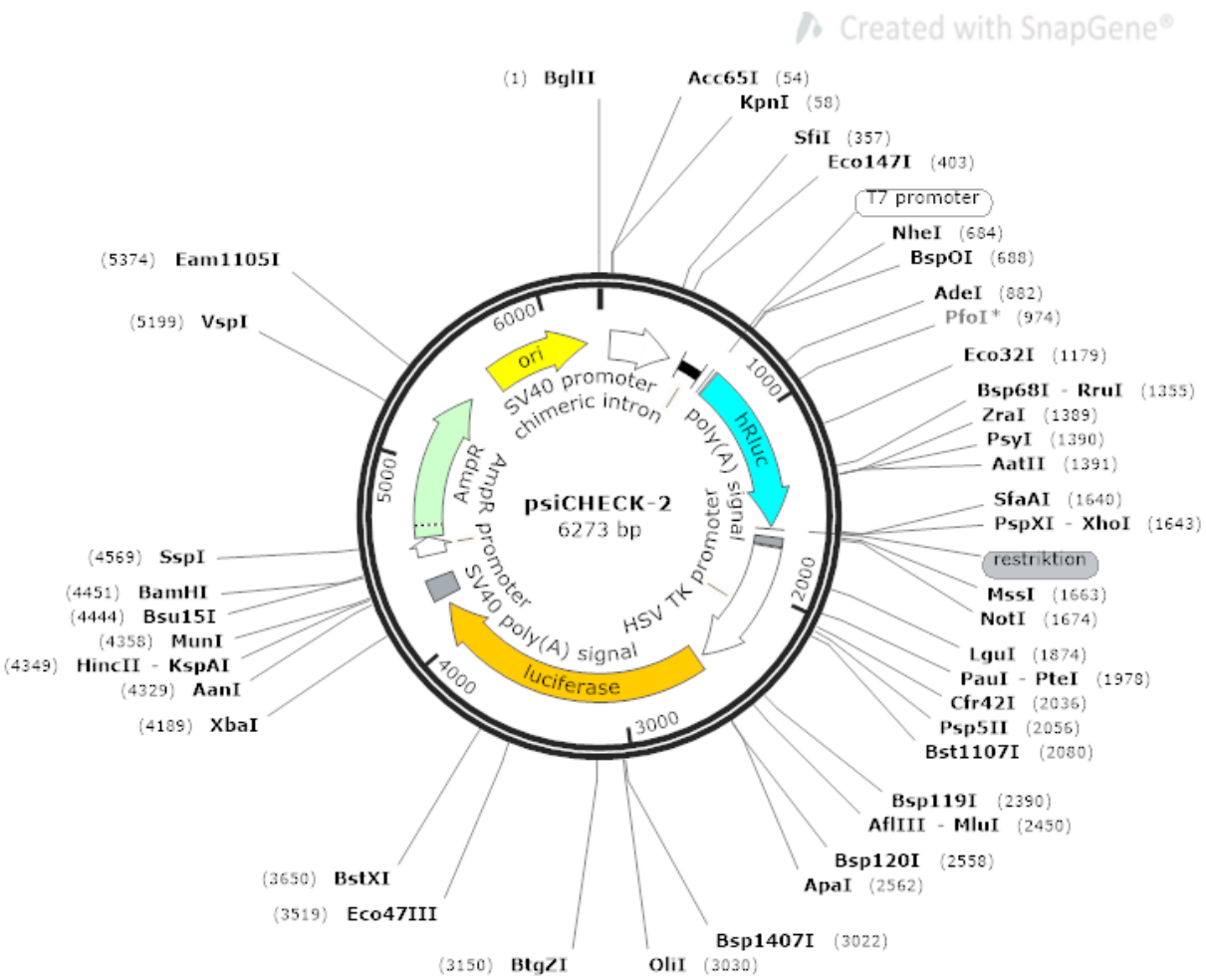

***Figure 32. psiCECK-2 plasmid map**. This plasmid was used for luciferase assay experiments.*

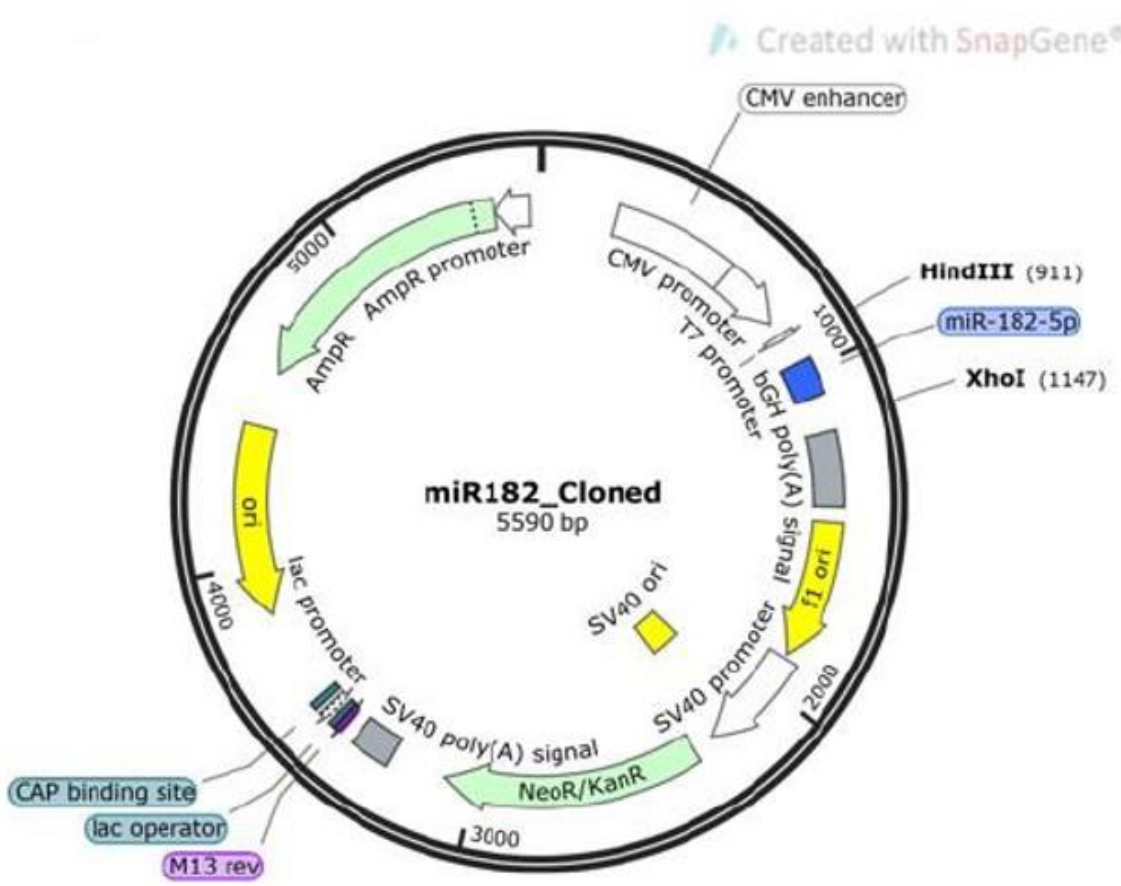

Figure 33. Plasmid map of miR-182-5p plasmid. *miRNA sequence was cloned into pcDNA3.1(+) vector via restriction cloning. Plasmid map was taken from the Masterthesis of Carina Seidl (93).*

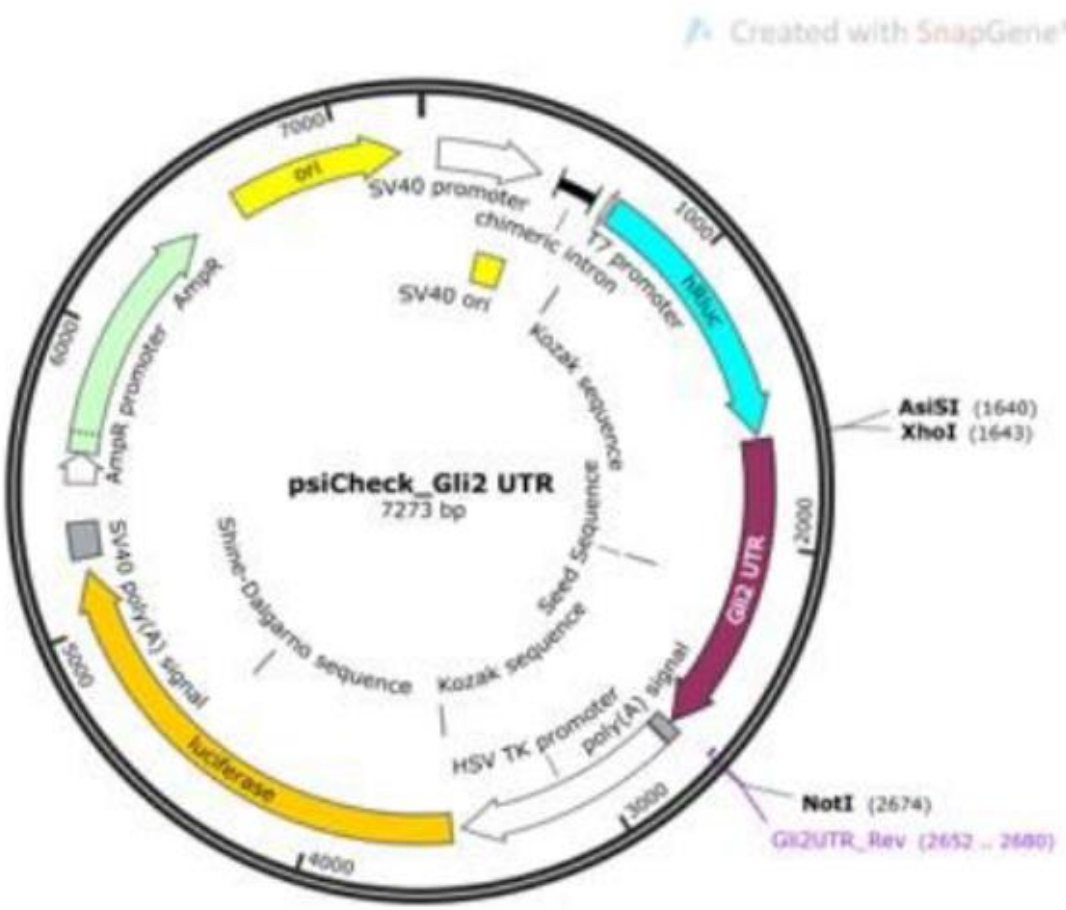

Figure 34. Plasmid map of Gli2 WT plasmid*. Gli2 UTR sequence was cloned into psiCHECK-2 vector via restriction cloning. Plasmid map was taken from the Masterthesis of Carina Seidl (93).*